

**CORTICAL REPRESENTATION OF LEARNING SOCIAL INTERACTIONS IN  
FREELY MOVING NON-HUMAN PRIMATES**

by

Melissa Christine Franch, B.S.

APPROVED:

---

Valentin Dragoi, Ph.D.

---

Fabricio H. Do Monte, DVM, Ph.D.

---

Xaq Pitkow, Ph.D.

---

Harel Shouval, Ph.D.

---

Danielle Garsin, Ph.D.

APPROVED:

---

Dean, The University of Texas  
MD Anderson Cancer Center UTHealth Graduate School of Biomedical Sciences

**CORTICAL REPRESENTATION OF LEARNING SOCIAL INTERACTIONS IN FREELY  
MOVING NON-HUMAN PRIMATES**

A  
DISSERTATION

Presented to the Faculty of

The University of Texas MD Anderson Cancer Center  
UTHealth Houston  
Graduate School of Biomedical Sciences

in Partial Fulfillment  
of the Requirements  
for the Degree of  
DOCTOR OF PHILOSOPHY

by  
Melissa Christine Franch, B.S.

Houston, Texas

*December, 2023*

## DEDICATION

*To my older brother with profound autism, Stefan Serafino Franch.*

*May you always know love.*

*I am me because of you.*

## ACKNOWLEDGEMENTS

Growing up, I had an extraordinary childhood experience that was instrumental in shaping my career as a neuroscientist. Being a witness and advocate to my sibling, Stefan, who has profound autism and intellectual disability promoted my curiosities in neuroscience from a young age. Specifically, my interests in Stefan's lack of eye contact and social motivation persisted into my postbaccalaureate and doctoral studies, ultimately leading to the research in this dissertation and that which I have yet to discover. Stefan, you will always be my greatest inspiration. While it's impossible to recognize every individual who has played a role in my graduate journey, I aim to spotlight those who have been essential in helping me achieve this milestone.

I would first like to sincerely thank my PhD advisor, Valentin Dragoi. Going into graduate school, I knew I wanted to study social behavior in primates. Therefore, the non-human primate model and innovative wireless recording technologies in the Dragoi lab really appealed to me. Thank you for providing me with the resources and support to accomplish my research goals. My independence cultivated in the Dragoi lab enabled me to have ownership of my research and develop critical skills and scientific questions that will continue to contribute success throughout my postdoctoral and faculty career.

I would also like to extend my gratitude to the members of my doctoral advisory committee for their invaluable feedback, suggestions, and constructive criticism. Their diverse perspectives and insights have enriched my research and helped me to develop a more well-rounded understanding of social and computational neuroscience.

In addition, I would like to acknowledge the financial support provided by the NIMH F31 Predoctoral Fellowship for supporting my stipend as well as many scholarships and fellowships provided by GSBS and the Neuroscience program, including the Russell and Diana Hawkins Fellowship, the Dee S. and Patricia Osborne Scholarship, and the Sam Taub and Beatrice Burton Fellowship. The support from these awards improved my livelihood and overall well-being, resulting in productive execution and completion of this research.

Some of the most important relationships have been those I've shared with my colleagues in the Dragoi lab. Over the years, members of the Dragoi lab have become my dear and close friends. Whether it is validating each other's analyses and code, providing assistance when troubleshooting, or discussing our moonshot projects and general challenges in our personal lives, we have overcome a lot together and are extremely supportive of each other. Continue to "violently execute!" Included in the lab, I also want to acknowledge the animals of our colony and the dedicated staff at CLAMC that care for them. Specifically, monkeys M, R, and G, have been my scientific collaborators throughout the years, and this work would certainly not be possible without them. Additionally, I am grateful to everyone who works behind the scenes at GSBS, the Neuroscience Graduate program, and the department of Neurobiology and Anatomy, for making my graduate experience not only possible but also enjoyable. I extend my deepest appreciation to all of you.

Furthermore, I am fortunate to have been "adopted" by families other than my own, including the Jensens, Meekins, and Gabelmans, and those of my high school "crew". You knew me during my critical periods of development when I arguably made the most mistakes, and yet you encouraged me with unrelenting patience and love. Thank you for never doubting who I could become. Another more recent adoption has been from the Pearadox Robotics team. Thank you for teaching me how to be an excellent leader and advocate for individuals who are underrepresented and under resourced in STEM fields. I can't wait to implement these inclusion efforts one day in the Franch lab.

Finally, I especially want to thank the individuals who have been my daily cheerleaders and unwavering supporters. Angad Mehrotra, you are the most remarkable partner, listener, and champion – always motivating me to reach my full potential. I am my best self because of you. To my brothers Daniel and Stefan, and to my parents, Regina and Serafino, advocates of 32 years and counting, you already know you are the greatest; the most unique and inspiring individuals. Mom and dad, despite unimaginable challenges that few can ever relate to, you cultivated family with a love and beauty that generates awe. I owe it all to you.

In conclusion, I am indebted to many individuals who have supported me throughout my doctoral studies. Their contributions, both big and small, have been invaluable in helping me to achieve my scientific goals. Your continued support and encouragement will enable my future success as neuroscientist. Thank you all for launching me in this trajectory – it is only the beginning.

## **ABSTRACT**

### **CORTICAL REPRESENTATION OF LEARNING SOCIAL INTERACTIONS IN FREELY MOVING NON-HUMAN PRIMATES**

Melissa C. Franch

Advisory Professor: Valentin Dragoi, Ph.D.

The motivation and capacity to be social is necessary for human survival. Successful learning of complex, prosocial behavior stems from the ability to perceive and respond to visual cues, such as the body language and facial expressions, from others in our environment. This dependence on visual information to guide social interaction is especially true for humans and non-human primates. Although recent studies in primate neurophysiology discovered neurons that can encode socially relevant variables, like reward and social actions, the underlying neural mechanisms of learning advanced social concepts, such as cooperation, are not well understood. Further, previous work has identified brain structures that are activated when restrained subjects passively view other agents in-person or socially interacting animals in videos, but examining how the brain processes social signals originating from interacting conspecifics in real time to initiate goal-directed behavior has not been explored – until now.

Limitations include the lack of a suitable framework to study how social cognition emerges in real time, and a lack of a neural population level approach to record from multiple brain regions simultaneously while animals perform naturalistic tasks. To this end, we developed a novel paradigm that combines behavioral monitoring with wireless eye tracking and neural recordings to study how pairs of freely moving, interacting macaques use visually-guided signals to learn social cooperation for food reward. By recording from visual (V4) and prefrontal (dorsolateral prefrontal cortex; dlPFC) brain regions simultaneously, I examined how visual representations relevant for social interactions are communicated from sensory to executive areas that encode reward and decision making.

During learning, animals improve coordination of their actions and likelihood of cooperating, and they cooperate more quickly. Notably, animals become more likely to cooperate after viewing a social cue, such as the reward or partner monkey. As social learning occurs, V4 and dlPFC refine the representation of viewing the reward or partner monkey by distributing socially-relevant information among neurons within each area. Additionally, dlPFC improves encoding of each animal's decision to cooperate, especially when social cues are viewed, highlighting the importance of visual monitoring to determine actions of oneself and predict or even influence other's actions in the creation of purposeful social behavior. Finally, learning social events increases the coordinated spiking between visual and prefrontal cortical neurons, with coordinated V4-dlPFC cells contributing more to encoding of social variables within each area. These results are the first to demonstrate how the visual-frontal cortical network prioritizes relevant sensory information to facilitate learning social interactions while freely moving macaques interact in a naturalistic environment.



## Table of Contents

<b>APPROVAL PAGE .....</b>	<b>i</b>
<b>DEDICATION.....</b>	<b>iii</b>
<b>ACKNOWLEDGEMENTS .....</b>	<b>iv</b>
<b>ABSTRACT .....</b>	<b>vii</b>
<b>LIST OF ILLUSTRATIONS .....</b>	<b>xii</b>
<b>ABBREVIATIONS .....</b>	<b>xiv</b>
<b>CHAPTER 1: INTRODUCTION.....</b>	<b>1</b>
1.1 Social behavior in primates .....	1
1.2 Neural processing of social information .....	2
1.3 Approaches to examine ecologically relevant social stimuli and behavior.....	5
1.4 The present study – overview, aims, and hypotheses .....	7
<b>CHAPTER 2: VIEWING SOCIAL CUES DRIVES COOPERATION DURING LEARNING.....</b>	<b>9</b>
2.1 Background.....	9
2.2 Methods .....	10
2.2.1 Animals.....	10
2.2.2 Social cooperation task .....	10
2.2.3 Opaque Divider Experiments .....	12
2.2.4 Cross-correlation of animals' pushes .....	12
2.2.5 Conditional Probability .....	13
2.2.6 Wireless eye tracking and fixations .....	13
2.2.7 Behavioral tracking .....	15
2.2.8 Hidden Markov Model .....	17
	ix

2.2.9 Statistics .....	17
2.3 Results .....	18
2.3.1 Animals learn to cooperate.....	18
2.3.2 Viewing the other monkey improves cooperation .....	20
2.3.3 Animals fixate on the reward and partner monkey the most before cooperation .....	21
2.3.4 Animals become more likely to cooperate after viewing a social cue .....	23
2.4 Discussion.....	25
<b>CHAPTER 3: POPULATION ENCODING OF SOCIAL EVENTS DURING LEARNING .....</b>	<b>26</b>
3.1 Background.....	26
3.2 Methods .....	27
3.2.1 Wireless electrophysiology .....	27
3.2.2 Receptive field mapping .....	29
3.2.3 Identifying stable units across sessions .....	31
3.2.4 Neural firing rate and response .....	33
3.2.5 Support vector machine decoder .....	34
3.2.6 Solo-and-social control experiments .....	35
3.2.7 Statistics .....	35
3.3 Results .....	36
3.3.1 Single cells respond to social cues and actions.....	36
3.3.2 Neural encoding of social cues and decisions improves during learning.....	40
3.3.3 Cells contribute more equally to encoding of social events during learning.....	45
3.3.4 Social context influences self-action.....	47
3.3.5 Neural activity is minimally correlated with animal's body and eye movements .....	48
3.4 Discussion.....	52

<b>CHAPTER 4: SPIKE TIMING COORDINATION BETWEEN BRAIN REGIONS DURING SOCIAL LEARNING .....</b>	<b>55</b>
4.1 Background .....	55
4.2 Methods .....	56
4.2.1 Cross-correlation of neuronal pairs .....	56
4.2.2 SVM weight normalization.....	57
4.2.3 Statistics .....	57
4.3 Results .....	58
4.3.1 Spiking coordination within and between areas improves during learning .....	58
4.3.2 Coordinated cells contribute more to encoding of social events .....	62
4.4 Discussion.....	63
<b>CHAPTER 5: DISCUSSION.....</b>	<b>65</b>
5.1 Summary of findings.....	65
5.2 Limitations and future directions .....	69
5.3 Clinical applications.....	70
<b>BIBLIOGRAPHY.....</b>	<b>73</b>
<b>VITA.....</b>	<b>91</b>

## LIST OF ILLUSTRATIONS

Figure 1. Social cooperation task .....	11
Figure 2. Opaque divider experimental setup .....	16
Figure 3. Wireless eye tracking .....	14
Figure 4. Viewing statistics .....	16
Figure 5. Action coordination improves during learning .....	18
Figure 6. Conditional probability to cooperate and motivation improves during learning.....	19
Figure 7. Disrupting viewing impairs cooperation .....	20
Figure 8. Identification of social cues .....	22
Figure 9. Relationship between action and viewing behaviors while learning to cooperate.....	24
Figure 10. Wireless neural recording methods.....	28
Figure 11. Identification of stimuli within neurons' receptive fields.....	30
Figure 12. Neural population stability.....	32
Figure 13. Viewing behavior during pushing.....	37
Figure 14. Neural responses to social events .....	38
Figure 15. Mixed selectivity in V4 and dIPFC .....	40
Figure 16. Encoding of social cues in V4 and dIPFC .....	42
Figure 17. Encoding of choice in V4 and dIPFC .....	43
Figure 18. Viewing social cues improves choice encoding .....	44
Figure 19. Learning distributes information among neurons .....	46
Figure 20. Effects of social context on self-action... ..	48
Figure 21. Neural activity correlations with oculomotor and body movements during pushing....	50
Figure 22. Neural activity correlations with body movements during fixations on social cues.....	51
Figure 23. Cross correlograms of neuronal pairs within and between brain regions.....	58
Figure 24. Spike timing coordination for social and nonsocial events.....	60
Figure 25. V4-dIPFC interactions are mostly feedforward.....	61

Figure 26. Social learning mechanisms in primate cortex.....	62
Figure 27. Social learning summary.....	68

## ABBREVIATIONS

ASD	autism spectrum disorder
CCG	cross-correlogram
dIPFC	dorsolateral prefrontal cortex
NHP	non-human primate
PSTH	peristimulus time histogram
V4	visual cortical area, V4
VTA	ventral tegmental area

## CHAPTER 1: INTRODUCTION

### ***1.1 Social behavior in primates***

Social interactions are essential for the well-being and survival of humans, non-human primates (NHPs), and other animals. Indeed, when we reflect on life's moments, our fondest memories often do not occur in isolation. Throughout life, we socially interact through play, cooperation, competition, friendship, mating, caring for young, and helping and leading others – just to name a few. Social interactions require the perception and integration of social cues through a complex cognition process (i.e. social cognition) that involves attention, memory, motivation, and empathy (Fernández et al., 2018; Wallace & Hofmann, 2021). Social cues in our environment such as context, features, and expressions of faces and bodies enable us to infer the identity, emotional status, and hidden thoughts of others, as well as to predict their potential actions (i.e. theory of mind) (BARON-COHEN & CROSS, 1992; Emery, 2000; Jamali et al., 2021). These computations guide decisions for appropriate behavioral responses, facilitating successful social interaction and engagement.

The correct functioning of the social cognition system has profound implications for human health. Impairments in social behavior are a common feature of many neuropsychiatric disorders, such as autism and depression (Association, 2013). Worldwide, there are as many as 450 million people suffering from a neuropsychiatric disorder, with devastating impacts for individuals and communities (Winsky et al., 2008). With a better understanding of how different brain regions mediate social interaction, targeted, individualized therapies for affected individuals could be implemented. For example, when behavioral therapy or medications fail, alternative forms of treatment involving brain stimulation and/or implants to a specific brain area are considered (Wickelgren, 2018). Thus, to develop more effective behavioral and neural strategies aimed at ameliorating social deficits, it is necessary to characterize the underlying mechanisms that support social behavior.

Both innate and learned social behavior is extremely complex and contingent, involving the perception and monitoring of self and others' actions to determine context-appropriate and productive responses. Specifically, cooperation - an advanced social concept critical for the evolution of intelligence - requires two or more agents to work together towards a common goal and thus relies heavily on perceiving social cues, such as the body language and expressions of the partner, and even the reward for cooperating. Although there is evidence for deep homologies in neuroanatomy and social behaviors across vertebrates (O'Connell & Hofmann, 2012), most visually-guided, strategic social behaviors are unique to primates (Platt et al., 2016). Social interactions, especially cooperative ones (Mendres & FB, 2000; Mesterton-gibbons & Dugatkin, 1997), are essential to the survival of humans (Strang & Park, 2017) and non-human primate (NHP) groups (Schulke et al., 2010; Silk et al., 2009, 2010), and typically involve complex cognitive processing (Tremblay et al., 2017). Rhesus macaques, a well-studied species of NHP, exhibit social behaviors similar to humans. They live in large, hierarchical groups (Noonan et al., 2014), displaying cohabitation, cooperation (Silk et al., 2009; Visco-Comandini et al., 2015), and competition (Maestriperi & Georgiev, 2016), and strategically acquire social information from facial expressions and eyes (Emery et al., 1997; Mosher et al., 2014). In addition, the primate brain is specialized to acquire information about conspecifics, indicating that particular information is valuable to the individual (Sliwa & Freiwald, 2017). This sensitivity to social bonds and the well-being of others that humans and NHPs share makes rhesus macaques an ideal model to study social behavior.

## ***1.2 Neural processing of social information***

Recent studies have investigated the neural mechanisms of social interactions in variety of mammals - from humans and NHPs to mice and bats - finding a 'self and other' encoding of social variables, such as reward value (Aquino et al., 2020; Chang et al., 2013; Grabenhorst et al., 2019; Noritake et al., 2018), actions (Falcone et al., 2016; Haroush & Williams, 2015; Jamali et al., 2021; Rose et al., 2021), agent identity (Báez-Mendoza et al., 2021; Rose et al., 2021),



and social rank (Kingsbury et al., 2019; Li et al., 2022; Padilla-Coreano et al., 2022) within many different brain regions. Indeed, cognition arises from dynamic interactions in neural networks distributed across the whole brain in addition to localized neural populations. However, only a few brain areas have been studied with single cell recordings during cooperation specifically (Haroush & Williams, 2015; Ong et al., 2020), limiting the amount of collected neural information from one part of the social pathway. Specifically, Haroush and Williams discovered neurons in the anterior cingulate cortex that predict another individual's unknown actions during cooperation (Haroush & Williams, 2015). Additionally, Song Ong and colleagues discovered neurons in the medial superior temporal sulcus that selectively signaled rewards obtained by cooperation (Song Ong et al., 2018). This research remains the only experimental evidence to examine the neural basis of cooperation in NHPs with single cell resolution, therefore our understanding of the neural computations underlying cooperation is limited. Furthermore, these experiments used traditional paradigms where animals were restrained, performing unnaturalistic tasks and viewing synthetic stimuli on monitors, so the neural mechanisms underlying the role of viewing relevant cues in the organic emergence of social decisions remain unknown.

Given the importance of viewing socially-relevant cues during social interactions, previous NHP work identified brain regions that are activated when viewing other agents in-person or socially interacting animals in videos (Dal Monte et al., 2022; Mosher et al., 2014; Sliwa & Freiwald, 2017). Notably, these studies found neurons in the amygdala and prefrontal cortical regions that respond selectively to fixations on the eyes of others and mutual eye contact, and can discriminate between social and nonsocial objects (Dal Monte et al., 2022; Mosher et al., 2014). Similar to the work summarized in the above paragraph, these data were examined from stationary animals performing passive or unnaturalistic tasks (Dal Monte et al., 2022; Mosher et al., 2014; Sliwa & Freiwald, 2017) with animals viewing social visual stimuli (i.e. images of monkey faces or videos of monkeys interacting) on monitors and not in real life (Mosher et al., 2014; Sliwa & Freiwald, 2017). Certainly, examining how the brain processes continuous “real-

world” social visual inputs from an interacting conspecific to initiate goal-directed behavior has not yet been explored – until now.

Social learning is a broad term that refers to any form of learning via social context including observing, imitating, and interacting with others. During observational and imitation learning, an individual observes and even mimics actions from another agent to acquire knowledge (Cross, 2012; Laland & Rendell, 2010). Previous work has shown observational learning is facilitated by the mirror neuron system, a network of neurons in premotor and parietal cortex that become active both when an individual performs an action and when they observe someone else performing the same action (Fogassi & Ferrari, 2011; Rizzo et al., 2008). The mirror neuron system is thought to be important for imitation, empathy, and understanding the actions and intentions of others (i.e. – learning from others) (Ramsey et al., 2021). Notably, in both humans and macaques, the dorsolateral prefrontal cortex (dlPFC) plays a role in social learning, imitation, and decision-making (Burke et al., 2010; Falcone et al., 2016; Feng et al., 2021; Gariépy et al., 2014; Suzuki et al., 2012; Yoshida et al., 2010).

However, learning of complex social behaviors like cooperation also requires interactive learning which involves the exchange of reciprocal social signals and information flow between two or more interacting agents (i.e. – learning with others) (Ramsey et al., 2021; Rogoff et al., 2001). Despite the critical role of social cognition in the process of social learning, neural mechanisms that facilitate interactive learning such as cooperation have yet to be explored. Specifically, identifying neural computations that support the perception and exchange of social stimuli will reveal how sensory information is used to predict and/or influence the actions of others during goal-directed, interactive learning. Two brain regions that could support such operations are V4 and dlPFC, given their roles in processing visual information and action planning. Cortical area V4 is an intermediate visual area, encoding complex objects and visual features (Gallant et al., 1998; Kim et al., 2019; Kobatake & Tanaka, 1994; Pasupathy & Connor, 1999; Schein & Desimone, 1990), and dlPFC is an executive region that encodes the goals of self and other (Falcone et al., 2016; Tanji & Hoshi, 2008), and is involved in tracking the decisions of others

during social learning (Gariépy et al., 2014; Suzuki et al., 2012). Additionally, dIPFC is downstream from V4 and integrates informational content and behavioral relevance of visual stimuli in perceptual decision-making (Heekeren et al., 2004; E. K. Miller et al., 1996; E. K. Miller & Cohen, 2001; Rainer et al., 1998; Rainer & Miller, 2000; Rao et al., 1997). Finally, sensory, task, choice, and attention related information is communicated between these areas (Brincat et al., 2018; Gregoriou et al., 2014; Siegel et al., 2015; Tremblay et al., 2015). Certainly, V4 and dIPFC emerge as relevant brain areas to record neural activity to understand how visual information is transformed and communicated across the cortical hierarchy to inform social decisions during learning cooperation.

### ***1.3 Approaches to examine ecologically relevant social stimuli and behavior***

Despite the clear importance of social cognition and learning of advanced social concepts, the underlying neural mechanisms are not well understood. One of the major limitations preventing this understanding is the lack of a suitable framework that would allow us to study how social cognition emerges in real time and how it influences brain networks. Indeed, most of our knowledge of social cognition originates from studies performed (i) in restrained animals engaged in simple tasks involving the movement of the eyes or touching a computer screen while recording neuronal responses (Chang et al., 2013; Dal Monte et al., 2022; Haroush & Williams, 2015; Mosher et al., 2014; Noritake et al., 2018; Ong et al., 2020) or (ii) by observing freely moving animals exhibiting social cognition in a naturalistic environment without attempting to record neural activity (Brosnan & de Waal, 2014; Brosnan & De Waal, 2003; Fletcher, 2008; Mendres & FB, 2000; Silk, 2009).

Previous approaches to understanding the neural network mechanisms of social cognition were limited for several reasons. First, social interactions span a wide range, from pairs of animals engaged in mating, grooming, and social communication to groups of animals engaged in complex cooperative interactions, such as collective foraging, in large open-field environments. What these interactions have in common is that animals are freely moving to

produce naturalistic, and often complex, patterns of behavior underpinning social interactions. Unfortunately, because of technical limitations, neural recordings in freely moving animals coupled with advanced behavioral monitoring have been extremely rare until now. Importantly, in those rare situations when neural responses were compared in restrained vs. unrestrained and naturalistic conditions, they were found to exhibit marked differences. For instance, the responses of visual cortical neurons were stronger, sparser, and more selective when stimuli were natural and animals were moving (Niell & Stryker, 2010; Tang et al., 2018; Vinck et al., 2015; Vinje & Gallant, 2000; Walker et al., 2019). Additionally, the same prefrontal cortical neurons generated different responses to vocalizations that were produced from a restrained or unrestrained animal during naturalistic communication (Jovanovic et al., 2022; McMahon et al., 2015). Third, merely rewarding restrained animals in non-effortful body-restrained tasks fails to generate the same (necessary) behaviors that more effortful tasks do, such as needing to make dozens of partner-coordinated responses in each trial (van Wolkenten et al., 2007). Hence, previous studies in non-effortful tasks were unlikely to address the full complexity and the most important aspects of social interactions.

Despite a cost of experimental control, recent work emphasizes the importance of studying the neurobiology of social interactions in more ecologically valid and naturalistic environments (Fan et al., 2021; C. T. Miller et al., 2022; Wallace & Hofmann, 2021). Technological advancements now enable the wireless recording of oculomotor and neural signals simultaneously with behavioral monitoring. While traditional restrained-animal paradigms provided the first steps towards understanding the neural basis of social cognition, designing experiments where behavioral diversity is permitted and not divorced from the dynamic context in which it naturally occurs is necessary to further understand the operation of neural circuits underlying social behavior (Fan et al., 2021; C. T. Miller et al., 2022).

#### **1.4 The present study – overview, aims, and hypotheses**

A fundamental goal in neuroscience has been to identify and understand neural computations that support natural behavior, such as social interaction. Research in the past decade discovered representations of social variables, including reward value (Aquino et al., 2020; Chang et al., 2013; Grabenhorst et al., 2019; Noritake et al., 2018), actions (Falcone et al., 2016; Haroush & Williams, 2015; Jamali et al., 2021; Rose et al., 2021), agent identity (Báez-Mendoza et al., 2021; Rose et al., 2021), and social rank (Kingsbury et al., 2019; Li et al., 2022; Padilla-Coreano et al., 2022), across many brain regions. However, they did not attempt to examine the neural processes that mediate the emergence of visually-guided social decision making during the learning of cooperation. Studies examining the neural underpinnings of social behavior have typically been performed with stationary animals performing passive or unnatural tasks using synthetic stimuli. Technical limitations have prevented the simultaneous recording of neural signals and visual cues from freely viewing and moving agents during social interactions.

Indeed, understanding how neurons in the brain represent learning of complex and effortful behaviors like cooperation has been challenging. This inspired me to investigate two important but unresolved questions in social neuroscience: 1) What are the behaviors and neural computations that promote cooperation, and 2) how do these behavioral and neural features change over time during *learning to cooperate*? Social interactions, including cooperation, rely heavily on visualizing social cues from the environment, such as the reward for cooperating and the partner's actions. In this study, to examine which social cues are encoded during learning cooperation and how they influence decision-making, I simultaneously record eye-tracking and neural population activity from a cortical network incorporating two regions - one that processes visual features (midlevel visual cortex, V4) and an executive region that processes social information (dlPFC). Critically, despite a cost of experimental control, recent work encourages an experimental paradigm shift to examine the neurobiology of social interactions in more ecologically valid and naturalistic environments (Fan et al., 2021; C. T. Miller et al., 2022; Wallace

& Hofmann, 2021). Here, the Dragoi lab and I acknowledged this call and created an ethologically relevant experimental regime for investigating neural mechanisms of learning cooperation in freely moving and behaving non-human primates. Our experiments are categorized as Level 4 out of 5 on the naturalism scale (1-5, from less to most naturalistic) as they include real-life social stimuli in a laboratory environment (Fan et al., 2021).

Harnessing the flexible and dynamic power of wireless neural and eye tracking recordings combined with markerless behavioral tracking (Mathis et al., 2018), I examine how macaque dyads learn to cooperate for a food reward, identify the visual cues used to guide decision-making, and discover their representations in a visual-social cortical pathway in the primate brain. My working hypothesis is learning social interactions will induce changes in 1) the encoding of social variables such as visual-social cues and choice within areas and 2) spike timing coordination between areas. These experiments can identify behavioral strategies used in social cooperation and will elucidate the functional role of visual and frontal brain areas, revealing new and alternative targets for therapies to improve social dysfunction in individuals with a variety of neuropsychiatric disorders. Overall, this research will contribute to understanding visuo-frontal cortical circuits that enable flexible, social behavior in an increasingly social world.

**Chapter 1 (current chapter):** provides background information about social behavior, social learning, the brain regions that support social cognition, and approaches used to answer questions about social behavior. These topics are referred to in the latter chapters of this dissertation.

**Chapter 2 | Aim 1:** Identifies changes in animals' actions and viewing behaviors during learning social cooperation.

**Chapter 3 | Aim 2:** Identifies neural correlates of learning social cooperation within each cortical area, including how social events are encoded and how individual neurons contribute to encoding of social events during learning cooperation.

**Chapter 4 | Aim 3:** Examines how learning social cooperation changes neural interactions between cortical areas.

**Chapter 5:** Summarizes the results from chapters 2-4 and considers these findings in the context of current research. It examines the constraints of the experiments and evaluates applicability of the findings to the wider community.

## **CHAPTER 2: VIEWING SOCIAL CUES DRIVES COOPERATION DURING LEARNING**

### ***2.1 Background***

Rhesus macaques cooperate for food acquisition in natural and laboratory environments (Mendres & FB, 2000; Mesterton-gibbons & Dugatkin, 1997; Molesti & Majolo, 2016; Silk, 2009; Visco-Comandini et al., 2015). The neural correlates of the decision to cooperate or defect in NHPs has previously been studied using game theory in economics, including the prisoner's dilemma (Haroush & Williams, 2015), and variants of the chicken game (Ong et al., 2020). In these experiments, animals were restrained and viewed synthetic stimuli on a monitor to determine when to cooperate. Therefore, our understanding of how social actions are guided by sensory information in a continuous, unrestrained social environment remains woefully lacking.

Animals exchange multiple sensory modalities, especially visual cues, to determine whether to explore, mate, compete, or cooperate with a conspecific. For example, primates, including rhesus macaques, spend much of their time looking at other individuals, especially at their faces and eyes (Emery, 2000; Nahm et al., 1997). This attention directed at the eyes often seems to be used to assess where an individual is looking, and many primate species will spontaneously orient to where other individuals are looking (Emery et al., 1997). Despite the clear role of behavioral cues in social interactions, few visual neurobiological studies focus on how socially relevant stimuli and stimulus features are processed by the brain. Furthermore, how animals' actions and viewing behaviors develop and change while learning cooperation has never been studied. Therefore, I use our lab's innovative and comprehensive approach to

investigate eye tracking and behavioral development from two monkeys while they learn to cooperate.

## **2.2 Methods**

### *2.2.1 Animals*

All experiments were performed under protocols approved by The University of Texas at Houston Animal Care and Use Committee (AWC) and the Institutional Animal Care and Use Committee (IACUC) for the University of Texas Health Science Center at Houston (UTHealth). Four adult male rhesus monkeys (*Macaca mulatta*; selfM1: 10 kg, 11 years old; partM1: 12 kg, 10 years old; selfM2: 14 kg, 12 years old; partM2: 12 kg, 16 years old) were used in the experiments.

### *2.2.2 Social cooperation task*

Two unique and familiar pairs of macaques learned to cooperate for food reward across weeks. Due to macaque's natural social hierarchy, each pair consisted of a subordinate ("self") and dominant monkey ("partner"). Animals cooperated in an arena, separated by a clear divider, so they could visually, but not physically, interact. The cooperation arena measured 7' x 4 x 3' (LxWxH) and was constructed out of pvc piping, plastic, and plexiglass. Each monkey could freely move around his side and each monkey had his own push button. At the start of a trial, perceivable but remote pellets dispensed in animal's respective trays, and animals could cooperate at any time by simultaneously pushing and holding individual buttons which moved their trays, delivering reward to each animal (**Fig. 1**). A trial begins when pellets dispense and ends when the trays reach the animals. Animals were acclimated to the arena and button before beginning social learning experiments. Buttons in the arena were strategically placed next to the clear divider so that monkeys could easily see each other's actions.

Each animal's tray contained his own amount of food reward (banana flavored pellet; not accessible by the other monkey), and the trays moved together at the same speed while animals



were simultaneously pressing. If one monkey stops pressing, trays stop at their location on the track, and continue moving forward only when both monkeys began pressing again. We labeled 'intertrial interval' the 20 s period consisting of a 10 s pause after a trial ends, followed by tray movement back to pellet dispensers (~5 s) and another 5 s pause before the next trial begins. Trial durations ranged from 10 seconds to 30 minutes, depending on how long it took for animals to cooperate.

A session, recorded once per day, included 100-130 trials where animals cooperated for one or three pellets each. I recorded 18 learning sessions from monkey pair 1 and 17 sessions from monkey pair 2. As animals performed the experiment, button pressing was recorded from each monkey. Simultaneously, neural and eye tracking data were wirelessly recorded from the subordinate ("self") monkey (**Fig.1**).

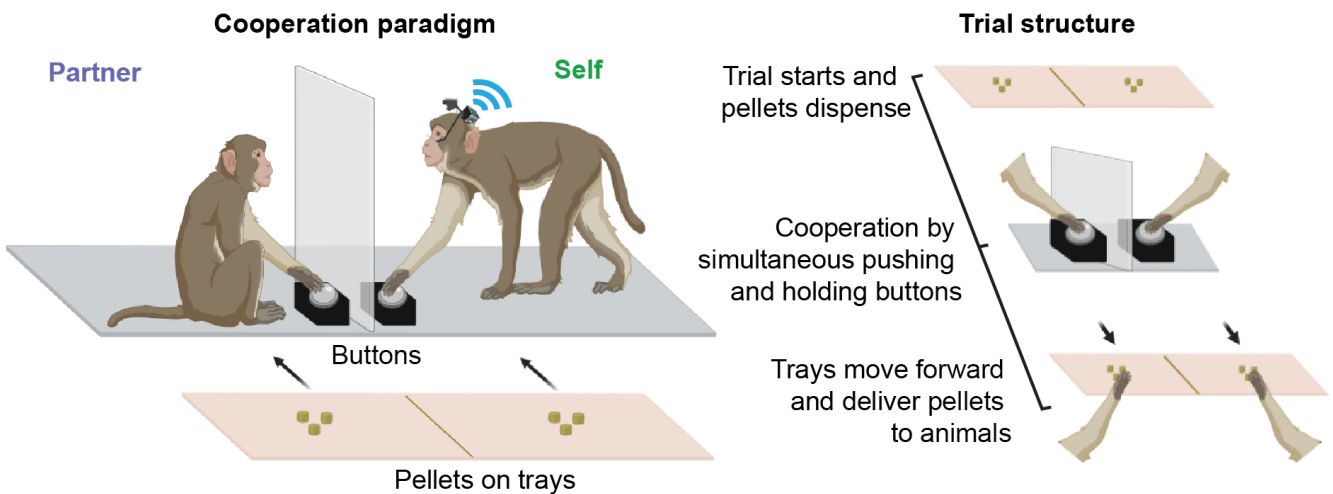


**Figure 1. Social cooperation task.** Two animals learn to cooperate for food. Behaviors were recorded from both animals; eye tracking and neural data recorded from self-monkey. Reward trays are positioned outside the arena. Macaque and graphics were created with BioRender.com

### 2.2.3 Opaque Divider Experiments

After learning cooperation sessions, I recorded opaque divider control sessions where animals completed the cooperation task with an opaque divider separating them, so animals could no longer see each other, but could still hear and smell one another. The opaque divider was a thin (6 mm thickness) piece of plexiglass that was painted in dark gray and cut to the correct dimensions to slide into the arena over the clear plexiglass that already divided the animals (**Fig. 2**). The side of the plexiglass near the buttons was designed to protrude out of the arena to ensure animals could not see each other pressing. Animals were aware the other animal was present as they could hear and smell each other, and they were brought into the experiment room together. I recorded 3 control sessions with the opaque divider from monkey pair 1 and 5 from monkey pair 2. Opaque divider sessions had the same number of trials with the same trial structure as regular learning cooperation experiments.



**Figure 2. Opaque divider experimental setup.** Two animals cooperate for food with an opaque divider between them, which prevents them from seeing each other.

### 2.2.4 Cross-correlation of animals' pushes

Cross correlograms (CCGs) in **Figure 5** were computed using animals' button push sequences occurring across a trial, represented as a series of zeros and ones in 100 ms time bins. For each cooperation trial within a session, push series for each monkey (sequences were of equal length)

were cross-correlated using the *xcorr* function in Matlab 2020b. Coeff normalization was used which normalizes the sequence so that the autocorrelations at zero lag equal 1. The cross-correlations were averaged across trials to create a session cross-correlogram, as plotted in **Figure 5B**. The maximum value, or peak, of each session’s CCG is plotted as the mean coordination for that session, as shown in **Figure 5C**. The time lag at which the peak occurred in each session is the push lag, shown in **Figure 5B**, right. Another “shuffled” analysis was performed for comparison, in which the push sequences derived for each monkey were shuffled randomly in time, for each trial. Trial cross-correlations between animal’s shuffled pushes were calculated and then averaged across trials to create a session CCG of shuffled presses, as shown in **Figure 5B**. As with the actual CCGs, the peak of each session’s shuffled CCG is plotted as the mean coordination for that session and shown in **Figure 5C**.

### 2.2.5 Conditional Probability

For each trial within a session, we computed the conditional probability of cooperating for the self and partner monkey respectively using the equations:

$$P(\text{Self}|\text{Part}) = \frac{P(\text{Self and Part})}{P(\text{Part})} \quad \text{and} \quad P(\text{Part}|\text{Self}) = \frac{P(\text{Self and Part})}{P(\text{Self})}$$

Where P(self|part) is the probability of the self monkey pushing given that his partner is pushing, and P(self and Part) is the probability of the self and partner monkey pushing at the same time (P(self)\*P(partner)). The probabilities were derived from button push sequences for each monkey that were represented as a time series of zeros and ones in 100 ms bins. Conditional probabilities were averaged across trials within a session to create the values plotted in **Figure 6A**.

### 2.2.6 Wireless eye tracking and fixations

We used a custom wireless eye tracker (ISCAN, Inc.) to measure pupil position and diameter from self-monkey during experiments. The portable wireless eye tracker mounted dorsally, right above the animal’s head, consisted of an eye mirror, eye camera for detecting

pupil size and eye position, and scene camera, situated above the eye camera (see also Milton et al., 2020), that records animal's field of view (**Fig. 3A**). All data was recorded at 30 Hz. To train animals to wear the device without damaging it, its 3D geometry was modeled (Sketchup Pro), and dummies were 3D printed and fitted with eye mirrors. To properly position the eye tracker and dummies relative to the eye, custom adapters were designed and 3D printed to attach directly to the animal's headpost and serve as an anchor point for the eye tracker. These adapters were designed to interface with the headpost, without touching the animal directly, to minimize discomfort, and reduce the likelihood of the device being tampered with. These dummy eye trackers were worn by animals for several mock recording sessions to adjust them to wearing

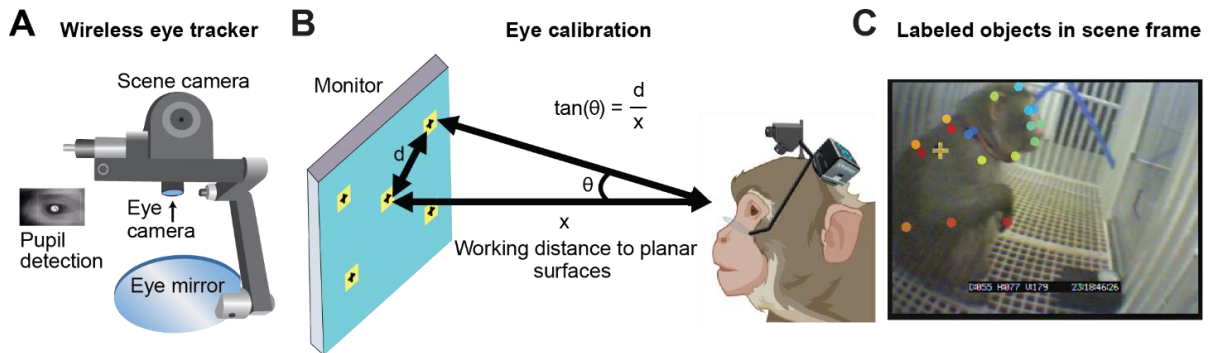


**Figure 3. Wireless eye tracking.** (A) Wireless eye tracker and components. Lower left: image from the eye camera showing tracking of animal's pupil size and eye movements. (B) Eye tracking calibration procedure. As the animal views five points on a monitor, this information is entered into the program (ISCAN Inc.), which projects a crosshair indicating the animal's point of gaze onto scene camera frames. (C) Using the equation in B, pixel space of the scene camera is converted to degrees to identify when objects in the scene camera frames are within the receptive fields of neurons. In this example, the animal's shoulder and upper arm are within receptive fields, which will be important for results in Chapter 4.

the device. Once the animals grew accustomed to wearing the dummy and stopped touching it altogether, the real device was used.

Before each experiment, the eye tracker was secured on the animal and we performed a calibration procedure ('point-of-regard' calibration) while the animal was head-fixed, which mapped the eye position data to the matrix of the head-mounted scene camera (**Fig. 3B**). Animals were trained to view 5 calibration points within the field of view of the scene camera

(640x480 pixel space of a scene camera frame maps to 35x28°, LxH), including a center calibration point and 4 outer points, positioned at  $\pm 8$  to  $\pm 10$  deg with respect to the center (we chose the distance between the animal's eye and calibration monitor based on the approximate range of eye-stimulus distances during free viewing, which was 70 cm). As the animal viewed each point, the eye calibration software synchronizes the eye movement data with the image frames recorded by the scene camera. After calibration, the animal's center of gaze is displayed on each scene camera frame in real time as a crosshair (**Fig. 3C** and **Fig. 8A**). If the animal looks outside the field of view of the scene camera frames, gaze location is not detected, and the crosshair will not appear on the scene camera frames. When this occurs, eye position data is reflected as zero (**Fig. 4A**). Therefore, only scene camera frames that included a crosshair were used in analysis, which mostly occurred (60-85%, **Fig. 4C**). We used the horizontal and vertical coordinates of the pupil to compute eye velocity. To extract fixations, we used velocity-threshold identification to determine the conservative velocity threshold that best separated the bimodal distribution of eye velocities in a session (Salvucci & Goldberg, 2000). A fixation was defined as a minimum 100 ms period when the eye velocity remained below this threshold (**Fig. 4A**). Most (70%) of fixations were 200 ms duration or less (**Fig. 4E**).

### *2.2.7 Behavioral tracking*

I captured a top-down, or overhead, video of the animals during the experiments using COSOOS CCTV LED home surveillance security camera. We recorded overhead and scene camera (wireless eye tracker) videos using the CORENTSC DVR (I.O. Industries). This DVR recorded videos at 30 frames/second and sent pulses to the Blackrock Cerebus neural recording system for every captured frame from each camera, as well as the start and end of video recording. I used the timestamps of these pulses to synchronize overhead video frames to neural and behavioral data. Due to imperfect transmission of wireless eye tracking data, frames were sometimes dropped from the recording. Therefore, to verify the timestamp of each scene camera frame, I used a custom object character recognition software (developed by Sudha Yellapantula,

PhD) to automatically read the timestamp listed on each scene camera frame and align with neural data. Using DeepLabCut, we trained a network to automatically label relevant objects in the frames, such as the crosshair (animal's point of gaze), reward dispensers and trays, each animal's button, and various body parts of the partner monkey including eyes, head, ears, nose, shoulders, limbs, chest, back, face, paws, and butt (**Fig. 3C and 4B**). The DeepLabCut output

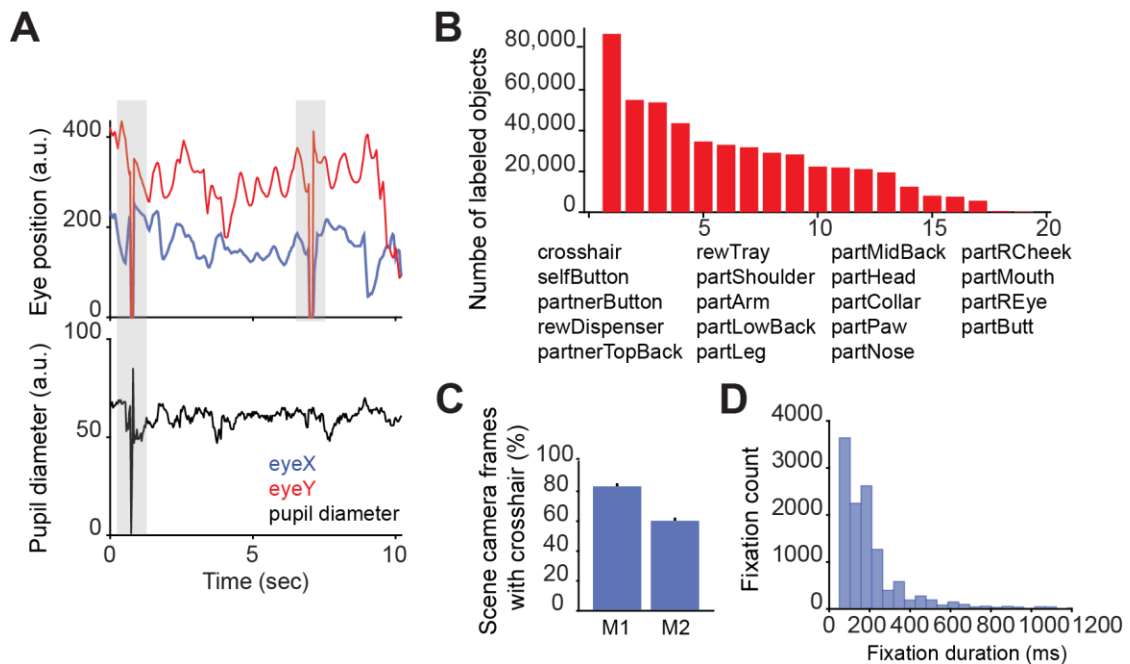


**Figure 4. Viewing statistics.** **(A)** Raw traces of eye x and y coordinates, and pupil diameter recorded with the wireless eye tracker. The zero values at 1 second are due to a blink, while the zero values of x and y coordinates at 7 seconds was due to the animal viewing an object located out of the field of view captured by the scene camera. **(B)** The total amount of objects that DeepLabCut labeled in the scene camera frames from one session, sorted from most to least present. **(C)** The session-averaged percentage of scene camera frames out of the total recorded that contained the crosshair for each monkey. **(D)** Histogram of fixation durations from one representative session that consisted of 12,378 fixations. 70% of the fixations were 200 ms duration or less.

included the location coordinates of all the objects found in the frames. Therefore, I used coordinates of the crosshair and objects to compute proximity and identify when the animal viewed (fixated on) them.

### 2.2.8 Markov Model

To explore interactions between fixation and push events, we used a Markov Model to estimate the transitional probabilities between social events as they occurred in a sequence across a trial, using the function, *hmmestimate* in Matlab2020b. Sequences consisted of 4 events/states: view reward, view partner, self-push and partner push, resulting in 16 event pairs and transitional probabilities. We only included trials where all 4 events occurred, which was on average, 40% of trials per session. For each event pair, transitional probabilities were averaged across trials for a session mean transitional probability, as seen in **Fig. 9A**.

### 2.2.9 Statistics

To assess systematic changes in behavioral and neural metric performance, or learning, I report the P-value from simple linear regression and Pearson's correlation coefficient to report the strength and direction of linear relationship. The percent increase or decrease of behavioral metrics was calculated by the percent change equation,  $C = \frac{x_2 - x_1}{x_1}$ , where C is the relative change,  $x_1$  was the value from session 1, and  $x_2$  is the value from the last session. Changes were then averaged across events or monkeys. When comparing two paired distributions, I used the two-sided Wilcoxon signed-rank test and for comparing two unpaired distributions, I used the Wilcoxon rank sum test. I chose these tests rather than parametric tests, such as the t-test, for their greater statistical power (lower type I and type II errors) when data are not normally distributed.

## 2.3 Results

### 2.3.1 Animals learn to cooperate

To quantify changes in cooperation performance over time, I analyzed features of both animals' actions, such as the coordination of their push onset and duration, the conditional probability of cooperating, and the delay to cooperate. The choice to cooperate, or the animal's response, is the moment the animal pushes and holds its button. Cross-correlation analysis between the button pushes of each monkey (see Methods) in each session revealed that their actions are coordinated and not random (**Fig. 5B**, left: shuffling push times resulted in near zero coincident pushing, red plot). In the first session, for each animal pair, cross-correlograms peaked at 0.6 coincidences, i.e., animals pushed together for 60% of the session, and increased to 80-90% coincident pushing in the last session (**Fig. 5B**, left: blue and gray plots). Indeed, animals learned to cooperate by significantly reducing the amount of time between each of their

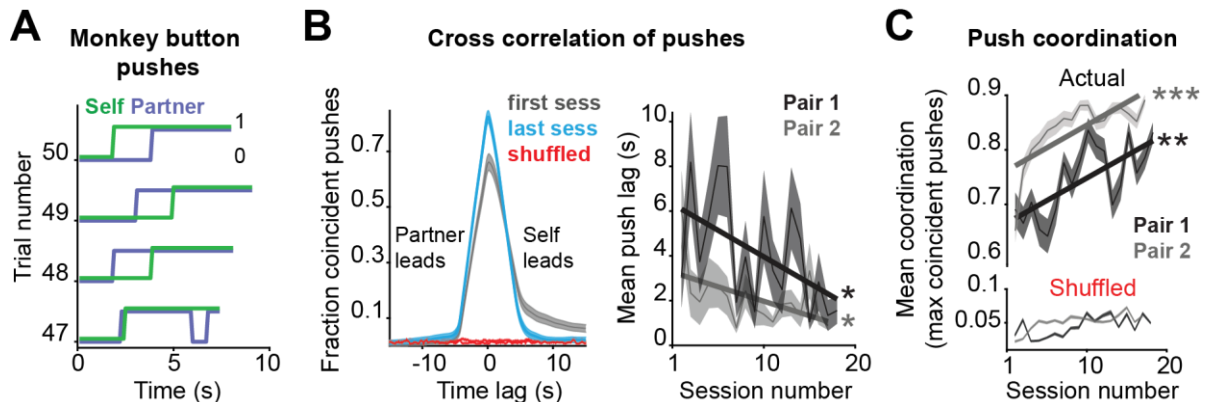


**Figure 5. Action coordination improves during learning.** (A) Example voltage traces of each animal's button push activity from Pair 1. A line increase to 1 indicates a monkey began pushing. (B) Left: example cross-correlograms of Pair 1's button pushes from the first and last session, using actual and shuffled data. Self-monkey lead cooperation more often in early sessions, as the maximum number of coincident pushes occurs at positive time lag (2 sec). Right: session average time lag between pushes when maximum coincident pushes occur. Pair 1  $P = 0.03$  and  $r = -0.5$ ; pair 2  $P = 0.02$  and  $r = -0.5$ , linear regression with Pearson correlation. (C) Session average maximum number of coincident pushes (i.e.: peaks) from cross-correlograms computed with actual and shuffled push data. Pair 1  $P = 0.001$  and  $r = 0.7$ ; pair 2  $P = 0.008$  and  $r = 0.7$ . All  $P$  values are from linear regression and  $r$  is Pearson correlation coefficient. On all plots, center line is mean with shaded SEM. \* $P < 0.05$ , \*\* $P < 0.01$ , \*\*\* $P < 0.001$ .



pushes (**Fig. 5B**: right, all  $P$ s < 0.05, linear regression), thereby improving response coordination across sessions (**Fig. 5B-C**, all  $P$ s < 0.01, linear regression).

Additionally, for each monkey, I computed the probability to cooperate given that the other monkey is pushing. Conditional probability exhibited a mean 54% increase across sessions, thus reflecting learning cooperation (**Fig. 6A**,  $P$  < 0.001, linear regression). Finally, the delay to cooperate, or amount of time it takes for a monkey to respond from trial start, decreased by 93% across sessions, suggesting that animals' motivation to cooperate increases during learning (**Fig. 6B**,  $P$  < 0.05, linear regression). Overall, this demonstrates that animals learned to cooperate across sessions by improving their action coordination, conditional probability, and reaction times.

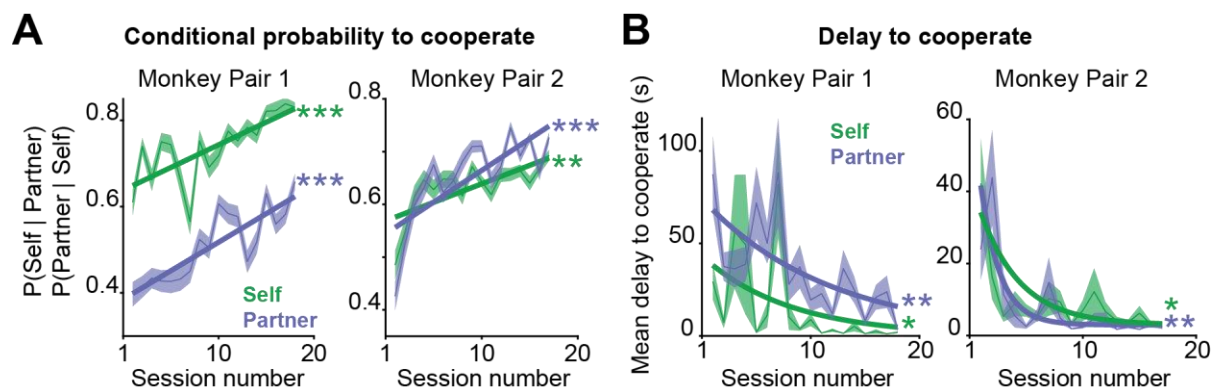


**Figure 6. Conditional probability to cooperate and motivation improves during learning.** (A) Session average conditional probability to cooperate for each monkey. Pair 1  $P = 0.0004$ ,  $r = 0.7$  and  $P = 6.02e^{-6}$ ,  $r = 0.8$ ; pair 2  $P = 0.001$ ,  $r = 0.7$  and  $P = 0.0004$  and  $r = 0.8$ , self and partner respectively. (B) Session average delay to cooperate, or response time, for each monkey. Pair 1  $P = 0.01$ ,  $r = -0.6$  and  $P = 0.001$ ,  $r = -0.6$ ; pair 2  $P = 0.01$ ,  $r = -0.6$  and  $P = 0.006$ ,  $r = -0.6$ , self and partner respectively. All  $P$  values are from linear regression and  $r$  is Pearson correlation coefficient. On all plots, center line is mean with shaded SEM. \* $P$  < 0.05, \*\* $P$  < 0.01, \*\*\* $P$  < 0.001.

### 2.3.2 Viewing the other monkey improves cooperation

In order to examine how the ability for animals to view each other affects cooperation, I completed opaque divider control experiments at the end of learning cooperation sessions in each monkey pair. The first opaque divider session completely confused the animals as they did not even attempt to push after reward dispensed. On the first trial for each animal pair, I had to prompt them. Animals did eventually figure out how to complete trials together without being able to see each other by using the ‘click’ sound of the button when it is pressed. Sometimes one monkey would push down on the button many times to signal his partner to push. Occasionally,

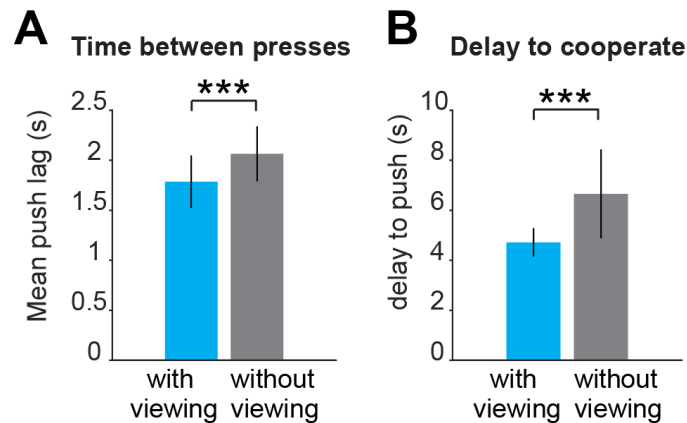


**Figure 7. Disrupting viewing impairs cooperation. (A)** Average amount of time between self and partner monkey presses during learning (‘with viewing’) sessions and control sessions with the opaque divider (‘without viewing’). Times were pooled across sessions (n = 8 sessions for each condition) and averaged across monkeys.  $P = 2.30e-08$ , Wilcoxon rank sum test. **(B)** Average delay to cooperate, or time for both monkeys to be pressing from the start of a trial, during learning (‘with viewing’) sessions and control sessions with the opaque divider (‘without viewing’). Times were pooled across sessions (n = 8 sessions for each condition) and averaged across monkeys.  $P = 4.64e-08$ , Wilcoxon rank sum test.

one monkey would tap his paw on the divider to get his partner’s attention. While macaques do vocalize, they did not produce vocalizations during these experiments and did not appear to use vocalizations to coordinate behavior.

To measure differences in cooperation behavior between the opaque divider (‘without viewing’) and learning (‘with viewing’) session conditions, I calculated the amount of time between each animal’s pushes on every trial as well as the delay to cooperate, or the amount of

time it took for both monkeys to be pushing together from the trial start. I used 3 learning sessions from pair 1 and 5 sessions from pair 2 to match the number of recorded control sessions in each pair. As expected, I found that animals exhibit more time in between pressing and are therefore less coordinated in control sessions (**Fig. 7A**,  $P < 0.001$ , Wilcoxon rank sum test). Additionally, animals take longer to cooperate during the control sessions when they can't see each other (**Fig. 7B**,  $P < 0.001$ , Wilcoxon rank sum test). These results suggest that visualization of the other monkey and his actions improve social cooperation.

### *2.3.3 Animals fixate on the reward and partner monkey the most before cooperation*

To determine which objects were salient for cooperation, I computed the fixation rate on each object during the cooperation trial and during the intertrial interval (objects and fixations shown in **Fig. 8A**). Fixation rates on the reward system (pellet and pellet dispenser) and partner monkey were significantly higher during the trial, particularly before cooperation, when both monkeys begin pushing, than during the intertrial period (**Fig. 8B**,  $P < 0.01$ , Wilcoxon signed-rank test). Therefore, fixations on the reward system ("view reward") and partner monkey ("view partner") constitute 'social cues.' Eye movement analysis revealed behavioral patterns where, at the beginning of a trial, the monkey typically views the reward followed by a push while frequently looking at his partner before partner's push (**Fig. 8C**). This led me to wonder if the relationship between events was changing across sessions during learning.

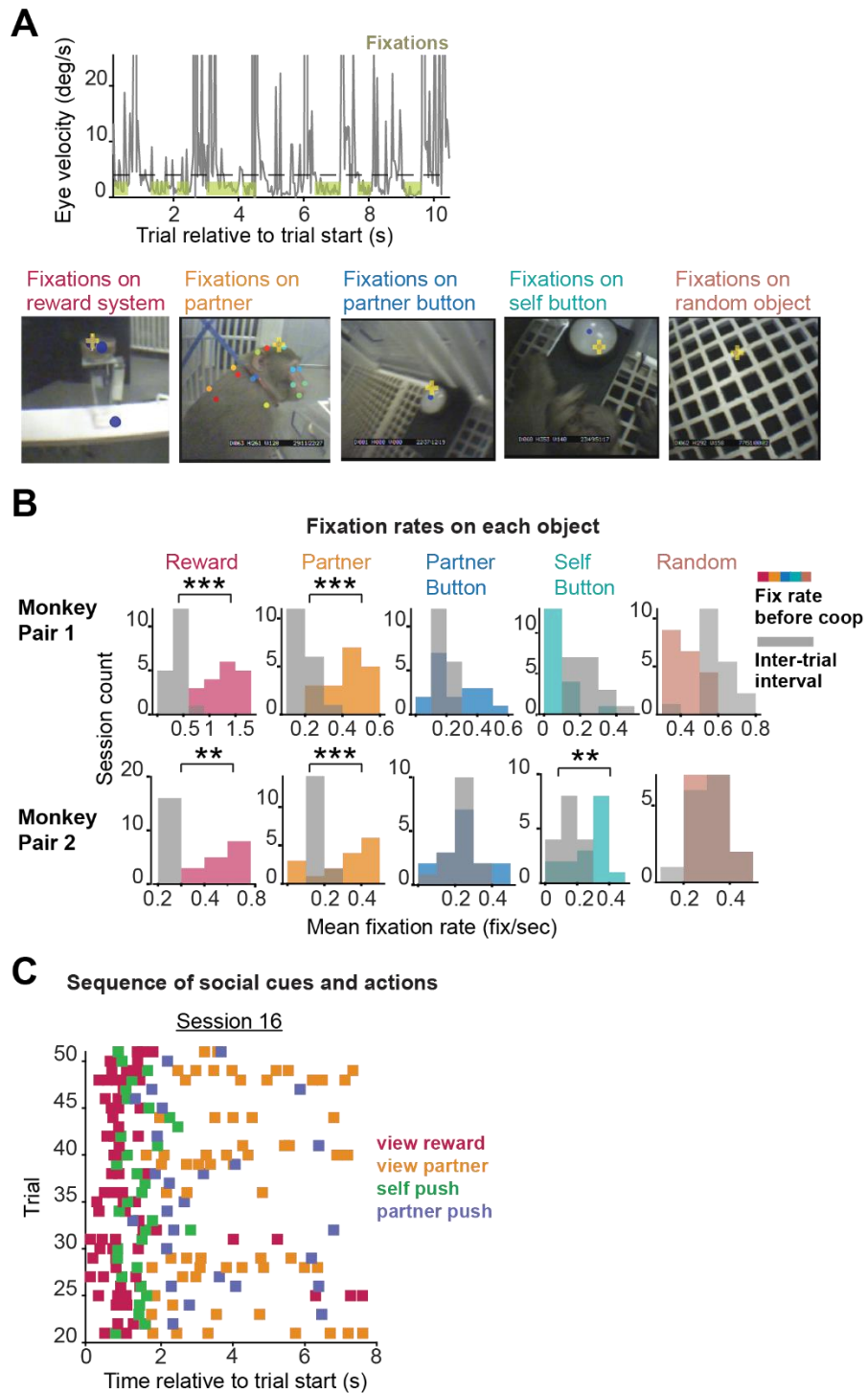
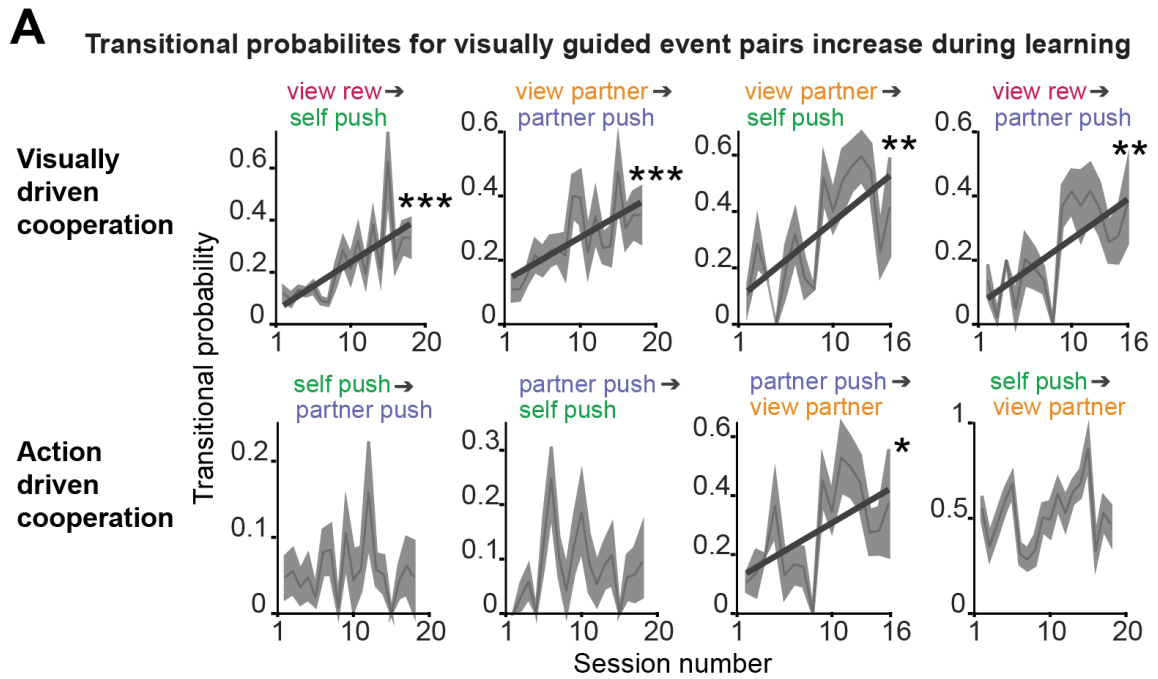


**Figure 8. Identification of social cues. (A)** Left: Fixations, highlighted in yellow, are periods when eye velocity remained below threshold (dashed line) for at least 100ms. Right: Scene camera images of objects the animal viewed, labeled with DeepLabCut (colored dots). Yellow cross represents self-monkey's point of gaze. **(B)** Histograms of session mean fixation rates for each object computed during the trial (before cooperation) and the inter-trial interval. Asterisks represent significance of Wilcoxon signed-rank test, only where fixations rates were higher during cooperation compared to inter-trial period. Pair 1  $P = 0.0002, 0.0002, 0.13, 0.002, \text{ and } 0.0002$ ; pair 2  $P = 0.005, 0.0004, 0.95, 0.001, \text{ and } 0.7$  for fixation rates on objects listed left to right. **(C)**

The sequence of action and viewing events that occur during cooperation across a random subset of trials within a session.

#### *2.3.4 Animals become more likely to cooperate after viewing a social cue*

To examine whether the relationship between social cues and actions changes during learning, I used a Hidden Markov Model to compute the probability of transitioning from one social event, or state, to another. Remarkably, the transitional probabilities between visually driven event pairs, but not action driven ones, significantly increased across sessions while learning to cooperate (**Fig. 9A**, all  $P < 0.01$ , linear regression). The lowest transitional probabilities (0.1) occurred between two actions (self-push to partner-push), indicating that monkeys cannot simply push their button to motivate the other monkey to cooperate (**Fig. 9**). Instead, there were high transitional probabilities (0.6 - 0.9) for event pairs where fixations on a social cue occurred before or after a push (i.e., view partner to self-push or self-push to view partner), thus demonstrating the importance of viewing social cues to promote cooperation (**Fig. 9A**). Indeed, I found a mean 220% increase in transitional probabilities for event pairs beginning with viewing social cues (**Fig. 9A**, top row, all  $P_s < 0.01$ ). These analyses reveal that across sessions, animals become more likely to cooperate after viewing social cues, indicating that fixations on social cues drive cooperation during learning.



**B** Transitions between social events

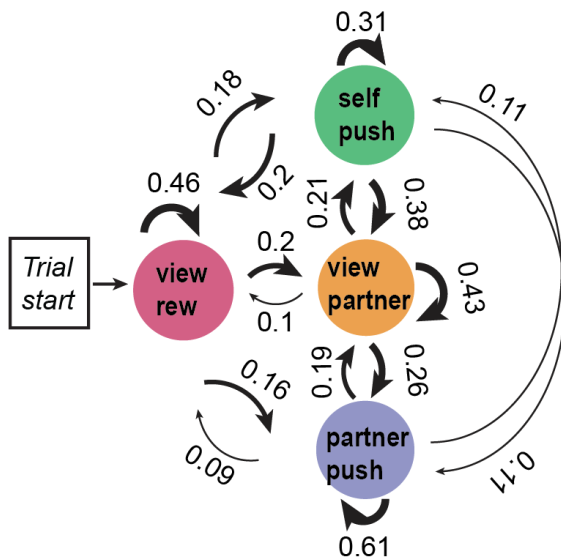


**Figure 9. Relationship between action and viewing behaviors while learning to cooperate.** (A) Markov Model transitional probabilities for example event pairs that begin with a viewing event (top row) or action event (bottom row). Top row:  $P = 0.0008$ ,  $P = 0.0008$ ,  $P = 0.003$ ,  $P = 0.003$ , and all  $r = 0.7$ ; Bottom row:  $P = 0.84$ ,  $0.9$ ,  $0.01$ , and  $0.2$ ;  $r = 0.6$  (partner push to view partner), from left to right, linear regression and Pearson correlation. Four plots, two on each row, came from each monkey pair. (B) Markov Model transitional probabilities averaged across both monkey pairs for all event pairs. \* $P < 0.05$ , \*\* $P < 0.01$ , \*\*\* $P < 0.001$ .

## **2.4 Discussion**

Here, I sought to identify the specific volitional behaviors between two animals that elicit cooperation. To accomplish this, I focused my study on a crucial period in the task: analyzing action and fixation events occurring between the start of a trial and the moment of cooperation (when both animals begin pushing). For the first time, wireless eye tracking and the permission of spontaneous behavior revealed how viewing social cues subserves learning to cooperate in freely moving NHPs. Indeed, a sole cooperating animal could have continuously pushed his button to elicit cooperation from his partner, but this is not the case. Instead, animals increase viewing and attention on social cues - the reward or their partner - to promote desired behavior over time, leading to improved action coordination between animals and reaction times, and thus learning of cooperation.

I always recorded eye tracking from the subordinate monkey, therefore, an interesting question for future studies is exploring whether social cue identity depends on social rank - are the important visual cues for the dominant, partner monkey also fixations on the reward system and his partner? One would expect a difference in social cue identity between social rank, as subordinate animals tend to pay more attention to others and can influence prosocial behavior in dominant partners (Gachomba et al., 2022; Ghazanfar & Santos, 2004; Kingsbury et al., 2019).

Although the monkeys' ability to view each other was obstructed in control experiments, animals were still able to complete cooperation trials and receive reward. This occurred because, while visual information did improve their performance, is it not the only sensory information required for or exchanged during social interactions. For instance, future studies should acquire comprehensive behavioral repertoires from interacting animals to determine exact sequences of behaviors, including viewing, gestures/movements, and vocalizations exchanged between agents that produce social interactions such as cooperating, grooming, or fighting.

Notably, I discovered how one monkey's viewing behavior can influence actions of *either* animal to promote cooperation. Viewing the partner monkey or reward could elicit cooperation

from the self or partner monkey (**Fig. 9**). Indeed, behavioral findings support the notion that viewing social cues is important for social monitoring, such as observing task goals and state of the partner, but also for social predicting, such as predicting when the partner monkey will cooperate, to determine contingent responses and learn cooperation, especially in primate species.

## **CHAPTER 3: POPULATION ENCODING OF SOCIAL EVENTS DURING LEARNING**

### ***3.1 Background***

Although social behavior relies heavily on viewing social cues, neural mechanisms of learning visually guided social interaction are not well known. Previous work has examined neural representations of social variables like reward, facial expressions, and choice in multiple brain regions involved in mentalizing, vicarious reinforcement, empathy, reward processing, and face perception (Chang et al., 2013; Dal Monte et al., 2022; Fogassi & Ferrari, 2011; Mosher et al., 2014; Noritake et al., 2018; Ong et al., 2020; Sliwa & Freiwald, 2017). Despite these efforts, neural activity was not recorded simultaneously from visual and/or executive brain regions during goal-directed behavior where animals could freely generate social decisions based on environmental cues in real time. Therefore, neural computations that underly perception and integration of sensory cues to support social decisions and learning of social interactions remain unknown. To address this gap in knowledge, I record from cortical areas involved in processing visual and social information, V4 and dlPFC. The dlPFC is part of an extensive, interconnected prefrontal network involved in social interactions and learning (Burke et al., 2010; Feng et al., 2021; Gariépy et al., 2014; Suzuki et al., 2012), action planning (Falcone et al., 2016; Yamagata et al., 2012), and perception of visual information (Haile et al., 2019; Rainer et al., 1998). V4 is a well-studied, midlevel visual area that encodes natural images (Okazawa et al., 2015) and a variety of visual features (Kim et al., 2019; Kobatake & Tanaka, 1994; Pasupathy & Connor, 1999; Schein & Desimone, 1990). I investigate my hypothesis by examining the neural encoding



of fixations on social cues and self-and-other decisions in V4 and dlPFC during learning cooperation.

## **3.2 Methods**

### *3.2.1 Wireless electrophysiology*

I chronically and simultaneously recorded from populations of neurons in mid-level visual cortex (area V4) and dorsolateral prefrontal cortex (area dlPFC) of the “self” animal, as these are key areas involved in processing complex visual features (Haile et al., 2019; Kim et al., 2019; Kobatake & Tanaka, 1994; Pasupathy & Connor, 1999, 2002; Russ & Leopold, 2015; Schein & Desimone, 1990; Viswanathan & Nieder, 2013; Wang et al., 2015) and planning social actions (Falcone et al., 2016; Gariépy et al., 2014; Stone et al., 1998; Tanji & Hoshi, 2008). In each monkey ( $n = 2$ ), I used Utah arrays to stably record from the same neural population (averaging 136 units/session in M1 and 150 units/session in M2, including single and multi-units; M1: 34 V4 cells, 102 dlPFC cells; M2: 104 V4 cells, 46 dlPFC cells) across multiple sessions (Dickey et al., 2009) (**Fig. 10** and **Fig. 12**).

After acclimatization and behavioral training (described in previous section), animals were implanted with a 64-channel dual Utah array in the left hemisphere dlPFC (anterior of the arcuate sulcus and dorsal of the principal sulcus), left V4 (ventrally anterior to lunate sulcus and posterior to superior temporal sulcus), and a pedestal on the caudal skull (Blackrock Microsystems). I used Brainsight, a neuronavigational system, and animal’s MRIs to determine the location for V4 and dlPFC craniotomies (Rogue Research). During surgery, visual identification of arcuate and principal sulci guided precise implantation of arrays into the dlPFC, and visual identification of the lunate and superior temporal sulci supported array placement in area V4. The dura was sutured over each array and two reference wires were placed above the dura mater and under the bone flap. Bone flaps from craniotomies were secured over the arrays using titanium bridges and screws. After the implant, the electrical contacts on the pedestal were always protected using

a plastic cap except during the experiment. Following array implantation, animals had a 3-week recovery period before recording from the arrays.

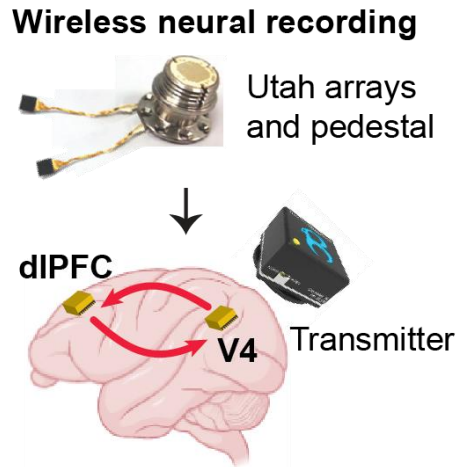


**Figure 10. Wireless neural recording methods.** Recording equipment. Two, 64-channel Utah arrays (gold squares) are attached to a pedestal. Red arrows represent the feedforward and feedback processing of information between areas. The wireless transmitter connects to the pedestal and transmits neural data recorded from each array.

To record the activity of neurons while minimizing interference with the animal's behavior, I used a lightweight, rechargeable battery-powered device (Cereplex-W, Blackrock Microsystems) that communicates wirelessly with a central amplifier and digital processor (Cerebus Neural signal processor, Blackrock Microsystems). First, the monkey was head-fixed, the protective cap of the array's pedestal was removed, and the wireless transmitter was screwed to the pedestal. The neural activity was recorded in the head-fixed position for 10 minutes to ensure the quality of the signal before releasing the monkey in the experimental arena. The arena was surrounded by eight antennas. Spikes from each brain area were recorded simultaneously at 30 kHz and detected online (Cerebus neural signal processor, Blackrock Microsystems) using a manually selected upper and lower threshold on the amplitude of the recorded signal in each channel. This thresholding was also helpful to eliminate noise from the animal chewing. I also eliminated noise using the software's automatic thresholding which was  $\pm 6.25$  times the standard deviation of the raw signal. The on-site digitization in the wireless device showed lower noise

than common wired head-stages. The remaining noise from the animal's movements and muscle activity was removed offline using the automatic algorithms in Offline Sorter (Plexon Inc.). Briefly, this was done by removing the outliers (outlier threshold = 4-5 standard deviations) in a 3-dimensional space that was formed by the first three principal components of the spike waveforms. Then, the principal components were used to sort single units using the k-means clustering algorithm. Each signal was then automatically evaluated and manually checked as multi or single unit using several criteria: consistent spike waveforms, waveform shape (slope, amplitude, trough-to-peak), and exponentially decaying ISI histogram with no ISI shorter than the refractory period (1 ms). The analyses here used all single and multiunit activity.

### *3.2.2 Receptive field mapping*

I identified receptive fields (RFs) of recorded neurons in a head-fixed task where the animal was trained to maintain fixation during stimulus presentation on a monitor. Neural activity was recorded and thresholded using a wired head-stage and recording system, alike the methods described above in *wireless electrophysiology* (Cerebus Neural signal processor, Blackrock Microsystems). I divided the right visual field into a 3 × 3 grid consisting of nine squares with each square covering 8° × 8° of visual space. The entire grid covered 24° × 24° of visual space. Each of the nine squares was further subdivided into a 6 × 6 grid. In each trial, one of the nine squares was randomly chosen, and the RF mapping stimuli were presented at each of the 36 locations in a random order. The RF mapping stimuli consisted of a reverse correlation movie with red, blue, green, and white patches (~1.33° each). A complete RF session is composed of 10 presentations of the RF mapping stimuli in each of the nine squares forming the 3 × 3 grid. I averaged the responses over multiple presentations to generate

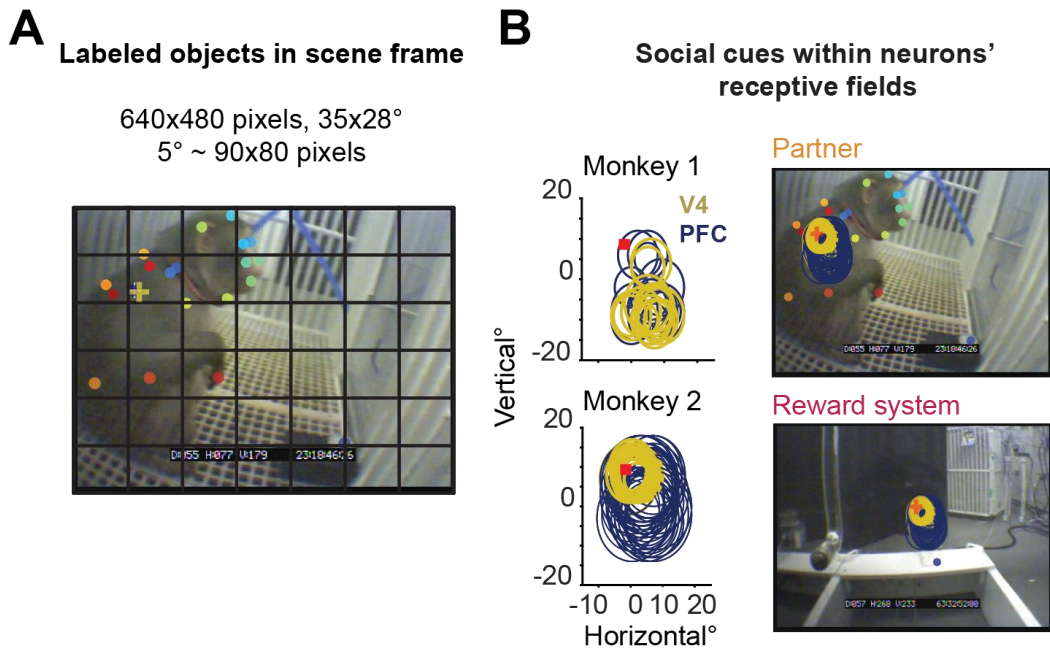


**Figure 11. Identification of stimuli within neurons' receptive fields.** (A) Using the equation in Fig. 3B, pixel space of the scene camera is converted to degrees to identify when objects in the scene camera frames are within the receptive fields of neurons. In this example, the animal's shoulder and upper arm are within receptive fields. (B) Left: Overlapping receptive fields (RF) of V4 and dIPFC neurons, identified in head-fixed recordings. V4 RF sizes: 4-6 deg; dIPFC RF sizes: 6-13 deg. Red square represents the point of fixation. Right: Scene camera images, measuring 35 x 28 degrees (LxH), where social cues were within receptive fields of recorded neurons during a fixation.

RF heatmaps and corresponding receptive field plots (as shown in **Fig. 11B**). Since recorded units remained stable across days, RF mapping was done prior to starting learning sessions, and performed once every month during recordings.

Similar to the behavioral tracking methods in chapter 2 (2.2.7), I trained a network in DeepLabCut, an markerless pose estimation software, to automatically label relevant objects in the frames, such as the crosshair, reward dispensers and trays, each animal's button, and various body parts of the partner monkey including eyes, head, ears, nose, shoulders, limbs, chest, back, face, paws, and butt (**Fig. 4B and 11A**). The DeepLabCut output included the location coordinates of all the objects found in the frames. Therefore, I used a degree-to-pixel conversion and the coordinates from the crosshair and object labels to identify which objects were in the receptive fields of the neurons in any given frame during a fixation (**Fig. 11 and 3B**,  $5^\circ = 90 \times 80$  pixels, based on the equation  $Tan\theta = d \div x$ , where  $d$  is the measured length and

height of the scene camera frame when viewing from distance  $x$ ). Finally, to compute body, torso, and limb velocity (movement) of the animal, as shown in **Figures 21-22**, I used DeepLabCut to label body parts of the self-monkey in the overhead camera frames. Head movements included labels from the center of the head, snout, and each ear. Limb movement was computed from the shoulder, elbow, and paw labels. Torso movement was calculated from the animal's upper and mid back labels.

### 3.2.3 Identifying stable units across sessions

I used principal component analysis (PCA) of waveforms from each session to identify consistent waveforms across sessions. First, we performed PCA on a matrix of 100 samples of waveforms of single and multi-units from every session using the *pca* function in Matlab 2020b. Then, for each session, I used the first 7 components of the principal component coefficients to compute the Mahalanobis distance (MD) between distributions of all waveforms for each combination of cell pairs within that session. Mahalanobis distance between two objects in a multi-dimensional vector space quantifies the similarity between their features as measured by their vector components. It takes into account the covariance along each dimension (Mahalanobis, n.d.). MD between two clusters of spike waveforms A and B belonging to a pair of neurons in 7-dimensional vector space was computed using the following formula:

$$MD = \sqrt{((A - B)^T V^{-1} (A - B))} ,$$

where T represents the transpose operation and  $V^{-1}$  is the inverse of the covariance matrix, and A and B are the first 7 components of the principal component coefficients for each neuron in the pair. Importantly, because this analysis was performed among cell pairs within a session, this distribution reflects the Mahalanobis distances for distinct, individual cells. I combined the distances across sessions to create one distribution and used this to identify a waveform threshold, which was the 5<sup>th</sup> percentile of the distribution. Therefore, Mahalanobis distances

between waveforms of cell pairs that are less than the threshold reflect waveform distributions that belong to the same neuron.

Then, for each channel (electrode), I computed MD using PCA waveform coefficients from all the neurons identified on that channel across all sessions. Some channels recorded 2 units each day, while others did not record any isolated SUA or MUA activity. 96 electrodes were recorded from each subject's brain, however, electrodes without single or multi units for at least 10 (i.e. half) of the learning sessions were not used in the analysis. Analysis included 90 total electrodes from M1 and 86 total electrodes from M2. MD values that were less than the threshold represented stable units, and cell pairs whose MD was above threshold indicated that the same

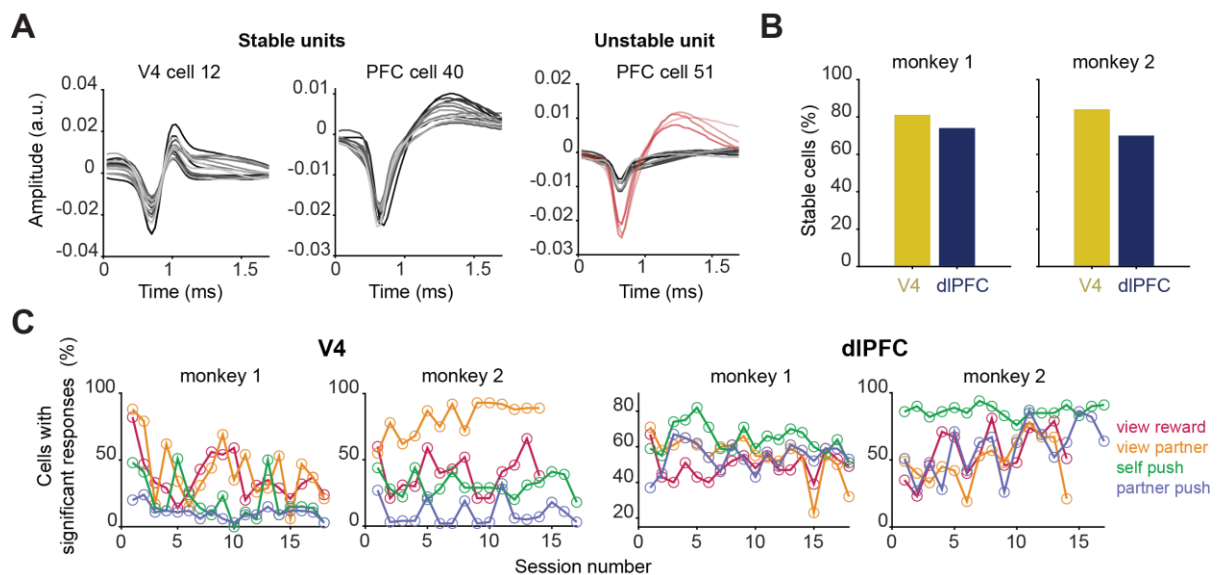


**Figure 12. Neural population stability.** (A) Example electrode channels from one monkey showing waveforms from a single unit recorded on that channel across sessions. Each waveform represents the average waveform of that unit from one session, with session one plotted in a dark color and increasing in transparency across sessions. The unstable unit shows a channel with waveforms that represent stable MUA (Black) and unstable SUA (red), as the single unit was only present for 4 out of the 18 sessions. (B) The number of stable cells divided by the total number of cells is the percentage of stable units in each area for each monkey. In monkey 1, 81% of recorded units (508/620 neurons) in V4 and 74% of recorded units in dIPFC (1362/1837 neurons) were consistent across sessions. In monkey 2, 84% of recorded units in V4 (1489/1773 neurons) and 70% of recorded units in dIPFC (560/794 neurons) were consistent. (C) For each brain region, the percentage of cells out of the total recorded per session (M1: 34 V4 cells, 102 dIPFC cells; M2: 104 V4 cells, 46 dIPFC cells) that exhibited a statistically significant change in firing rate from baseline (intertrial interval firing rate) during social events (as shown in Fig. 3E but plotted across sessions for each monkey). For each cell,  $P < 0.01$  Wilcoxon signed-rank test with FDR correction. The percentage of responding cells does not systematically change across sessions.

neuron was not recorded across both days/sessions. Channels with stable units and a channel with stable MUA but unstable SUA are shown in **Figure 12A**. The number of stable cells divided by the total number of cells is the percentage of stable units in each area for each monkey, as shown in **Figure 12B**. In monkey 1, 81% of recorded units (508/620) in V4 and 74% of recorded units in dlPFC (1362/1837) were consistent across sessions. In monkey 2, 84% of recorded units in V4 (1489/1773) and 70% of recorded units in dlPFC (560/794) were consistent (**Fig 12B**). Overall, my analysis yields results comparable to other electrophysiological studies with Utah array recordings who also found that chronically implanted Utah arrays typically record from the same neurons across days and months (Dickey et al., 2009; Fernandez-Leon et al., 2015; Luo & Maunsell, 2018).

#### *3.2.4 Neural firing rate and response*

I identified four salient events for cooperation: fixations on the reward, fixations on the partner monkey, self-pushes, and partner pushes. On average, there were 826 fixations on the reward, 936 fixations on the partner, 116 self-pushes, and 43 partner pushes per session for each animal pair. To determine if a cell was significantly responding to one or more of these events, I compared the firing rate in a baseline period (intertrial time, specifically 4.5 seconds before trial start) to the event onset using a Wilcoxon signed-rank test followed by FDR correction. Specifically, for each neuron I calculated its firing rate (20 ms bins) occurring 130 ms after fixation onset that accounted for visual delay (60 ms for V4 neurons and 80 ms for dlPFC). I chose this window as the fixation response period since most of the fixations were 100 – 200 ms in duration (**Fig. 4D**). For self and partner push, I chose 1000 ms before push onset as the response period since firing rates began to significantly increase during this time. For partner pushes on 'partner lead' trials only (**Fig. 13A**), I used 500 ms before and 500 ms after the push, since the self-monkey viewed him after this push (**Fig. 13A**, also trays were not moving as self-monkey was not pushing yet on these types of observations). Neural activity occurring between the moment trays began moving and the end of a trial was never used in any analysis in this

study. For each neuron, response firing rates were compared to baseline firing rates that were computed across the same duration as social event responses (130 ms for fixations and 1000 ms for pushes). The percentage of neurons responding to social events did not systematically differ across sessions (**Fig. 12C**).

### 3.2.5 Support vector machine decoder

I used a support vector machine decoder (Bishop, n.d.) with a linear kernel to determine whether the population firing rates in V4 or dlPFC carry information about visual stimuli and/or decision-making (**Fig. 16-20**). Specifically, I computed the mean firing rates of each neuron in the population for the response period (described above) in each observation of fixations or pushes (multiple observations of any social event could occur within one trial), and then classified binary labels specifying the event (for example, fixations on reward were class one, fixations on partner were class two) from neural responses. For each session, the number of fixations or pushes were always balanced across classes. Random selections of class observations were repeated for 100 permutations, giving the average classification accuracy over 1000 test splits of the data, for each session. To train and test the model, I used a 10-fold cross-validation. Briefly, the data was split into 10 subsets and in each iteration the training consisted of a different 90% subset of the data and the testing was done with the remaining 10% of the data. I utilized the default hyperparameters as defined in *fitcsvm*, MATLAB 2020b. Decoder performance was calculated as the percentage of correctly classified test trials. In each session and iteration, I trained a separate decoder with randomly shuffled class labels. The performance of the shuffled decoder was used as a null hypothesis for the statistical test of decoder performance (**Fig. 16-20**). For improved data visualization in **Fig. 16-18**, I plotted the shuffle-corrected decoder accuracy (actual – shuffled decoder performance), but learning trends remain even when only the actual decoder accuracy is evaluated.

For **Figure 16A-C** analyses, 14 sessions were analyzed from pair 2 due to an inadequate number of fixations on the stimuli in 3 out of the 17 sessions. Similarly, for **Figure 16B**, only 16



sessions were included in the analysis because Monkey 1 did not fixate on self-button during 2 sessions. Sessions with less than 30 fixations were not included in any neural analyses. For the analysis in **Figure 20C**, the number of observations for each class matched for “with cue” and “without cue” to enable fair comparison of decoder performance across conditions. In each session, for comparing feature weights across sessions (**Fig. 19**) and of correlated and non-correlated V4 and dlPFC neurons (**Fig. 26**), I first normalized weights across the entire population of neurons, using the equation below where  $W_o$  is the current cell weight divided by the square root of the sum of all the squared weights in the population (Koren, 2021). Finally, the absolute values of weights were averaged across neurons within each session for each monkey, then combined to create the distributions seen in **Fig. 26**.

$$normalized\ weight = \frac{W_o}{\sqrt{W_1^2 + W_2^2 + \dots + W_n^2}}$$

### 3.2.6 Solo-and-social control experiments

Solo-and-social control experiments occurred after learning experiments and included periods of solo trials where self-monkey was alone in the arena, pellets dispensed only in his tray, and he pushed his button to deliver reward. Another monkey was brought into the room for social trials and social periods behaved as the usual task. Solo-and-social sessions included 60 solo and 60 social trials, conducted in blocks to control for changes in neural recording quality within a session: 30 social trials – 60 solo trials – 30 social trials were performed, and this sequence of trial types alternated from day to day.

### 3.2.7 Statistics

To assess systematic changes in behavioral and neural metric performance, or learning, I report the P-value from simple linear regression and Pearson’s correlation coefficient to report the strength and direction of linear relationship. The percent increase or decrease of behavioral and neural metrics was calculated by the percent change equation,  $C = \frac{x_2 - x_1}{x_1}$ , where C is the relative

change,  $x_1$  was the value from session 1, and  $x_2$  is the value from the last session. Changes were then averaged across events or monkeys. For comparing two paired groups such as a cell's firing rate during an event and baseline period, I used the two-sided Wilcoxon signed-rank test. I chose this test rather than parametric tests, such as the t-test, for its greater statistical power (lower type I and type II errors) when data are not normally distributed. When multiple groups of data were tested, I used the False Discovery Rate multiple comparisons correction (Benjamini & Hochberg, 1995) whose implementation is a standard function in Matlab. When comparing two unpaired distributions, I used the Wilcoxon rank sum test.

### **3.3 Results**

#### *3.3.1 Single cells respond to social cues and actions*

I investigated the relationship between neural signals and social events leading to cooperation by analyzing the neural responses between the start of the trial and cooperation onset when both animals begin pushing. I identified fixations on social cues and non-social objects (i.e., monkey's buttons or arena floor) within the receptive fields of the recorded neurons (**Fig. 11B** and Methods). Neurons in both cortical areas significantly increased firing rates in response to fixations on social cues compared to baseline measured during the intertrial interval (**Fig. 14-15**,  $P < 0.01$ , Wilcoxon signed-rank test with False Discovery Rate, FDR, correction). A distinct feature of 'social brain' areas is the ability to process information about one's self and other (Haroush & Williams, 2015; Jamali et al., 2021; Kingsbury et al., 2019; Ong et al., 2020; Padilla-Coreano et al., 2022; Rose et al., 2021). I explored this feature by identifying self and partner monkey pushes, or decisions to cooperate, that occurred separately in time ( $> 1$  s from each other, **Fig. 13A**). Importantly, I hypothesized that self-monkey's neurons process allocentric information during partner choice, since he views the partner during most of partner's pushes, but not during his

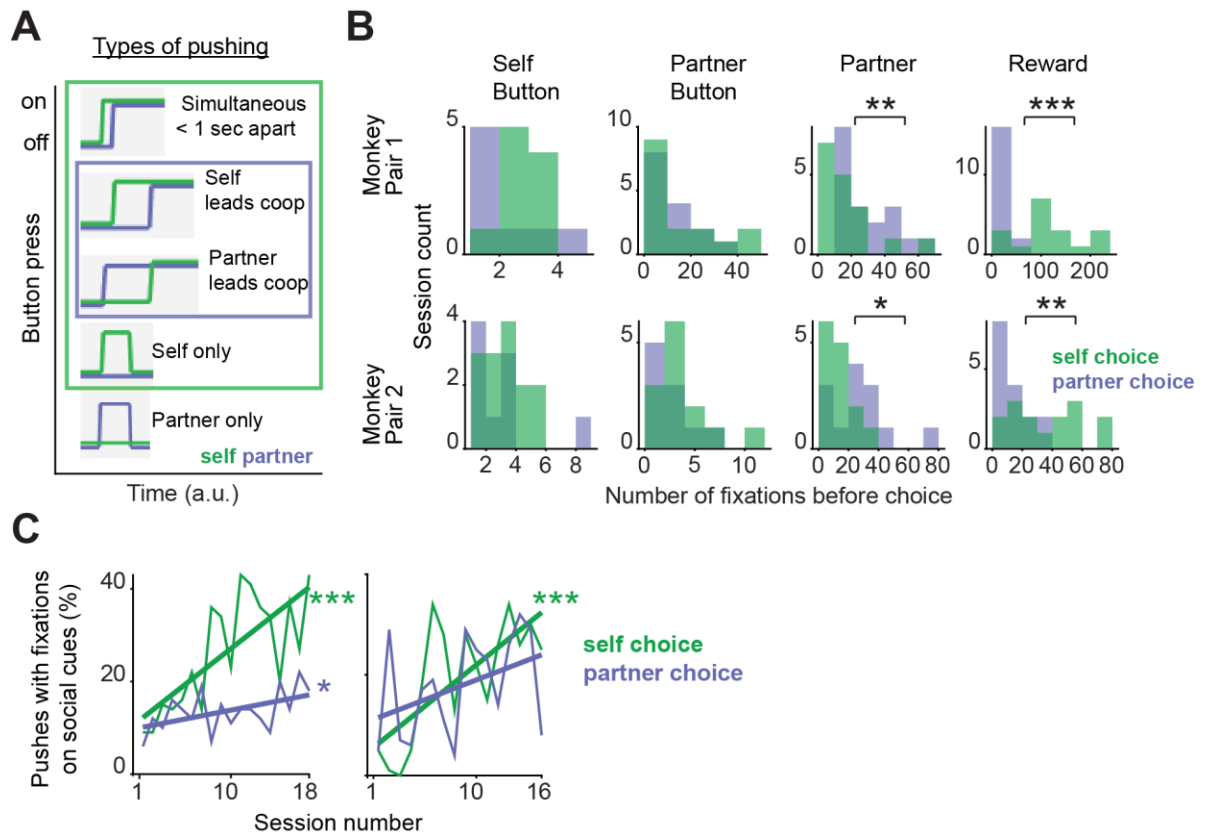


**Figure 13. Viewing behavior during pushing. (A)** Self and partner pushes consisted of push types that occurred in their respective outlined boxes. ‘Partner only’ pushes rarely occurred and were not used in analysis. For total number of pushes, see Methods 3.2.4: *Neural firing rate and response*. **(B)** The distribution of the number fixations on each object that occurred before (1000 ms pre) self and partner (1000 ms pre 500 ms post) pushes in each session. There are more fixations on the partner monkey before the partner pushes than self, and there are more fixations on the reward before the self-monkey pushes than partner. Pair 1 P Values: 0.005 and  $5.79e^{-5}$ , Pair 2 P values: 0.03 and 0.003, Wilcoxon rank sum test, \* $P < 0.05$ , \*\* $P < 0.01$ , \*\*\* $P < 0.001$ . **(C)** For each animal pair, the percentage of self and partner pushes where fixations on the partner and/or reward system occurred within 1000 ms of choice in each session. Pair 1  $P = 0.0003$ ,  $r = 0.7$  and  $P = 0.03$ ,  $r = 0.5$ ; pair 2  $P = 0.0005$ ,  $r = 0.8$  and  $P = 0.06$ ,  $r = 0.4$ , self and partner choice respectively, linear regression and Pearson correlation.

own push (**Fig. 13B**). I find that self-monkey typically fixates on the reward before his own push and fixates on the partner monkey before partner pushes (**Fig. 13B**). Over time, the self-monkey increased viewing of social cues (reward or partner) before pushing, indicating that viewing social cues informs decision-making as learning emerges (**Fig. 13C**,  $P < 0.05$ , linear regression).

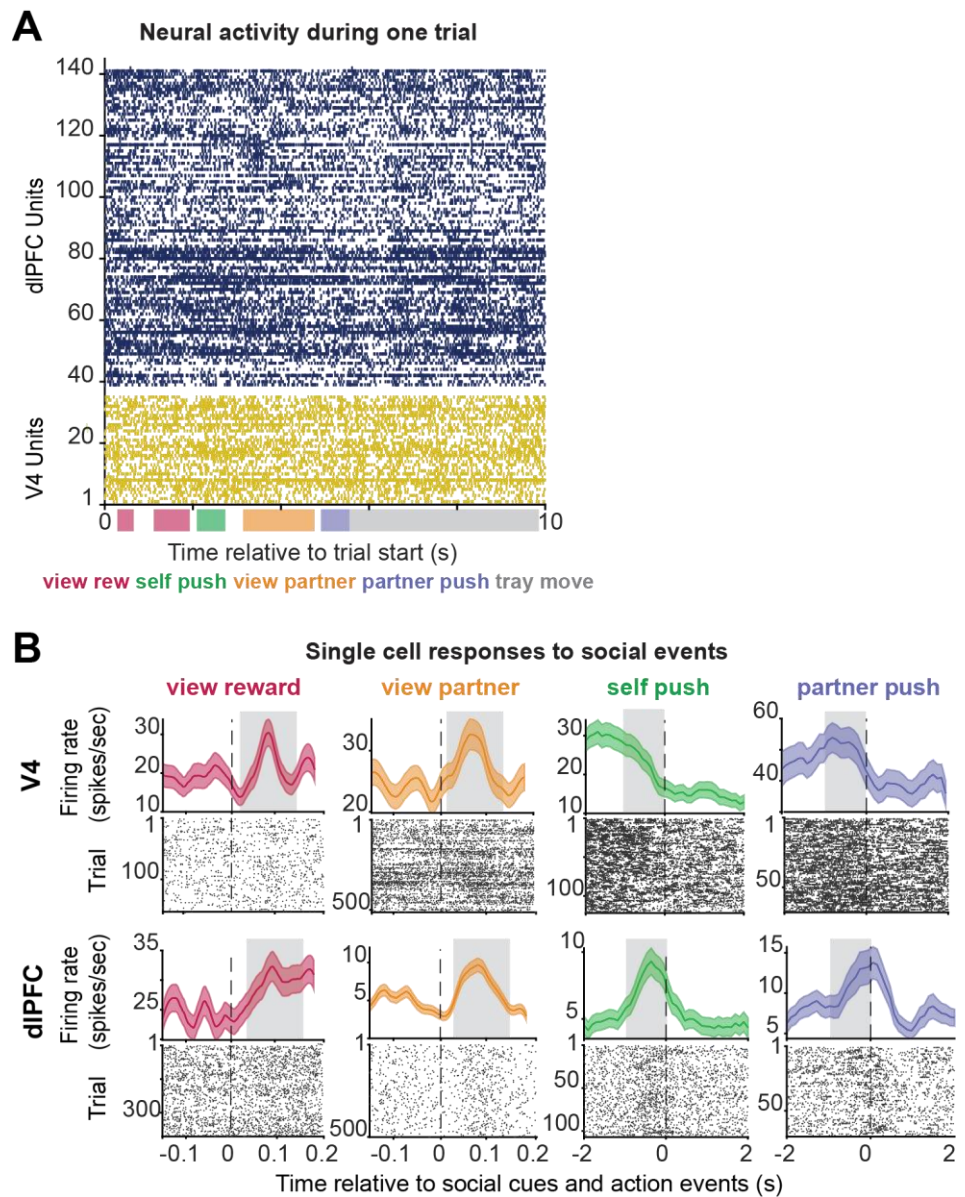


**Figure 14. Neural responses to social events. (A)** Raster plot of spiking activity from M1 self-monkey's V4 (units 1-35) and dIPFC (units 36-140) cells across one trial. **(B)** Peri-event time histogram and raster examples of four distinct V4 and dIPFC cells responding to each social event. Dashed lines represent event onset and gray shaded box represents the response period used in all further analyses (also see Methods). Center line is mean firing rate averaged across the number of observations of each event with shaded SEM.

Indeed, 70% of dIPFC units increased their firing rate during each animal's push relative to baseline, with responses beginning 1000 ms before push onset (**Fig. 14B** and **Fig. 15A**,  $P < 0.01$ , Wilcoxon signed-rank test with FDR correction). Notably, a majority of dIPFC cells responded to *both* self and partner's choice (66%), and reward and partner fixations (43%) as opposed to just one or the other (**Fig. 15B-C**). Overall, dIPFC neurons

responded to both fixations and choice (**Fig. 15A**, left, all  $P < 0.01$  Wilcoxon signed-rank test with FDR correction), with 55% of dIPFC neurons exhibiting mixed selectivity (**Fig. 15A**, right). While a fraction of V4 neurons (28%) exhibited a change in firing rate around push time, the great majority responded to fixations on social cues (36 and 52%, fixations on reward and partner respectively). In contrast to dIPFC, most units in V4 responded only to fixations; 22% of V4 neurons exhibited mixed selectivity and most V4 neurons responded to partner monkey fixations (**Fig. 15A and C**). My results indicate that these mixed selectivity neurons, especially in dIPFC, may support the behavioral diversity observed in such a naturalistic and cognitively demanding social environment (Fusi et al., 2016; Parthasarathy et al., 2017; Rigotti et al., 2013).

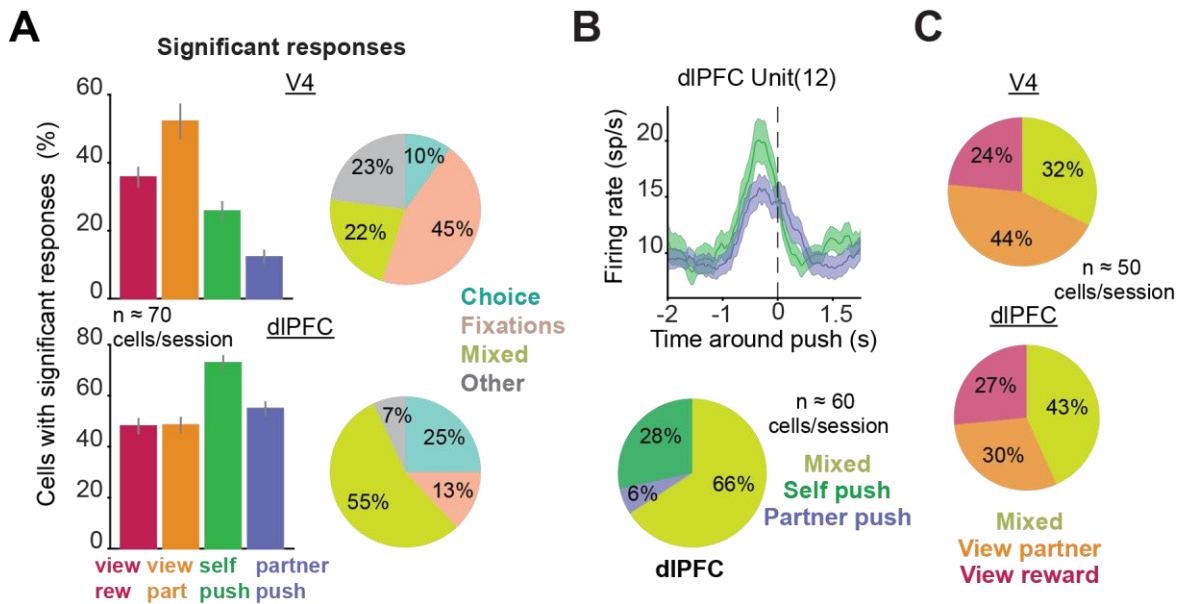


**Figure 15. Mixed selectivity in V4 and dIPFC.** (A) Left: for each area, the percentage of cells out of the total recorded (M1: 34 V4 cells, 102 dIPFC cells; M2: 104 V4 cells, 46 dIPFC cells) that exhibit a significant change in firing rate from baseline (intertrial interval firing rate) during social events, averaged across sessions and monkeys. For each cell,  $P < 0.01$  Wilcoxon signed-rank test with FDR correction. Right: for each area, the percentage of neurons out of the total recorded that responded only to choice (self and/or partner), only to fixations (reward and/or partner), both fixations and choice (“mixed”), or none at all (“other”). (B) PSTH from an example dIPFC unit that shows an increase in firing rate before both the self-monkey and partner monkey pushes. Bottom: pie chart reflecting the percentage of push-modulated dIPFC units that respond only to self-push, only to partner push, or to both (“mixed”). Percentages averaged across sessions and monkeys. M1: 102 total dIPFC cells, 73 are push responsive; M2: 46 total dIPFC cells, 41 are push responsive. (C) Pie chart reflecting the percentage of fixation-modulated V4 and dIPFC units that respond only to reward fixations, only to partner fixations, or to both (“mixed”). Percentages averaged across sessions and monkeys. M1: 73 dIPFC cells and 20 V4 cells are fixation responsive; M2: 30 dIPFC and 80 V4 cells are fixation responsive.

### 3.3.2 Neural encoding of social cues and decisions improves during learning

Next, I examined the ability of neural populations to encode social cues and animals’ choice to cooperate during learning. A support vector machine (SVM) classifier with 10-fold cross-validation was trained to decode fixations on social cues and cooperation choices from single observations (see *Methods* 3.2.5). Fixations on the reward system and partner monkey were accurately decoded from the population response in each area. Decoding accuracy for social cues in each area increased on average by 328% during learning (Fig. 16A, all  $P < 0.01$ ,

linear regression). In contrast, while non-social objects, such as fixations on self-monkey's button and random floor objects, could be reliably decoded from V4 and dIPFC activity, decoder performance did not improve across sessions (**Fig. 16B**). Thus, during learning cooperation both V4 and dIPFC selectively improve the encoding of visual features of social objects (e.g., reward system and partner), but not that of other objects. Furthermore, dIPFC neurons accurately discriminated between social and non-social object categories as decoder performance significantly improved by 228% during learning (Fig. 16C, all  $P < 0.01$ , linear regression). Thus, dIPFC representations of social visual cues as well as their distinction from non-social cues strengthen while animals learn to cooperate (**Fig. 16C**).

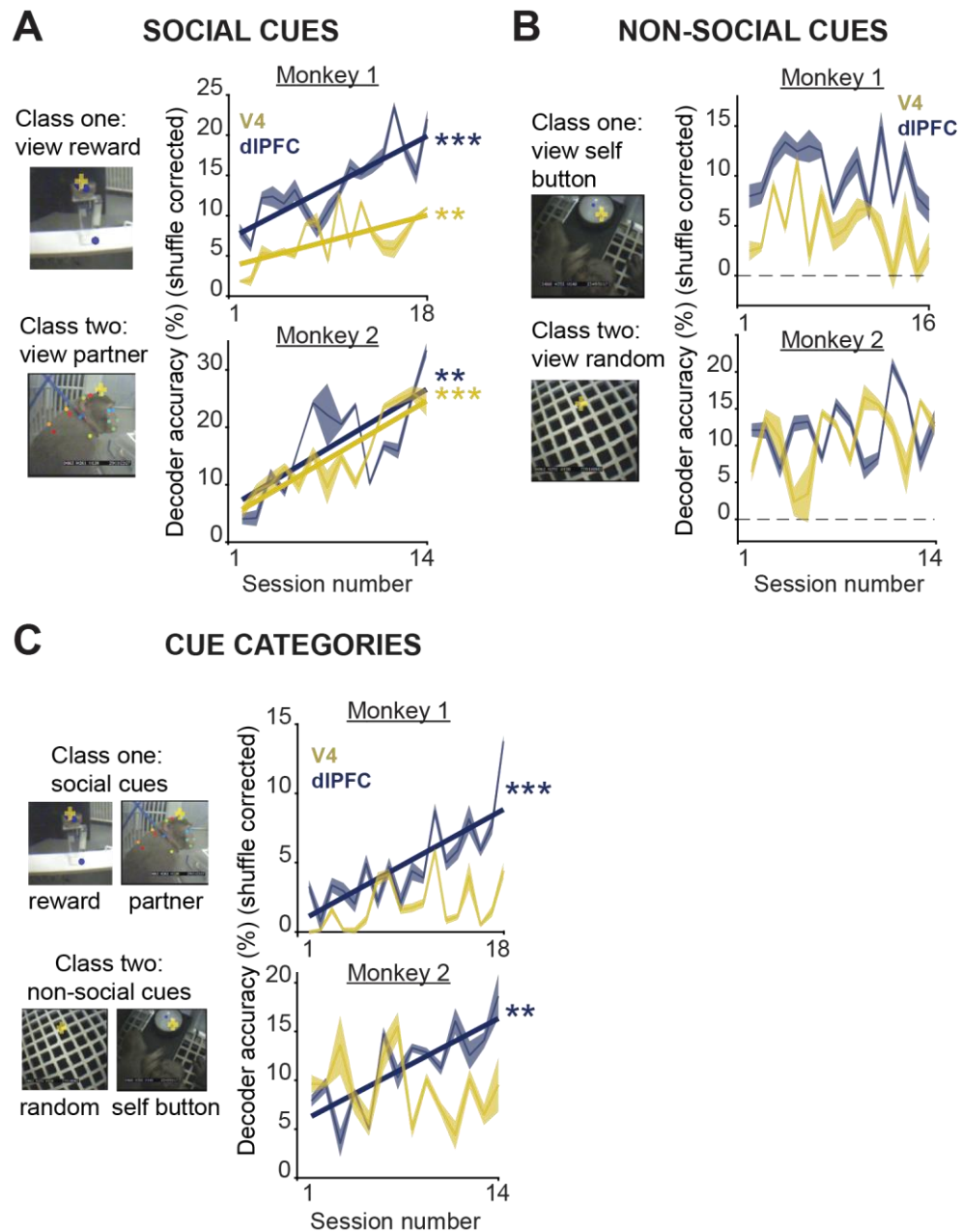


**Figure 16. Encoding of social cues in V4 and dIPFC. (A)** Decoding accuracy for fixations on the reward system and partner monkey. Decoders were trained and tested using 10-fold cross validation where chance is 50%, or 0% shuffle-corrected (dashed lines). M1:  $P = 0.006$ ,  $r = 0.6$  and  $2.31 \times 10^{-5}$ ,  $r = 0.8$ ; M2:  $P = 3.01 \times 10^{-5}$  and  $0.004$ , V4 and dIPFC respectively, linear regression and Pearson correlation. Plots display shuffle-corrected mean prediction accuracy on test observations ( $\pm$ SEM) **(B)** Decoding performance for fixations on two non-social objects. Session number does not predict accuracy. M1:  $P = 0.26$  and  $0.41$ ; M2:  $P = 0.18$  and  $0.52$ , V4 and dIPFC respectively, linear regression. **(C)** Decoding performance for object categories: fixations on social cues and non-social cues. M1:  $P = 0.08$  and  $P = 0.0001$ ,  $r = 0.8$ ; M2:  $P = 0.3$  and  $P = 0.001$ ,  $r = 0.8$  for V4 and dIPFC accuracy respectively, linear regression and Pearson correlation.



I further examined whether neural populations encode each monkey's decisions to cooperate. By decoding population activity before a push, I found that in V4, choice events can be decoded only in a small number of sessions (**Fig. 17**). In contrast, in dIPFC decoding performance increased on average by 5,320% while animals learned to cooperate (**Fig. 17**, all  $P < 0.01$ , linear regression).

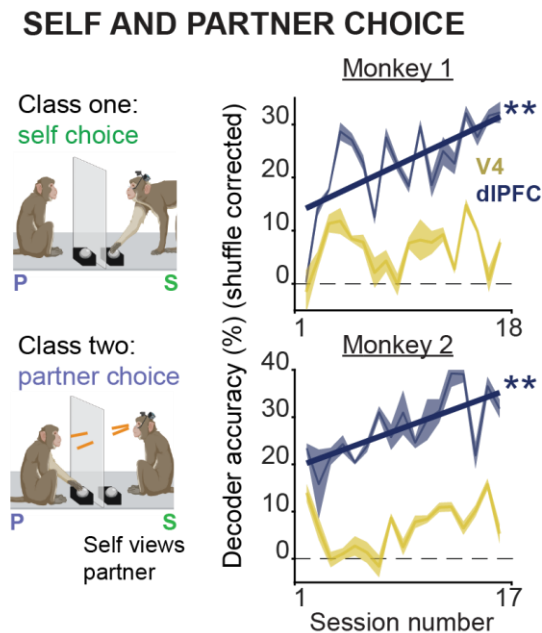


**Figure 17. Encoding of choice in V4 and dIPFC.** Decoding performance for each animal's choice to cooperate. M1:  $P = 0.54$  and  $P = 0.003$ ,  $r = 0.7$ ; M2:  $P = 0.1$  and  $P = 0.002$ ,  $r = 0.7$  for V4 and dIPFC accuracy respectively, linear regression and Pearson correlation.

Importantly, I found that self-monkey viewed different social cues during self and partner pushes (**Fig. 13B**), so I examined whether neural activity during pushing reflected decision-making or changes in visual input. To investigate this, I decoded each animal's choice to cooperate during two scenarios: 1) pushes with preceding (within 1000-ms) fixations on social cues (reward system or partner), and 2) pushes without preceding fixations on social cues. Events in scenario 1 were balanced to match those in scenario 2 (see Methods). In both V4 and dIPFC, decoder performance for choice was significantly reduced by 65% and 24% respectively, when pushes with preceding fixations on social cues were excluded (**Fig. 18**, gray,  $P < 0.001$ , Wilcoxon signed-rank). However, in dIPFC, the choice to cooperate could be reliably decoded and decoder

accuracy remained correlated with learning (**Fig. 18**, bottom row, all  $P < 0.05$ , linear regression). This demonstrates that dIPFC encodes each animal's decision to cooperate and that viewing social cues during decision-making improves choice encoding. In contrast, V4 decoder performance was close to chance when button pushes preceded by fixations on social cues were removed from the analysis, suggesting that V4 activity before choice mostly represents viewing social cues and not decision-making (**Fig. 18**). Altogether, this demonstrates that improved encoding of egocentric (self) and allocentric (partner) choice in dIPFC, but not V4, correlates with learning cooperation.

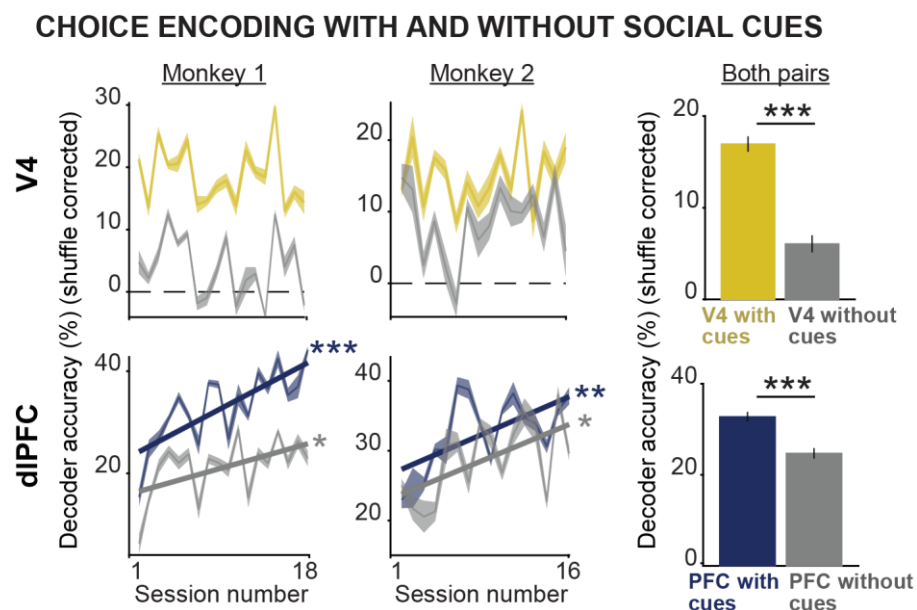


**Figure 18. Viewing social cues improves choice encoding.** Left: Decoding performance for each animal's choice using self and partner pushes that always had preceding fixations on either social cue within 1000 ms of push (navy and gold) compared to pushes that did not have fixations on social cues (gray). V4: M1  $P = 0.48$  and  $P = 0.4$ ; M2  $P = 0.49$  and  $P = 0.71$ , V4 accuracy with and without social cues respectively, linear regression. dIPFC: M1  $P = 0.0002$ ,  $r = 0.8$  and  $P = 0.02$ ,  $r = 0.5$ ; M2  $P = 0.008$ ,  $r = 0.6$  and  $P = 0.02$ ,  $r = 0.6$  for dIPFC accuracy with and without social cues respectively, linear regression and Pearson correlation. Right: Decoding accuracy for choice averaged across both monkeys during with and without social cue conditions. V4  $P = 7.44e-7$  and dIPFC  $P = 3.46e-6$ , Wilcoxon signed-rank test.

### 3.3.3 Cells contribute more equally to encoding of social events during learning

Given the improvement in decoding performance for social events, I wondered if neuronal weights were increasing during learning. In linear SVM decoding models, as I've applied here, weights are assigned to each neuron and represent a neuron's contribution to the decision boundary for separating one decoded event from another (i.e. – self and partner choice, reward and partner stimuli). The sign (+ or -) of the weight indicates which class/event the neuron is most representing. Additionally, the higher the magnitude of the weight, the more important that neuron is for classification. I first normalized the weights of all neurons within a session (see Methods 3.2.5). Since within each animal, data was recorded from nearly the same neural population across sessions (including single and multi-units; M1: 34 V4 cells, 102 dlPFC cells; M2: 104 V4 cells, 46 dlPFC cells), I then compared the absolute value of weight distributions across sessions during learning (Koren, 2021).

Surprisingly, weight values did not increase, but rather, the variance, kurtosis, and skewedness of weight distributions decreased across sessions for decoding models that showed improved decoding performance (**Fig. 19**). This finding was consistent across brain areas and learning models from each monkey (**Fig. 19D**). Importantly, decreasing variance, kurtosis, skewedness, or maximum value of weights was not observed in models where decoding performance did not improve, such as non-social cues (**Fig. 19B**). The decrease in these weight metrics suggests that, during learning, information about social events is distributed more evenly across the population, such that a few neurons are no longer contributing most of the information, as seen in earlier, 'naïve', sessions (**Fig. 19A**). The decrease in weight variance corresponded to a decrease in the maximum value of weights across sessions, supporting the idea that learning distributes information across neurons (**Fig. 19C**).

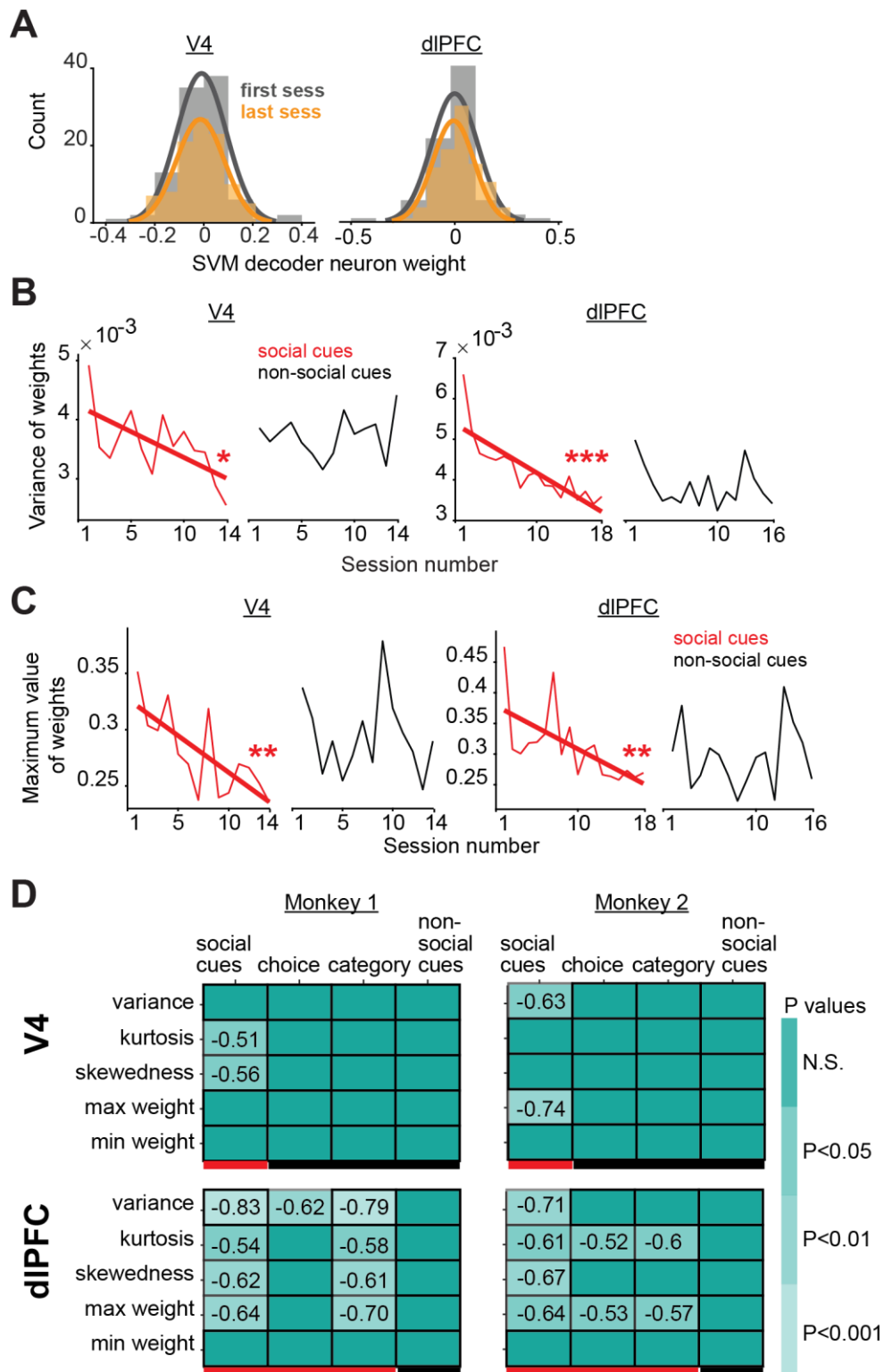


**Figure 19. Learning distributes information among neurons. (A)** Distribution of neurons' weights from the SVM model for decoding social cues for the first session and last session (V4 from Monkey 2, 98 and 102 neurons in first and last session respectively. dIPFC from Monkey 1, 90 and 101 neurons in first and last session respectively). Histogram of weights with normal distribution fit is plotted. **(B)** For each brain area, the variance of weight distributions (absolute valued) for each session from SVM models decoding social or non-social cues, as seen in Fig.

16A-B. V4 (average 104 cells/session) from M2 and PFC (average 102 cells/session) from M1. V4 social cues variance,  $P = 0.01$ ,  $r = -0.63$ , and PFC social cues variance,  $P = 1.67e-5$ ,  $r = -0.83$ , linear regression and Pearson correlation. **(C)** For each brain area, the maximum weight value (absolute valued) from each session in SVM models decoding social or non-social cues. V4 social cues maximum weight,  $P = 0.002$ ,  $r = -0.74$  and PFC social cues maximum weight,  $P = 0.004$ ,  $r = -0.64$ , linear regression and Pearson correlation. **(D)** Summary of decoding models that exhibit decreased variance, kurtosis, skewedness, or maximum value of weights for each brain area and monkey. For each decoding model, the P value, represented in shades of teal color, reflects linear regression of each weight metric with session number, as shown in B and C. The value in each box is Pearson correlation coefficient from correlating session number and weight metric. Learning models are SVM models where classification accuracy increased, such as decoding social cues. Significant decrease of these decoding weight metrics is associated with learning models exclusively.

### 3.3.4 Social context influences self-action

I considered whether dIPFC activity before button pushing during cooperation reflected the animal's decision to cooperate (i.e., pushing with social intention) or simply his decision to push the button. To investigate this, I recorded 9 additional sessions using 'solo blocks' whereby the self-monkey completed sets of 'cooperation' trials entirely by himself (see Methods 3.2.6). Solo blocks were interspersed with regular cooperation blocks conducted in two animals. Overall, the percentage of dIPFC cells that responded before push did not differ between contexts when compared to baseline activity (session averaged intertrial activity, **Fig. 20B**: bar plot, both 88%. all  $P < 0.01$ , Wilcoxon signed rank with FDR correction). However, social context did modulate a cell's firing rate before pushing, affecting 25% of recorded neurons. (**Fig. 20A-B**,  $P < 0.01$ , Wilcoxon rank sum test). Strikingly, I discovered a gain modulation effect of social context, where 61% of modulated dIPFC neurons exhibited higher firing rates before pushing during the solo context than social (**Fig. 20B**: pie chart,  $n = 10$  neurons/session). Furthermore, the type of trial – solo or social – could be decoded from the pre-push neural population activity of all dIPFC units ( $n = 40$  units/session, **Fig. 4C**). These findings in dIPFC suggest that social context affects neural representation of action and confirms the activity examined in Figures 17-18 reflects the self-monkey's decision to cooperate.

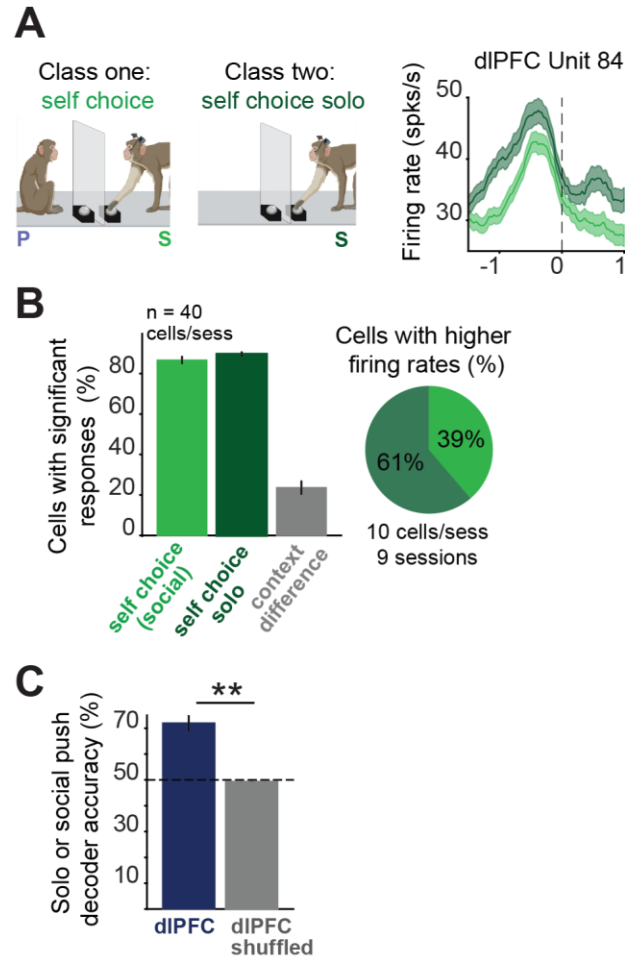


**Figure 20. Effects of social context on self-action. (A)** Social and solo trial schematic with peri-event time histogram for a dIPFC cell that exhibits a significant change in firing rate between solo and social conditions **(B)** Mean percentage of cells ( $n \sim 40$  cells/session from 9 sessions) responding significantly to self-choice in each condition when compared to baseline and compared across conditions (context difference),  $P < 0.01$  Wilcoxon signed-rank test with FDR correction and Wilcoxon rank sum test for context difference. Pie chart: session averaged percentage of modulated (context difference) cells that exhibit significantly higher firing rates before self-choice during solo or social condition. **(C)** Actual and shuffled decoding performance for solo and social trials using dIPFC activity occurring 1000 ms before self-choice, averaged across sessions,  $P = 0.004$ , Wilcoxon signed-rank test. Dashed line represents chance. SEM is represented with error bars or shading. \* $P < 0.05$ , \*\* $P < 0.01$ , \*\*\* $P < 0.001$ .

### 3.3.5 Neural activity is minimally correlated with animal's body and eye movements

dIPFC is one of the many interconnected regions of the prefrontal cortex, which receives convergence of multiple, more modular systems, such as sensory cortices, to plan actions (Fuster, 2000; Fuster & Bressler, 2015). The decision to cooperate in dIPFC is at a higher

hierarchical level than the execution of the motor action (i.e., button pushing), although both are parts of control, generally speaking (Botvinick, 2007; Fine & Hayden, 2022; Fuster, 2000). Therefore, it is expected that dIPFC orchestrates goal-directed actions and is not without premotor representations. Indeed, a recent study shows that dIPFC neurons are modulated by both task variables and uninstructed movements, but that this mixed selectivity does not hinder the ability to decode variables of interest (Tremblay et al., 2022). Movement driven activity is mostly orthogonal to task-driven activity, preventing movements from contaminating the neural representation of task-relevant variables (Stringer et al., 2019).

However, because motor variables such as head, body, and eye movement and pupil size during pushes may influence neuronal activity in cortex (Musall et al., 2019; Talluri et al., 2022; Tremblay et al., 2022), I quantified the correlation between these movements and neural activity in V4 and dIPFC. Consistent with our previous work and that of others (Shahidi et al., 2022; Talluri et al., 2022), I found only a small percentage of V4 and dIPFC neurons whose activity was correlated with movements or pupil size during pushing (**Fig. 21**, all metrics < 12% of correlated neurons (n = 1157 neurons), Pearson correlation  $P < 0.01$ ). Additionally, neural activity in V4 and dIPFC during fixations was only minimally associated with the animal's head and body movements (**Fig. 22**). With these findings, I confirm that the population activity examined in **Figures 16-28** (chapters 3 and 4) represents task-relevant variables such as visual social cues and social decisions.

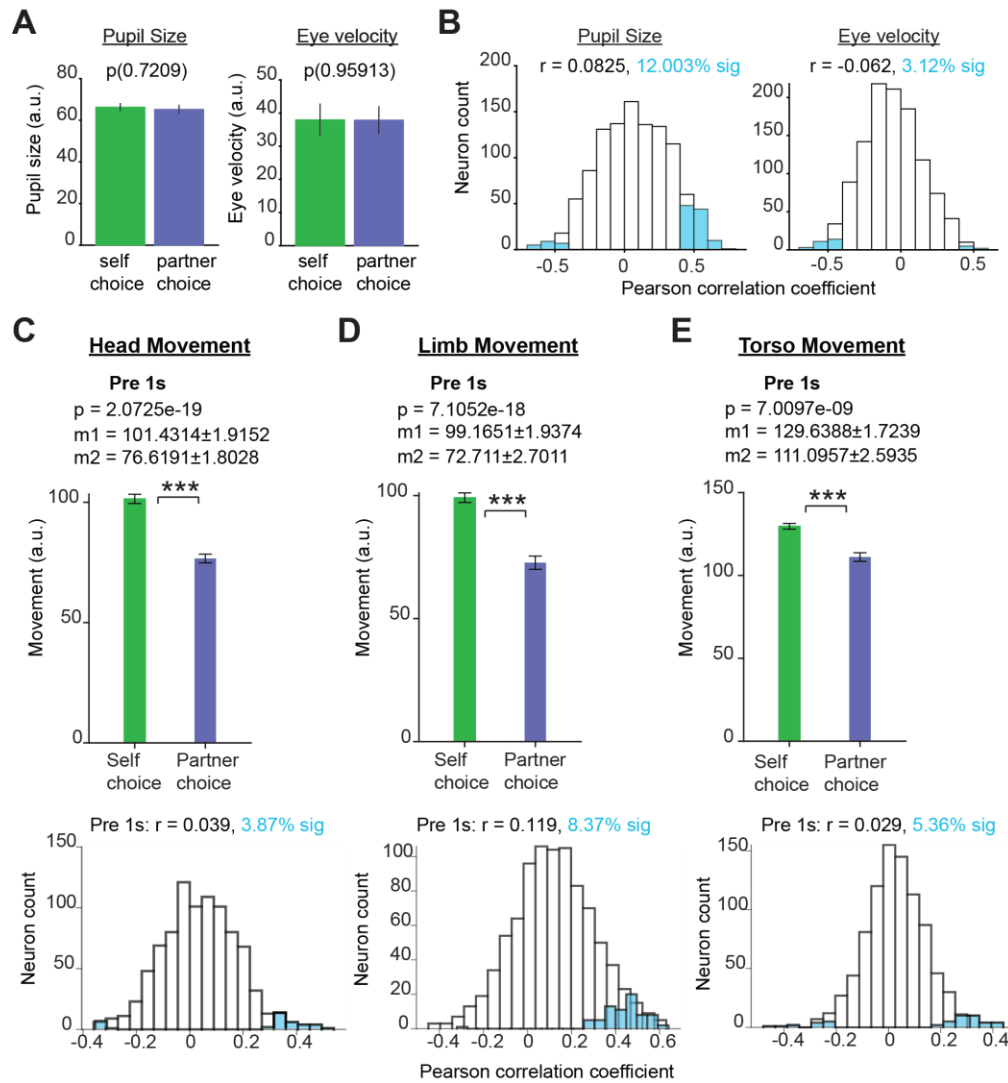


**Figure 21. Neural activity correlations with oculomotor and body movements during pushing.** (A) Pupil size and eye velocity, averaged across sessions and animals, that occurred before (1000 ms pre) the self and partner monkey pushes. There is no significance difference in pupil size and eye velocity between animal's choices, Wilcoxon rank sum test,  $P > 0.05$ . (B) The distribution of Pearson correlation coefficients from the correlation of V4 and dIPFC neuron's firing rates with pupil size and eye velocity occurring before (1000 ms pre) self and partner pushes.  $N = 1157$  neurons from eight sessions across two animals. Percent significant represents neurons with a significant correlation coefficient,  $P < 0.01$ . (C) Self-monkey's head movement occurring 1000 ms before self or partner monkey pushes, averaged across six sessions from two monkeys.  $M1$  and  $m2$  represent the mean movement for each choice type. Significance between groups was assessed using Wilcoxon rank sum test.  $*P < 0.05$ ,  $**P < 0.01$ ,  $***P < 0.001$ . Below - The distribution of Pearson correlation coefficients from the correlation of V4 and dIPFC neuron's firing rates with head movement occurring 1000 ms before self and partner pushes.  $N = 900$  neurons from six sessions across two animals. Percent significant represents neurons with a significant correlation coefficient,  $P < 0.01$ . (D) The same as in C but shows histograms of neural firing rate correlations with limb movement. (E) The same as in C but displaying neural firing rate correlations with torso movement.



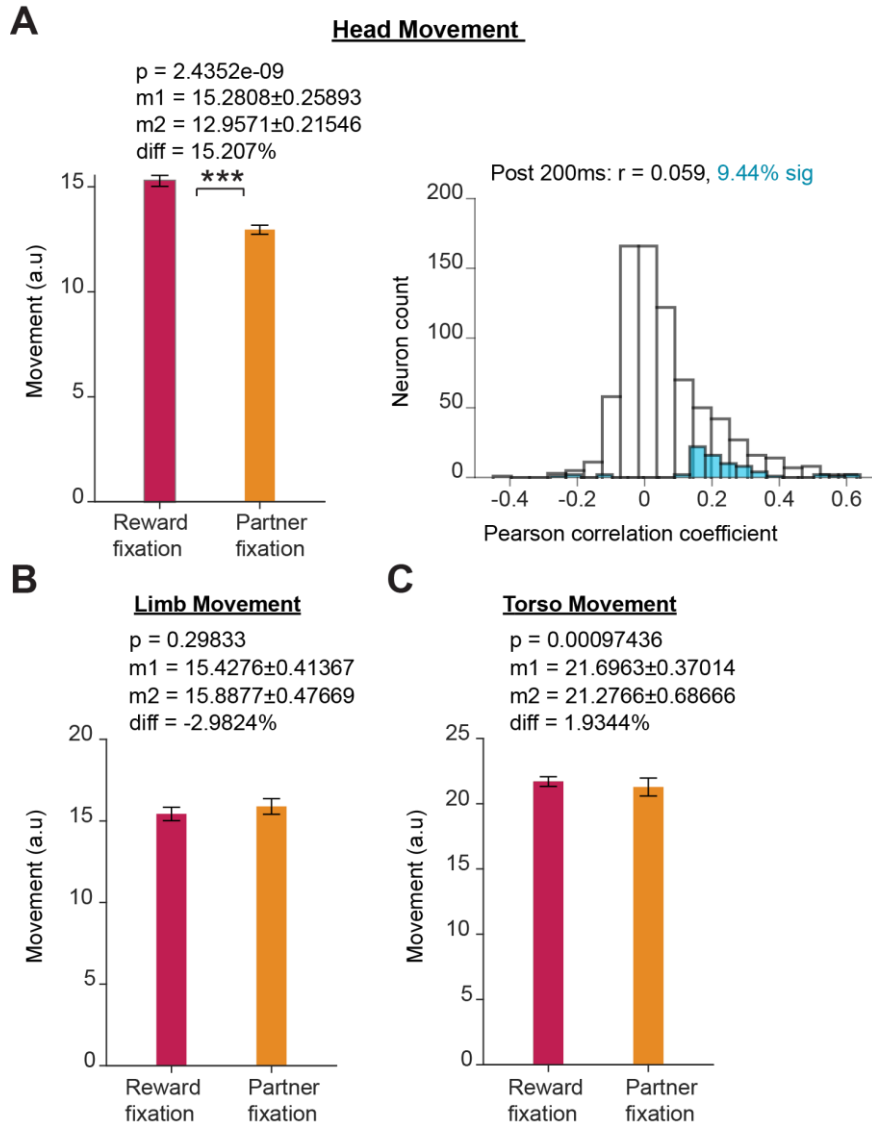


**Figure 22. Neural activity correlations with body movements during fixations on social cues. (A)** Left - Self-monkey's head movement occurring 200 ms after onset of fixations on the reward and partner monkey, averaged across six sessions from two monkeys. M1 and m2 represent the mean movement for each fixation type. Diff is the difference between the means. Significance between groups was assessed using Wilcoxon rank sum test. \* $P < 0.05$ , \*\* $P < 0.01$ , \*\*\* $P < 0.001$ . Right - the distribution of Pearson correlation coefficients from the correlation of V4 and dIPFC neuron's firing rates with head movement occurring 200 ms after fixations on the reward system and partner monkey.  $N = 900$  neurons from six sessions across two animals. Percent significant represents neurons with a significant coefficient,  $P < 0.01$ . **(B)** The same as in A, left but for limb movement. **(C)** The same as in A, left but for torso movement. While there is a significant difference in torso movement across reward and partner fixations, the magnitude of the difference is less than 2%.

### **3.4 Discussion**

I found single cell and population representations of viewing social cues in each brain area. Specifically, during learning, V4 and dIPFC population encoding of social cues (fixations on reward and partner) improved across sessions, but did not improve for other, non-social objects (fixations on self-button and random objects). Since the objects within these social and non-social categories have distinct visual features, improvement in decoding performance is most likely related to an improvement in V4 and dIPFC ensemble representation of *social* visual features exclusively, as non-social objects can be decoded but performance does not correlate with learning behavior. While V4 has been previously shown to process visual information, such as object shape, color, and texture (Kim et al., 2019; Kobatake & Tanaka, 1994; Schein & Desimone, 1990), my findings reveal that V4 encoding of visual features in a 3D, goal-directed, social environment is modulated by feature salience, particularly social relevance, inviting further investigation of V4 in social cognition research.

Likewise, these findings in dIPFC further previous work demonstrating dIPFC's ability to represent visual features beyond spatial information, such as categories of visual stimuli (i.e. – numerosity) and object identity (Rao et al., 1997; Viswanathan & Nieder, 2013; Wallis & Miller, 2003; Wutz et al., 2018). Indeed, dIPFC not only improved discrimination for social cues but also for social and non-social categories, which complements a recent study showing neurons in other prefrontal regions (dorsomedial prefrontal cortex, anterior cingulate cortex, and orbitofrontal cortex) prioritize social discriminability between viewing faces and other objects during free viewing with another monkey (Dal Monte et al., 2022). Social gaze interaction is important for social behavior and whether V4 and dIPFC are modulated by the gaze of others remains to be discovered, as I did not record eye tracking data from the partner monkey. Interestingly, decoding accuracy for predicting social and non-social cues was consistently higher in dIPFC than V4. I suspect this is because dIPFC receives and integrates many sensory modalities (E. K. Miller & Cohen, 2001; Wang et al., 2015), enabling better prediction of incoming stimuli. Therefore, future

studies could explore how prefrontal and sensory cortices support tactile, auditory, vocal, and visual communication during learning of social interactions.

Neural processing of allocentric information is essential for social learning. In primates especially, evidence gathered from visually monitoring of other agents is used to determine actions of oneself and predict other's actions. The temporal fluidity and spontaneous behavior in this ethologically relevant experiment enabled the examination of neural mechanisms underlying self and other decisions in V4 and dlPFC during learning to cooperate. The period preceding push is most likely when animals are forming the decision to cooperate. Importantly, animals increase viewing of social cues before pushing during learning, and monkeys exhibited a diversity of viewing and push sequences before cooperating across trials and sessions (**Fig. 8-9, and Fig. 13**). This allowed examination of neural population activity during both independent and overlapping events (i.e. – pushes with or without fixations on social cues). I explored encoding of the egocentric (self-monkey) and allocentric (partner monkey) decision to cooperate by using self and partner pushes that occurred separately from other events, such as the start of the trial (to avoid relation to reward), and the other animal's push (**Fig. 13A**). Critically, these isolated partner pushes occurred during moments when the self-monkey was likely to be thinking and mentalizing about the partner, as evidenced by fixations on the partner during these times (**Fig. 13B**). For instance, if self-monkey is the only monkey pushing and holding his button, he might be anticipating when the partner will also cooperate, especially right before the partner pushes, explaining why allocentric information is encoded in dlPFC during this time. dlPFC population encoding of egocentric and allocentric choice significantly improved during learning, even when pushes with immediate (occurring within one sec of push) preceding fixations on social cues were removed from analysis, emphasizing the important and persistent role of dlPFC in social choice during learning. This finding contributes to previous work describing dlPFC's contribution to social action planning and goal-directed behavior (Falcone et al., 2016; Tanji & Hoshi, 2008; Yamagata et al., 2012).

Notably, dlPFC decoding performance and learning trend for choice that excluded preceding fixations on social cues was significantly lower than model performance that included preceding fixations on social cues, suggesting that, while dlPFC does not depend on viewing social cues for planning or predicting self and other decisions, the additional visual information does improve neural representation of social decisions in dlPFC. Indeed, this finding supports a possible role for dlPFC in mentalization and theory of mind, as the self-monkey could have been thinking about the partner monkey without looking directly at him around these critical decision periods. Moreover, my analysis did not include time points when the mirror neuron system would have been activated and influencing dlPFC activity, such as during post-push periods when self-monkey observed partner monkey pushing his button (i.e. during other-action execution). This invites further investigation of the role of mirror neuron regions in social learning (di Pellegrino et al., 1992; Fogassi & Ferrari, 2011; Rozzi et al., 2008). As expected, V4 did not encode self and other decisions, as decoding performance for choice decreased to near chance levels when pushes with fixations on social cues were removed from analysis. In other words, when accounting for changes in visual input, choice events could not be decoded in V4.

Overall, V4 and dlPFC neurons isolate and process socially pertinent visual information that is used to improve coding of social decisions in dlPFC. These computations highlight the importance of visual monitoring to determine actions of oneself and predict or even influence other's actions in the creation of purposeful social behavior. Additionally, I examined how neurons within V4 and dlPFC populations represent social variables during learning by analyzing features of neural weight distributions across sessions. Decoding models for social events that exhibit increased performance were characterized by a decrease in the variance, kurtosis, and skewedness of neuronal weight distributions during learning (**Fig. 19**). The maximum value of weights also decreased across sessions exclusively in learning models. The decrease in these metrics suggests that, during learning, information about social events is distributed more evenly across the population, such that a few neurons are no longer contributing most of the information, as seen in the first few sessions before information is learned. Certainly, once relevant

information is learned, it would be beneficial for learned information to be represented among a group of neurons and not restricted to only a few neurons.

The distribution of information among neurons and improved encoding of social cues and choice in V4 and dlPFC during learning is likely gated by dopaminergic signaling from the mesocortical limbic pathway (Stalter et al., 2020). D1 and D2 dopaminergic receptors are expressed in V4 and dlPFC neurons (Lidow et al., 1991), with prefrontal cortex receiving direct projections from dopaminergic neurons in the midbrain (Björklund & Dunnett, 2007; Williams & Goldman-Rakic, 1998). Activation of these dopaminergic receptors in prefrontal cortex have been shown to control neural responses to visual stimuli in V4 (Noudoost & Moore, 2011) and enhance sensory sensitivity of dlPFC neurons (Stalter et al., 2020). As social stimuli, such as the partner monkey, become more rewarding during learning, this could increase dopamine levels in cortex to improve neural encoding of social variables – a framework that should be explored in future studies. Collectively, the findings in this chapter provide mechanistic insights into how neural systems encode and process social information during learning cooperation.

## **CHAPTER 4: SPIKE TIMING COORDINATION BETWEEN BRAIN REGIONS DURING SOCIAL LEARNING**

### ***4.1 Background***

In addition to the individual roles of V4 and dlPFC, studies outlining their cytoarchitecture show that both areas share indirect neuronal projections via parietal and temporal areas (Gregoriou et al., 2014; Kolster et al., 2014; Saleem et al., 2014; Ungerleider et al., 2008). These multisynaptic connections facilitate the feedforward processing of information from V4 to dlPFC, with V4 encoding mostly visual features that integrate in dlPFC to make decisions and plan actions (Brincat et al., 2018; Choi et al., 2018; Siegel et al., 2015). Additionally, V4 receives feedback modulation from dlPFC, such as attention (Gregoriou et al., 2014), task-related information, and choice signals (Choi et al., 2018; Siegel et al., 2015). Although we know that temporal

coordination of neuronal spiking activity supports signal transmission and behavior, the neural interactions between V4 and dlPFC during social behavior remains unknown. I expect that the back-and-forth relay of electrical signals, or spike timing coordination, between V4 and dlPFC during socially relevant events should support social learning. Therefore, I will use simultaneous neural recordings during learning social cooperation experiments to understand neural interactions within and between V4 and dlPFC. This analysis will determine whether, in addition to patterns and covariance of neurons' firing rates as observed in chapter 4, spike timing coordination between neurons can also contribute to learning social interactions.

## **4.2 Methods**

### *4.2.1 Cross-correlation of neuronal pairs*

Cross correlograms (CCGs) in **Figure 23** were computed by sliding the spike trains of each cell pair and counting coincident spikes within 1 ms time bins for each social event and pair of neurons (within and between areas) using the *xcorr* function in Matlab 2020b. Cross-correlations were normalized by the geometric mean spike rate, and corrected for stimulus-induced correlations by subtracting an all-way shuffle predictor (Bair et al., 2001; Pojoga et al., 2020). I computed CCGs using spiking activity that occurred 800 ms before choice or random events and 200 ms after fixation onset with visual delay (see section *3.2.4 Neural firing rate and response*). For cross-correlation of v4-dlPFC responses to fixations, I used an 80 ms visual delay. A CCG was considered significant if the peak (occurring within -6 to +6 ms lag interval for within area and  $\pm 15$ -60 ms lag interval between areas) exceeded 4.5 times the standard deviations of the noise (tail) level occurring  $\pm 60$  ms from the peak range during non-fixation events and  $\pm 25$  ms from the peak range for fixation events. Mean coordination values for each session are the average of the CCG peaks of all significant cell pairs. For random events, I used times from the inter-trial period and, for random fixations, I used fixations on objects that were not social cues. Within a session, the number of random observations matched those of the social event.

#### 4.2.2 SVM weight normalization

In each session, for comparing feature weights of correlated and non-correlated V4 and dIPFC neurons (**Fig. 26**), I first normalized weights across the entire population of neurons, using the equation below where  $W_o$  is the current cell weight divided by the square root of the sum of all the squared weights in the population (Koren, 2021).

$$\text{normalized weight} = \frac{W_o}{\sqrt{W_1^2 + W_2^2 + \dots + W_n^2}}$$

Finally, the absolute values of weights were averaged across neurons within each session for each monkey, then combined to create the distributions seen in **Fig. 26**. For each brain area, I used the weights from SVM models for decoding social cues or each animal's choice to cooperate.

#### 4.2.3 Statistics

To assess systematic changes in behavioral and neural metric performance, or learning, I report the P-value from simple linear regression and Pearson's correlation coefficient to report the strength and direction of linear relationship. The percent increase or decrease of behavioral and neural metrics was calculated by the percent change equation,  $C = \frac{x_2 - x_1}{x_1}$ , where C is the relative change,  $x_1$  was the value from session 1, and  $x_2$  is the value from the last session. Changes were then averaged across events or monkeys. For comparing two paired groups such as a cell's firing rate during an event and baseline period, I used the two-sided Wilcoxon signed-rank test. I chose this test rather than parametric tests, such as the t-test, for its greater statistical power (lower type I and type II errors) when data are not normally distributed. When multiple groups of data were tested, I used the False Discovery Rate multiple comparisons correction (Benjamini & Hochberg, 1995) whose implementation is a standard function in Matlab. When comparing two unpaired distributions, I used the Wilcoxon rank sum test.

## 4.3 Results

### 4.3.1 Spiking coordination within and between areas improves during learning

Temporal coordination of neuronal spiking within and between cortical areas is believed to be correlated with signal transmission (45). I computed spike time correlations between pairs of cells in V4, dIPFC, and across areas. Only significant cross-correlograms (CCGs) were used in the analysis (the peak of shuffle-corrected CCGs was  $> 4.5$  standard deviation of the tails (46), see Methods). To account for the delay of information transmission within and between areas, I only analyzed within-area CCGs (average of 668 cell pairs/session) that peaked at  $\pm 0-6$  ms time lag, and inter-areal CCGs (average of 45 cell pairs/session) that peaked at  $\pm 15-60$  ms lag (**Fig. 23**).

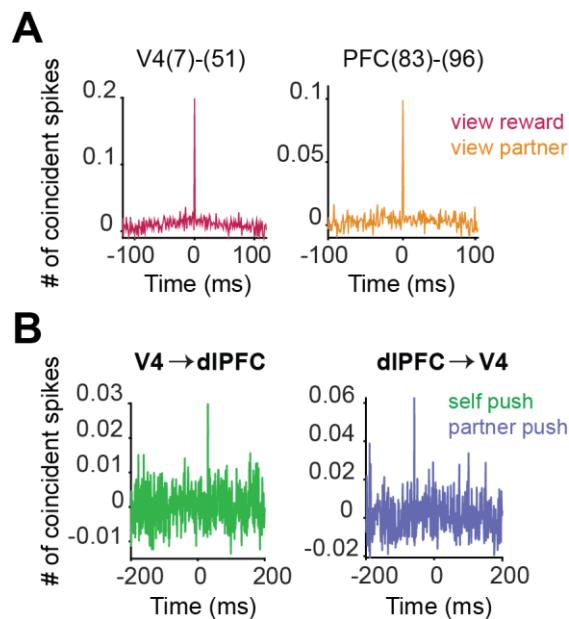


**Figure 23. Cross-correlograms of neuronal pairs within and between brain regions.** (A) Example cross-correlograms (CCGs) of V4-dIPFC cell pairs during two of the four social events, averaged across observations. (B) Example CCGs of V4-dIPFC cell pairs during two of the four social events. CCGs were computed with 1 ms time bins during neural response periods for each event, displayed in Figure 14B.

The mean coordination and average of significant cell pair maximum coincident spikes (CCG peaks) significantly increased across sessions during social events (**Fig. 24**). Within V4,



pairwise synchrony increased by 114% across sessions during fixations on social cues, but not before choice events. In dIPFC, synchronized spiking increased on average by 137% during fixations on social cues and self-choice, but not during partner choice. As animals learned to cooperate, coordination between V4 and dIPFC increased by 160% for all social events except partner choice (**Fig. 24**). Importantly, both within and between areas, coordination during fixations on random floor objects or random time periods (e.g., inter-trial interval) did not change across sessions, indicating that increased coordination exclusively correlates with learning of social events (**Fig. 24**).

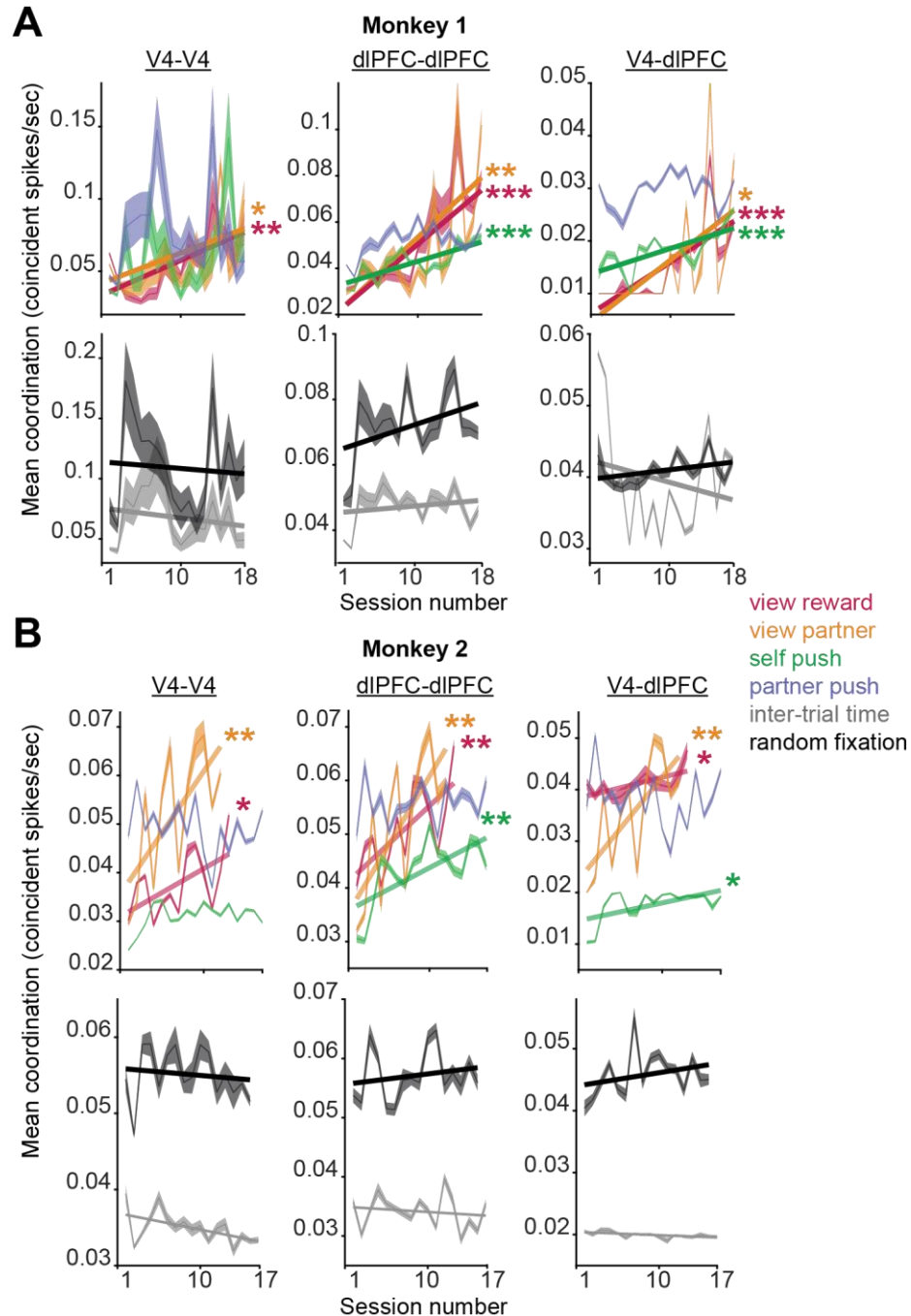


**Figure 24. Spike timing coordination for social and non-social events. (A)** Top row: Mean coordination plotted across sessions for each social event in V4, dIPFC, and between areas (V4:  $P = 0.001$ ,  $r = 0.7$ ;  $P = 0.01$ ,  $r = 0.6$ ;  $P = 0.09$  and  $P = 0.8$ . PFC:  $P = 5.68e-6$ ,  $r = 0.9$ ;  $P = 0.003$ ,  $r = 0.7$ ;  $P = 1.25 \times 10^{-4}$ ,  $r = 0.7$  and  $P = 0.07$ . V4-dIPFC:  $P = 2.89 \times 10^{-4}$ ,  $r = 0.8$ ;  $P = 0.01$ ,  $r = 0.6$ ;  $P = 9.93 \times 10^{-4}$ ,  $r = 0.7$  and  $P = 0.27$ . Linear regression with Pearson's correlation coefficient for view reward, view partner, and self-push events, respectively). Bottom row: Mean coordination during fixations on random objects and during random events (inter-trial period) for V4, dIPFC and inter-areal cell pairs. V4:  $P = 0.4$  and  $0.7$ ; PFC:  $P = 0.4$  and  $0.09$ ; V4-dIPFC:  $P = 0.4$  and  $0.1$ , for random event and fixations, respectively. **(B)** Top row: Mean coordination plotted

across sessions for each social event in V4, dIPFC, and between brain areas (V4:  $P = 0.03$ ,  $r = 0.6$ ;  $P = 0.005$ ,  $r = 0.7$ ;  $P = 0.1$  and  $P = 0.2$ . PFC:  $P = 0.008$ ,  $r = 0.7$ ;  $P = 0.003$ ,  $r = 0.8$ ;  $P = 0.002$ ,  $r = 0.7$  and  $P = 0.44$ . V4-dIPFC:  $P = 0.02$ ,  $r = 0.6$ ;  $P = 0.006$ ,  $r = 0.7$ ;  $P = 0.01$ ,  $r = 0.6$  and  $P = 0.48$ . Linear regression with Pearson's correlation coefficient for view reward, view partner, self-push and partner push events respectively). For 'view reward' and 'view partner' events, only 14 sessions were analyzed due to an inadequate number of fixations on the stimuli in 3 out of the 17 sessions. Sessions with less than 30 fixations were not included in the analysis. Bottom row: Mean spike timing coordination during fixations on random objects and during random events (intertrial period, 4.5 seconds before trial start) for V4, dIPFC, and inter-areal cell pairs. V4:  $P = 0.03$  and  $0.9$ ; PFC:  $P = 0.53$  and  $0.45$ ; V4-dIPFC:  $P = 0.01$  and  $0.14$ , for random events and random fixations, respectively. Significant  $P$  values correspond to decreasing trends.

Additionally, while significant V4-dIPFC pairs exhibited maximum coincident spiking at both positive (V4 leads) and negative time lags (dIPFC leads) during social events, there were consistently more inter-areal cell pairs with positive time lags (**Fig. 25**). This indicates that information between V4 and dIPFC during social cooperation is typically communicated in a feedforward direction (**Fig. 25**), consistent with my finding that social cues are used to guide animals' decision to cooperate (**Fig. 9**). The number of cell pairs with negative and positive time lags, or therefore directionality of information, did not systematically change across sessions.

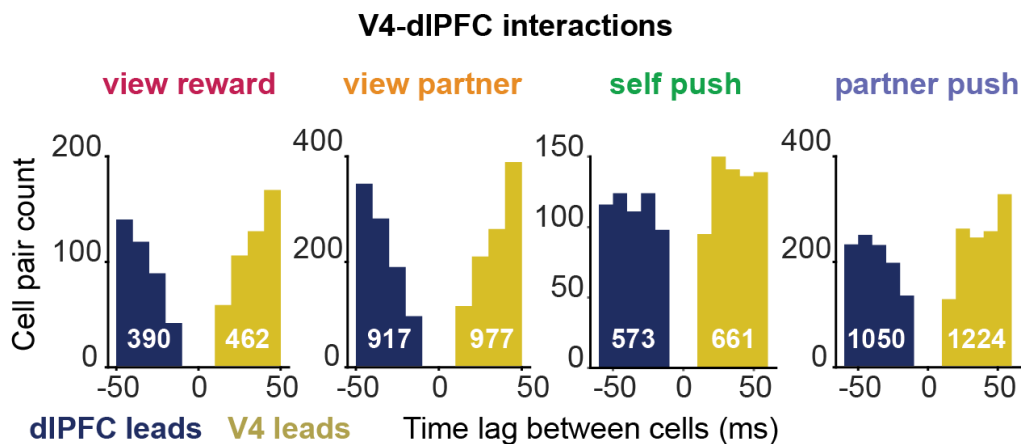


**Figure 25. V4-dIPFC interactions are mostly feedforward.** Histograms of time lag values of CCG peaks between all significantly correlated V4-dIPFC cell pairs across sessions and monkeys, for each social event.

#### *4.3.2 Coordinated cells contribute more to encoding of social events*

Finally, I asked whether the V4 and dIPFC cells that were coordinated in their spike timing would also exhibit improved encoding of social variables. Notably, significantly correlated pairs of V4-dIPFC neurons contributed more to the encoding of social events in each brain area, as their normalized weight values from decoding models for social cues and choice were significantly higher than the weights of the remaining population of cells (**Fig. 26A**, Wilcoxon signed-rank test,  $P < 0.01$ ). In V4, this result applied for the encoding of social cues but not choice, whereas in dIPFC it applied for all events except partner choice (**Fig. 26A**). Taken together, we propose a general mechanism for learning social interactions, whereby increased spike timing coordination between areas V4 and dIPFC during social events leads to improved encoding and distributed representation of social variables within each area (**Fig. 26B**).

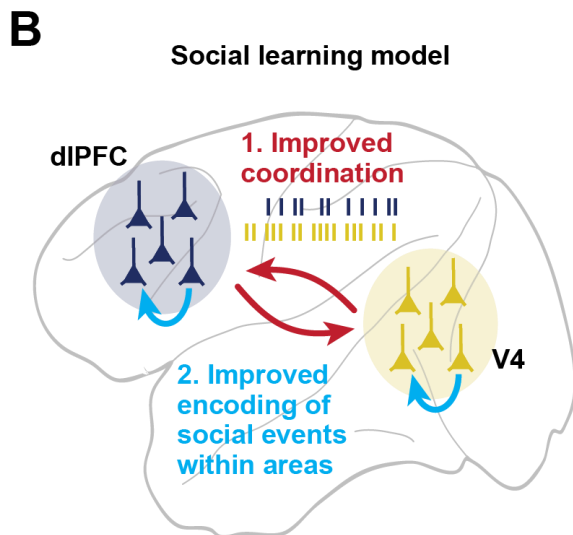
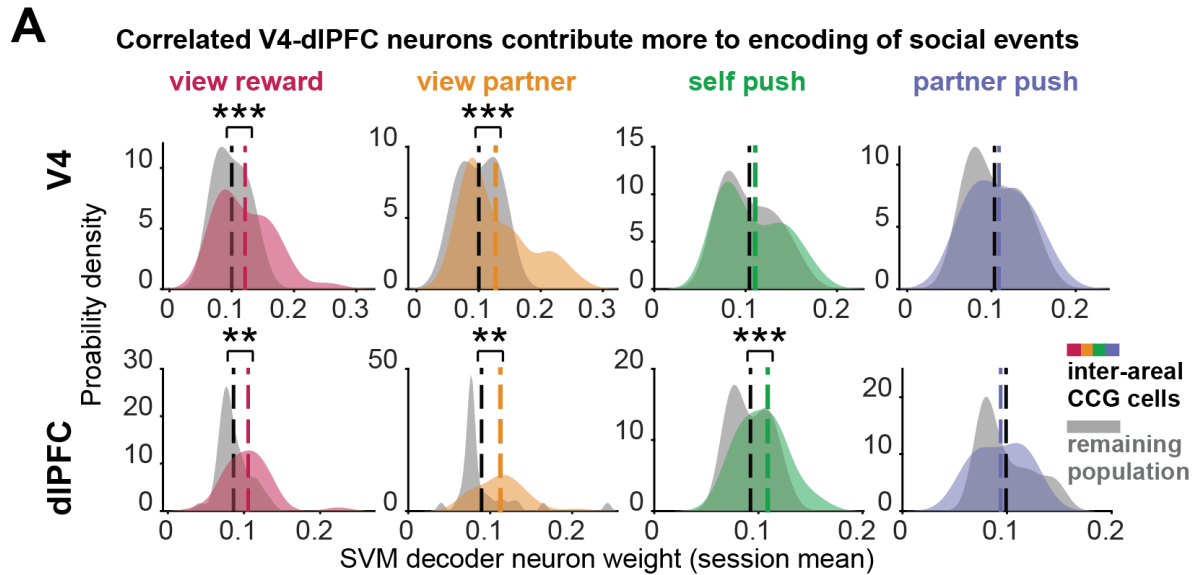


**Figure 26. Social learning mechanisms in primate cortex. (A)** Probability density plots of decoder weights of V4 and dIPFC neurons significantly correlated during each social event. Weights were averaged across neurons within each session for each monkey, then combined. V4 from left to right:  $P = 6.48 \times 10^{-4}$ ,  $P = 6.38 \times 10^{-4}$ ,  $P = 0.33$ ,  $P = 0.24$ ; PFC:  $P = 0.002$ ,  $P = 0.001$ ,  $P = 7.41 \times 10^{-4}$ ,  $P = 0.14$ , Wilcoxon signed-rank comparing weight distributions of correlated and non-correlated neurons. **(B)** Cartoon of social learning model: increased inter-area spike timing coordination improves the encoding of social variables to mediate learning social interaction.

#### 4.4 Discussion

Associative learning of social signals relies on successive transformations of sensory inputs within local and long-range cortical networks (Brincat et al., 2018; Haruno & Kawato, 2006; Siegel et al., 2015). These data support that enhanced communication, or coordinated spiking,

between visual and prefrontal cortical areas mediates learning social interactions. Specifically, although V4-V4 coordination did not increase during learning when aligned to self-choice, coordination between pairs of V4-dIPFC cells did increase, and coordination consistently improved within and between areas following fixations on social cues, indicating that visual and decision information is communicated. Surprisingly, an increase in spiking coordination was not observed either within dIPFC or between V4-dIPFC before partner-choice, suggesting that dIPFC codes the prediction of other's behavior in mean firing rates but not spike timing coordination. I expect that increased coordination occurs between dIPFC and other cortical areas around allocentric events during learning and should be explored. Candidate areas, given their reciprocal connections to dIPFC and/or role in processing allocentric information, include the orbitofrontal cortex, dorsomedial prefrontal cortex, anterior cingulate cortex, and superior temporal sulcus (Dal Monte et al., 2022; Haroush & Williams, 2015; Moessnang et al., 2017; Ong et al., 2020). Additionally, while some significantly correlated inter-areal cell pairs exhibited maximum coordination at negative lag, meaning dIPFC spiked first, most cell pairs exhibited maximum coordination at positive lag, meaning V4 cells spiked first, suggesting a mostly feedforward processing of information throughout learning. For any social event, the directionality of spiking coordination did not consistently change across sessions (i.e. – increasing pairs with positive or negative lag was not observed during learning).

Notably, for each brain area, spike timing coordination results correlated with that of neural encoding for social events. For example, V4 ensembles did not encode choice and likewise did not exhibit increased coordination for either self or partner choice, however, V4 improved encoding of social cues and also exhibited increased synchronized spiking after fixations on social cues during learning. Strikingly, I found that significantly correlated V4-dIPFC neurons contribute more to the encoding of social cues within V4, and social cues and egocentric choice in dIPFC, as reflected by their increased weights in classification models compared to neurons that did not significantly correlate with a cell in the other brain region.

These findings led to my development of a social learning mechanism whereby an increase in coordinated spiking between visuo-frontal circuits leads to improved encoding of social events within each area. This theory is consistent with sensorimotor associative learning circuit models where coincident activity between brain regions during task-relevant stimulus-response events permits Hebbian plasticity at the cortico-cortical synapses that correspond to the associations (Makino et al., 2016). For example, in my experiments, monkeys learn the association between viewing certain cues and cooperating (fixating on the reward or partner can cause either monkey to push, receiving reward), and learn that pushing and holding the buttons together leads to reward. As learning occurs, animals increase viewing of social cues before pushing (**Fig.13**), so increased spiking coordination between V4 and dIPFC during these times could elicit synaptic changes between neurons within each area (Hedrick et al., 2022), thus improving encoding of sensory and/or decision-making signals within each region, resulting in the improved motor output that I observed via decreased reaction times and increased action coordination across sessions. The increased magnitude of coordinated spiking between V4 and dIPFC is likely influenced by reward prediction error or causal association signals from dopaminergic neurons in the ventral tegmental area, as cortico-striatal synapses are a site of plasticity during associative learning and could strengthen specific feedforward sensory input synapses from V4 to dIPFC neurons involved in social decisions (Jeong et al., 2022; Law & Gold, 2009; Makino et al., 2016; Pasupathy & Miller, 2005; Schultz, 1998; Xiong et al., 2015).

## **CHAPTER 5: DISCUSSION**

### ***5.1 Summary of findings***

“The eyes of men converse as much as their tongues, with the advantage that the ocular dialect needs no dictionary, but is understood all the world over.”

- Ralph Waldo Emerson, 1876

Essentially, vision is the social language of primates.

Social interaction, especially cooperation, requires interpretation and exchange of sensory information, including relevant visual cues, among interacting agents. However, it has long been unclear how visual information is encoded and passed on to executive areas to guide social decisions and learning cooperation behavior. My results reveal that across sessions, animals learn to cooperate by improving the coordination of their actions and reaction times. Further, animals become more likely to cooperate after viewing social cues. This is supported by the increase in coordinated spiking between visual and prefrontal cortical neurons during learning to cooperate, which was associated with improved accuracy of neural populations to encode social cues and the decision to cooperate. This provides the first evidence for the role of visual cortex in encoding of socially relevant information. Somewhat surprisingly, dIPFC neurons outperformed those in V4 in their ability to discriminate between multiple visual social cues, such as fixations on reward and partner, and those on social and non-socially relevant information. This is likely due to the fact that dIPFC receives and integrates diverse sensory modalities (E. K. Miller & Cohen, 2001; Wang et al., 2015), which may enable a better prediction of highly-dimensional incoming stimuli. Overall, V4 and dIPFC neurons prioritize socially pertinent visual information that is used to improve coding of social decisions in dIPFC. These computations highlight the importance of visual monitoring to determine actions of oneself and predict or even influence other's actions in the creation of purposeful social behavior.

Here, I propose a social cooperation learning model whereby an increase in coordinated spiking between feedforward visuo-frontal circuits during social viewing improves the coding of social events and distributes their representation in each area (**Fig. 27**). This model is supported by the finding that, remarkably, the strongest coupled neurons across areas were those that contributed the most to the encoding of social events. Furthermore, early during learning, a select number of cells contributed most to social interactions compared to the rest of the population. However, as learning progressed, the information about social and decision-making signals



became more evenly distributed across the neural population. Essentially, *inter-areal* neurons that fire together, wire together (Hebb, 1949; Shatz, 1992), to distribute and contribute social information among *intra-areal* neurons. This is consistent with sensorimotor associative learning models in which Hebbian plasticity may occur during coincident responses between brain areas during task-relevant stimulus-response events (Makino et al., 2016; Xu et al., 2012). As learning progresses, animals increase viewing of social cues before deciding to cooperate (**Fig. 13**). Thus, increased spiking coordination between V4 and dlPFC during viewing social cues could elicit synaptic changes between neurons within each area (Hedrick et al., 2022). Subsequently, the improved encoding of sensory and decision-making signals within each cortical area may underlie the improved motor output observed via decreased reaction times and increased action coordination across sessions (**Fig. 5-6**).

Finally, by allowing animals to move freely during social cooperation, this study represents a pioneering move toward examining the neural underpinnings of naturalistic behavior in a free-roaming setting. While this paradigm shift has long been suggested (Dell et al., 2014; Ghazanfar & Santos, 2004; Wallace & Hofmann, 2021), recent advances in low-power, high-throughput electrophysiological devices coupled with wireless behavioral monitoring and large-scale computing (Fernandez-Leon et al., 2015; Milton et al., 2020; Shahidi et al., 2022) made this research feasible only now. Critical to this work is simultaneous use of wireless neural and eye tracking recordings to examine how visual events and social cues guide the decision to cooperate. Analyzing the relationship between the behavioral repertoires of each freely interacting agent allowed me to uncover the neural computations involving prioritization of social visual cues that were essential to social learning. Thus, vision may be the social language of primates likely governing learning of various social activities, such as grooming, play, and collective foraging. A shift toward more natural behavior in which multi-sensory information is recorded wirelessly in conjunction with large-scale population recordings will be essential for understanding neural mechanisms of social cognition (Fan et al., 2021; C. T. Miller et al., 2022). Collectively, my findings reveal a visuo-frontal cortical network representation of learning visually

driven cooperation in the primate brain, inspiring research that promotes holistic understanding of how multiple brain areas guide social interactions in our increasingly social world.

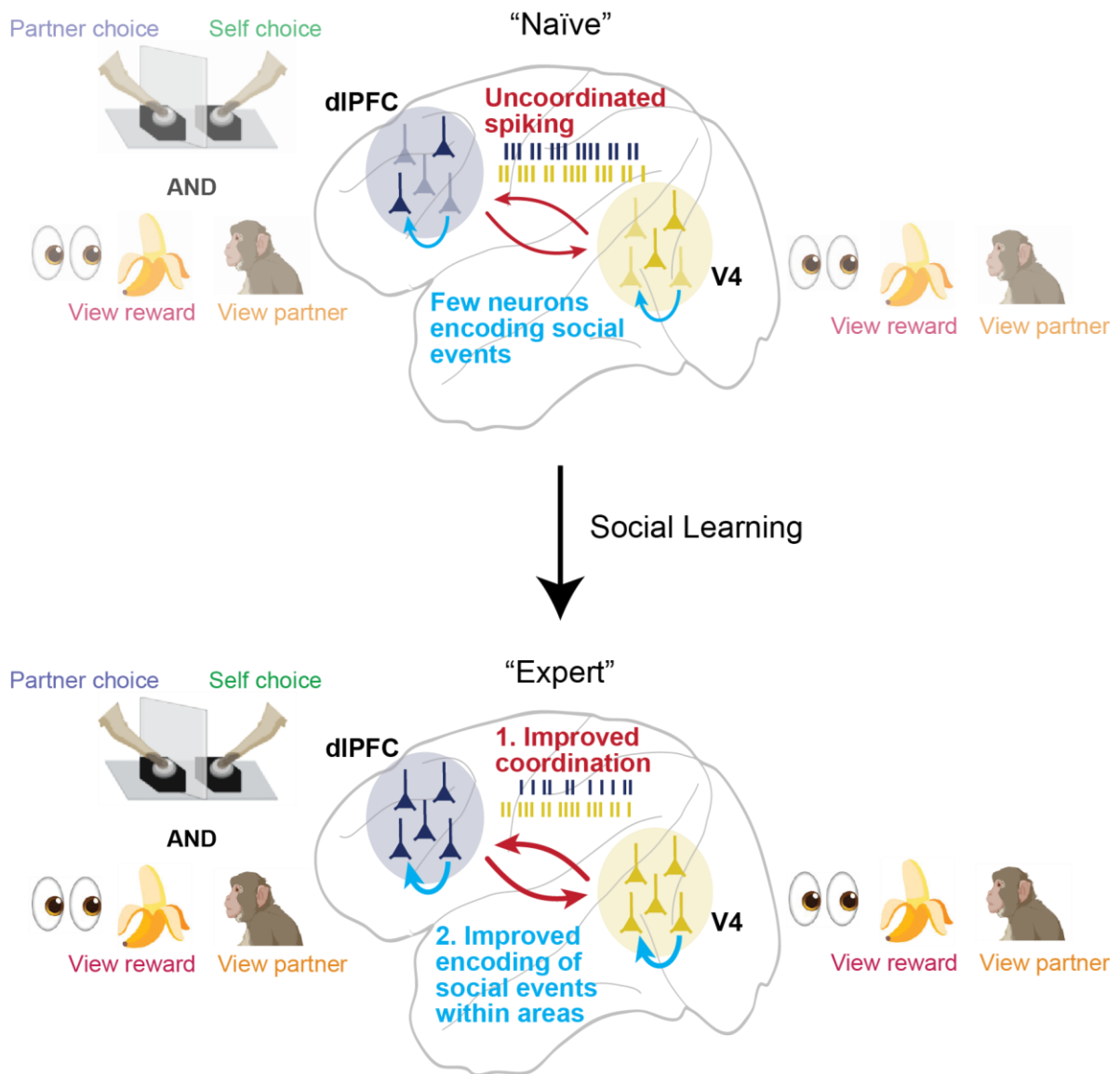


**Figure 27. Social learning summary.** In early sessions when the animals were naïve to cooperation, the timing of spiking activity between areas was not coordinated during social events and a few neurons encoded most of the social information relative to the rest of the population. As learning progresses, mostly feedforward spike timing coordination improves between regions during social events and subsequently, information is more evenly distributed among neurons, correlating with improved encoding of social events within each area. V4 improves encoding of social visual cues whereas dIPFC improves encoding of social visual cues and decisions of self and other.

## **5.2 Limitations and future directions**

While this innovative approach combining wireless eye tracking and neural recordings provides discovery of neural computations that subserve learning of voluntary social behavior, every study has its limitations. Probably the most apparent limitation is that I did not perform combined neural and eye tracking recordings from both monkeys simultaneously. When my experiments began in 2017, it was not technologically possible to accomplish this feat. However, the technology exists today and future studies in social cognition should examine the neural correlates of interacting agents simultaneously. This would be particularly valuable in the context of social learning and in order to study teacher-learner interactions where both agents are concurrently engaged in the learning process – observing, imitating, and learning from and with each other (De Felice et al., 2022; Gariépy et al., 2014). One could examine the neural mechanisms underlying gaze information from each agent prior to vocal communication or action exchange between agents. Cognitive research of such an interactive process would contribute valuable information to social neuroscience.

A central dogma in neuroscience is that dopaminergic projections from the ventral tegmental area to limbic regions including the prefrontal cortex mediate learning by modulating synaptic plasticity through reinforcement and prediction error (Dioconescu et al., 2017; Schultz, 1998) or causal associative signaling (Jeong et al., 2022) . Therefore, it would be beneficial to measure dopamine levels in cortex during social learning. One way this could be done is through fast-scan cyclic voltammetry (FCSV), which is a technique that uses a carbon fiber electrode to measure changes in dopamine concentrations in a behaving animal in real time (Venton & Cao, 2020). FCSV could be paired with chronic electrophysiological recordings to measure changes in dopamine and neural activity, respectively, in any brain region. Analyzing dopamine levels and neural activity simultaneously during social learning would inform whether changes in dopamine correlate with changes in the neural population and network representations I observed here.

Although primates rely heavily on visual cues during social behavior, social interactions are extremely complex and involve multisensory integration. Future research should investigate how other sensory cues, such as odors, vocalizations, and touch (Contestabile et al., 2021; Froesel et al., 2022; Jovanovic et al., 2022; Martin et al., 2023) , complement visual information to guide neural computations underlying social decisions. Additionally, most primates live in groups and exhibit a social hierarchy (Noonan et al., 2014; Schulke et al., 2010). Therefore, features such as social identity, rank, and familiarity likely influence social decisions and sensory cues exchanged amongst individuals (Gachomba et al., 2022; Ghazanfar & Santos, 2004). A study examining neural processing of these multimodal cues and social relationships could identify whether certain behaviors are salient or irrelevant for specific types of social interactions. For instance, investigating the neural basis of multisensory events that constitute distinct social behaviors such as grooming and fighting/competition would elucidate neural mechanisms that facilitate integration of sensory cues and social status to support social competence. Overall, combined multiplexed behavioral and neural recordings from a network of brain regions during rich, naturalistic social behavior will enable a more wholistic understanding of social cognition. Such knowledge could potentially provide novel behavioral or neural strategies for interacting with others during different social roles (i.e. - parenting vs. professional leadership) and for improving neuropsychiatric disorders.

### ***5.3 Clinical applications***

Elucidating the correct functioning of the social cognition system has profound implications for human health. Understanding the neural basis of social interactions can help us comprehend the complex behaviors and emotions that underlie our social relationships. Unfortunately, persistent deficits in social interaction and communication characterize many neuropsychiatric disorders, especially ASD, schizophrenia, and depression, affecting millions of people worldwide (Association, 2013; Winsky et al., 2008). Importantly, the findings from this study contribute to our limited knowledge about the neural computations underlying advanced

forms of *learning* social interaction, such as cooperation. The discoveries described here can have significant consequences for human health and well-being, including improved treatments for psychiatric disorders and enhanced social functioning in everyday life.

First, this work exposes how two cortical brain regions process and respond to real, three-dimensional, social stimuli, such as viewing another conspecific and the reward for performing a social action (cooperating) in a naturalistic, free roaming environment. This research revealed that neural population encoding within each region and spiking coordination between brain regions during viewing social, but not non-social, stimuli improved while animals learned to cooperate and social stimuli became more salient. Therefore, such selective improvement in neural encoding of social stimuli indicates this visual information is valuable during social behavior. With this knowledge, wireless eye tracking methods like those used here can be employed for individuals with social dysfunction to promote viewing of salient social information. Indeed, closed-loop therapeutic activities could be incorporated into daily behavior where an individual receives a local food/juice reward for viewing salient social information, such as viewing the person who is speaking or even fixating on the lips or eyes of others when engaging in social interaction. Such a real-time, feedback driven system would help individuals associate social stimuli as rewarding, improving healthy development of social interactions.

In addition to informing behavioral therapies, this research furthers development of neural enhancement of social behavior, which would be especially helpful for individuals with severe social deficits. For example, when behavioral therapy or medications fail, alternative forms of treatment involving brain stimulation and/or implants to a specific brain area are considered (Qiu et al., 2021; Wickelgren, 2018). This work demonstrates how, unlike the role of the mirror neuron system which engages during action observation and execution (Fogassi & Ferrari, 2011; Rozzi et al., 2008), dlPFC is involved in *predicting* another agent's action as well as planning an individual's own action. This finding motivates dlPFC as a potential target for neurotherapy. Moreover, this work informs studies using neurofeedback to train individuals with autism to

interpret social cues, which have shown promising results in improving an individual's social functioning and reducing disadvantageous symptoms (Datko et al., 2018; Friedrich et al., 2015).

Lastly, this research can help us develop better tools for enhancing our social skills and improving our everyday functioning. Social skills are essential for success in both personal and professional contexts. The neural basis of viewing social information discovered from this work informs the development of interventions to improve our social skills, such as training programs to improve social cognition or virtual reality simulations to enhance social communication. These interventions can have practical applications in various settings, such as schools, workplaces, and mental health clinics, helping individuals to improve their social interactions and overall quality of life.

## BIBLIOGRAPHY

- Aquino, T. G., Minxha, J., Dunne, S., Ross, I. B., Mamelak, A. N., Rutishauser, U., & O'Doherty, J. P. (2020). Value-Related Neuronal Responses in the Human Amygdala during Observational Learning. *The Journal of Neuroscience : The Official Journal of the Society for Neuroscience*, *40*(24), 4761–4772. <https://doi.org/10.1523/JNEUROSCI.2897-19.2020>
- Association, A. P. (2013). *DSM 5*. American Psychiatric Association.
- Báez-Mendoza, R., Mastrobattista, E. P., Wang, A. J., & Williams, Z. M. (2021). Social agent identity cells in the prefrontal cortex of interacting groups of primates. *Science (New York, N.Y.)*, *374*(6566), eabb4149. <https://doi.org/10.1126/science.abb4149>
- Bair, W., Zohary, E., & Newsome, W. T. (2001). Correlated firing in macaque visual area MT: time scales and relationship to behavior. *The Journal of Neuroscience : The Official Journal of the Society for Neuroscience*, *21*(5), 1676–1697.
- BARON-COHEN, S., & CROSS, P. (1992). Reading the Eyes: Evidence for the Role of Perception in the Development of a Theory of Mind. *Mind & Language*, *7*(1–2), 172–186. <https://doi.org/https://doi.org/10.1111/j.1468-0017.1992.tb00203.x>
- Benjamini, Y., & Hochberg, Y. (1995). Controlling the False Discovery Rate: A Practical and Powerful Approach to Multiple Testing. *Journal of the Royal Statistical Society: Series B (Methodological)*, *57*(1), 289–300. <https://doi.org/https://doi.org/10.1111/j.2517-6161.1995.tb02031.x>
- Bishop, C. M. (n.d.). *Pattern recognition and machine learning*. New York : Springer, [2006] ©2006. <https://search.library.wisc.edu/catalog/9910032530902121>
- Björklund, A., & Dunnett, S. B. (2007). Dopamine neuron systems in the brain: an update. *Trends in Neurosciences*, *30*(5), 194–202. <https://doi.org/10.1016/j.tins.2007.03.006>
- Botvinick, M. M. (2007). Multilevel structure in behaviour and in the brain: a model of Fuster's hierarchy. *Philosophical Transactions of the Royal Society of London. Series B, Biological*

*Sciences*, 362(1485), 1615–1626. <https://doi.org/10.1098/rstb.2007.2056>

Brincat, S. L., Siegel, M., von Nicolai, C., & Miller, E. K. (2018). Gradual progression from sensory to task-related processing in cerebral cortex. *Proceedings of the National Academy of Sciences of the United States of America*, 115(30), E7202–E7211. <https://doi.org/10.1073/pnas.1717075115>

Brosnan, S. F., & de Waal, F. B. M. (2014). Evolution of responses to (un)fairness. *Science (New York, N.Y.)*, 346(6207), 1251776. <https://doi.org/10.1126/science.1251776>

Brosnan, S. F., & De Waal, F. B. M. (2003). Monkeys reject unequal pay. *Nature*, 425(6955), 297–299. <https://doi.org/10.1038/nature01963>

Burke, C. J., Tobler, P. N., Baddeley, M., & Schultz, W. (2010). Neural mechanisms of observational learning. *Proceedings of the National Academy of Sciences of the United States of America*, 107(32), 14431–14436. <https://doi.org/10.1073/pnas.1003111107>

Chang, S. W. C., Gariépy, J.-F., & Platt, M. L. (2013). Neuronal reference frames for social decisions in primate frontal cortex. *Nature Neuroscience*, 16(2), 243–250. <https://doi.org/10.1038/nn.3287>

Choi, H., Pasupathy, A., & Shea-Brown, E. (2018). Predictive Coding in Area V4: Dynamic Shape Discrimination under Partial Occlusion. *Neural Computation*, 30(5), 1209–1257. [https://doi.org/10.1162/NECO\\_a\\_01072](https://doi.org/10.1162/NECO_a_01072)

Contestabile, A., Casarotto, G., Girard, B., Tzanoulinou, S., & Bellone, C. (2021). Deconstructing the contribution of sensory cues in social approach. *The European Journal of Neuroscience*, 53(9), 3199–3211. <https://doi.org/10.1111/ejn.15179>

Cross, E. S. (2012). *Observational Learning of Complex Motor Skills: Dance BT - Encyclopedia of the Sciences of Learning* (N. M. Seel (ed.); pp. 2491–2493). Springer US. [https://doi.org/10.1007/978-1-4419-1428-6\\_78](https://doi.org/10.1007/978-1-4419-1428-6_78)

Dal Monte, O., Fan, S., Fagan, N. A., Chu, C.-C. J., Zhou, M. B., Putnam, P. T., Nair, A. R., & Chang, S. W. C. (2022). Widespread implementations of interactive social gaze neurons in



the primate prefrontal-amygdala networks. *Neuron*, 110(13), 2183-2197.e7.  
<https://doi.org/10.1016/j.neuron.2022.04.013>

Datko, M., Pineda, J. A., & Müller, R.-A. (2018). Positive effects of neurofeedback on autism symptoms correlate with brain activation during imitation and observation. *The European Journal of Neuroscience*, 47(6), 579–591. <https://doi.org/10.1111/ejn.13551>

De Felice, S., Hamilton, A. F. de C., Ponari, M., & Vigliocco, G. (2022). Learning from others is good, with others is better: the role of social interaction in human acquisition of new knowledge. *Philosophical Transactions of the Royal Society B: Biological Sciences*, 378(1870), 20210357. <https://doi.org/10.1098/rstb.2021.0357>

Dell, A. I., Bender, J. A., Branson, K., Couzin, I. D., de Polavieja, G. G., Noldus, L. P. J. J., Pérez-Escudero, A., Perona, P., Straw, A. D., Wikelski, M., & Brose, U. (2014). Automated image-based tracking and its application in ecology. *Trends in Ecology & Evolution*, 29(7), 417–428. <https://doi.org/10.1016/j.tree.2014.05.004>

di Pellegrino, G., Fadiga, L., Fogassi, L., Gallese, V., & Rizzolatti, G. (1992). Understanding motor events: a neurophysiological study. *Experimental Brain Research*, 91(1), 176–180. <https://doi.org/10.1007/BF00230027>

Diaconescu, A. O., Mathys, C., Weber, L. A. E., Kasper, L., Mauer, J., & Stephan, K. E. (2017). Hierarchical prediction errors in midbrain and septum during social learning. *Social Cognitive and Affective Neuroscience*, 12(4), 618–634. <https://doi.org/10.1093/scan/nsw171>

Dickey, A. S., Suminski, A., Amit, Y., & Hatsopoulos, N. G. (2009). Single-unit stability using chronically implanted multielectrode arrays. *Journal of Neurophysiology*, 102(2), 1331–1339. <https://doi.org/10.1152/jn.90920.2008>

Emery, N. J. (2000). The eyes have it: the neuroethology, function and evolution of social gaze. *Neuroscience & Biobehavioral Reviews*, 24(6), 581–604. [https://doi.org/https://doi.org/10.1016/S0149-7634\(00\)00025-7](https://doi.org/https://doi.org/10.1016/S0149-7634(00)00025-7)

- Emery, N. J., Lorincz, E. N., Perrett, D. I., Oram, M. W., & Baker, C. I. (1997). Gaze following and joint attention in rhesus monkeys (*Macaca mulatta*). *Journal of Comparative Psychology (Washington, D.C. : 1983)*, 111(3), 286–293. <https://doi.org/10.1037/0735-7036.111.3.286>
- Falcone, R., Brunamonti, E., Ferraina, S., & Genovesio, A. (2016). Neural Encoding of Self and Another Agent's Goal in the Primate Prefrontal Cortex: Human-Monkey Interactions. *Cerebral Cortex (New York, N.Y. : 1991)*, 26(12), 4613–4622. <https://doi.org/10.1093/cercor/bhv224>
- Fan, S., Dal Monte, O., & Chang, S. W. C. (2021). Levels of naturalism in social neuroscience research. *iScience*, 24(7), 102702. <https://doi.org/10.1016/j.isci.2021.102702>
- Feng, C., Eickhoff, S. B., Li, T., Wang, L., Becker, B., Camilleri, J. A., Héту, S., & Luo, Y. (2021). Common brain networks underlying human social interactions: evidence from large-scale neuroimaging meta-analysis. *Neuroscience & Biobehavioral Reviews*. <https://doi.org/https://doi.org/10.1016/j.neubiorev.2021.03.025>
- Fernandez-Leon, J. A., Parajuli, A., Franklin, R., Sorenson, M., Felleman, D. J., Hansen, B. J., Hu, M., & Dragoi, V. (2015). A wireless transmission neural interface system for unconstrained non-human primates. *Journal of Neural Engineering*, 12(5), 56005. <https://doi.org/10.1088/1741-2560/12/5/056005>
- Fernández, M., Mollinedo-Gajate, I., & Peñagarikano, O. (2018). Neural Circuits for Social Cognition: Implications for Autism. *Neuroscience*, 370, 148–162. <https://doi.org/https://doi.org/10.1016/j.neuroscience.2017.07.013>
- Fine, J. M., & Hayden, B. Y. (2022). The whole prefrontal cortex is premotor cortex. *Philosophical Transactions of the Royal Society of London. Series B, Biological Sciences*, 377(1844), 20200524. <https://doi.org/10.1098/rstb.2020.0524>
- Fletcher, G. E. (2008). Attending to the outcome of others: disadvantageous inequity aversion in male capuchin monkeys (*Cebus apella*). *American Journal of Primatology*, 70(9), 901–905. <https://doi.org/10.1002/ajp.20576>

- Fogassi, L., & Ferrari, P. F. (2011). Mirror systems. *Wiley Interdisciplinary Reviews. Cognitive Science*, 2(1), 22–38. <https://doi.org/10.1002/wcs.89>
- Friedrich, E. V. C., Sivanathan, A., Lim, T., Suttie, N., Louchart, S., Pillen, S., & Pineda, J. A. (2015). An Effective Neurofeedback Intervention to Improve Social Interactions in Children with Autism Spectrum Disorder. *Journal of Autism and Developmental Disorders*, 45(12), 4084–4100. <https://doi.org/10.1007/s10803-015-2523-5>
- Froesel, M., Gacoin, M., Clavagnier, S., Hauser, M., Goudard, Q., & Ben Hamed, S. (2022). Socially meaningful visual context either enhances or inhibits vocalisation processing in the macaque brain. *Nature Communications*, 13(1), 4886. <https://doi.org/10.1038/s41467-022-32512-9>
- Fusi, S., Miller, E. K., & Rigotti, M. (2016). Why neurons mix: high dimensionality for higher cognition. *Current Opinion in Neurobiology*, 37, 66–74. <https://doi.org/10.1016/j.conb.2016.01.010>
- Fuster, J. M. (2000). Executive frontal functions. *Experimental Brain Research*, 133(1), 66–70. <https://doi.org/10.1007/s002210000401>
- Fuster, J. M., & Bressler, S. L. (2015). Past makes future: role of pFC in prediction. *Journal of Cognitive Neuroscience*, 27(4), 639–654. [https://doi.org/10.1162/jocn\\_a\\_00746](https://doi.org/10.1162/jocn_a_00746)
- Gachomba, M. J. M., Esteve-Agraz, J., Caref, K., Maroto, A. S., Bortolozzo-Gleich, M. H., Laplagne, D. A., & Márquez, C. (2022). Multimodal cues displayed by submissive rats promote prosocial choices by dominants. *Current Biology: CB*. <https://doi.org/10.1016/j.cub.2022.06.026>
- Gallant, J. L., Connor, C. E., & Van Essen, D. C. (1998). Neural activity in areas V1, V2 and V4 during free viewing of natural scenes compared to controlled viewing. *Neuroreport*, 9(7), 1673–1678. <https://doi.org/10.1097/00001756-199805110-00075>
- Gariépy, J.-F., Watson, K. K., Du, E., Xie, D. L., Erb, J., Amasino, D., & Platt, M. L. (2014). Social learning in humans and other animals. *Frontiers in Neuroscience*, 8, 58.

<https://doi.org/10.3389/fnins.2014.00058>

Ghazanfar, A. A., & Santos, L. R. (2004). Primate brains in the wild: the sensory bases for social interactions. *Nature Reviews. Neuroscience*, 5(8), 603–616.

<https://doi.org/10.1038/nrn1473>

Grabenhorst, F., Báez-Mendoza, R., Genest, W., Deco, G., & Schultz, W. (2019). Primate Amygdala Neurons Simulate Decision Processes of Social Partners. *Cell*, 177(4), 986–998.e15. <https://doi.org/10.1016/j.cell.2019.02.042>

Gregoriou, G. G., Rossi, A. F., Ungerleider, L. G., & Desimone, R. (2014). Lesions of prefrontal cortex reduce attentional modulation of neuronal responses and synchrony in V4. *Nature Neuroscience*, 17(7), 1003–1011. <https://doi.org/10.1038/nn.3742>

Haile, T. M., Bohon, K. S., Romero, M. C., & Conway, B. R. (2019). Visual stimulus-driven functional organization of macaque prefrontal cortex. *NeuroImage*, 188, 427–444. <https://doi.org/10.1016/j.neuroimage.2018.11.060>

Haroush, K., & Williams, Z. M. (2015). Neuronal prediction of opponent's behavior during cooperative social interchange in primates. *Cell*, 160(6), 1233–1245. <https://doi.org/10.1016/j.cell.2015.01.045>

Haruno, M., & Kawato, M. (2006). Heterarchical reinforcement-learning model for integration of multiple cortico-striatal loops: fMRI examination in stimulus-action-reward association learning. *Neural Networks*, 19(8), 1242–1254. <https://doi.org/https://doi.org/10.1016/j.neunet.2006.06.007>

Hebb, D. O. (1949). *The organisation of behaviour*, New York. Wiley.

Hedrick, N. G., Lu, Z., Bushong, E., Singhi, S., Nguyen, P., Magaña, Y., Jilani, S., Lim, B. K., Ellisman, M., & Komiyama, T. (2022). Learning binds new inputs into functional synaptic clusters via spinogenesis. *Nature Neuroscience*, 25(6), 726–737. <https://doi.org/10.1038/s41593-022-01086-6>

Heekeren, H. R., Marrett, S., Bandettini, P. A., & Ungerleider, L. G. (2004). A general mechanism

- for perceptual decision-making in the human brain. *Nature*, 431(7010), 859–862.  
<https://doi.org/10.1038/nature02966>
- Jamali, M., Grannan, B. L., Fedorenko, E., Saxe, R., Báez-Mendoza, R., & Williams, Z. M. (2021). Single-neuronal predictions of others' beliefs in humans. *Nature*, 591(7851), 610–614.  
<https://doi.org/10.1038/s41586-021-03184-0>
- Jeong, H., Taylor, A., Floeder, J. R., Lohmann, M., Mihalas, S., Wu, B., Zhou, M., Burke, D. A., & Nambodiri, V. M. K. (2022). Mesolimbic dopamine release conveys causal associations. *Science (New York, N.Y.)*, 378(6626), eabq6740. <https://doi.org/10.1126/science.abq6740>
- Jovanovic, V., Fishbein, A. R., de la Mothe, L., Lee, K.-F., & Miller, C. T. (2022). Behavioral context affects social signal representations within single primate prefrontal cortex neurons. *Neuron*, 110(8), 1318-1326.e4. <https://doi.org/10.1016/j.neuron.2022.01.020>
- Kim, T., Bair, W., & Pasupathy, A. (2019). Neural Coding for Shape and Texture in Macaque Area V4. *The Journal of Neuroscience : The Official Journal of the Society for Neuroscience*, 39(24), 4760–4774. <https://doi.org/10.1523/JNEUROSCI.3073-18.2019>
- Kingsbury, L., Huang, S., Wang, J., Gu, K., Golshani, P., Wu, Y. E., & Hong, W. (2019). Correlated Neural Activity and Encoding of Behavior across Brains of Socially Interacting Animals. *Cell*, 178(2), 429-446.e16. <https://doi.org/10.1016/j.cell.2019.05.022>
- Kobatake, E., & Tanaka, K. (1994). Neuronal selectivities to complex object features in the ventral visual pathway of the macaque cerebral cortex. *Journal of Neurophysiology*, 71(3), 856–867. <https://doi.org/10.1152/jn.1994.71.3.856>
- Kolster, H., Janssens, T., Orban, G. A., & Vanduffel, W. (2014). The retinotopic organization of macaque occipitotemporal cortex anterior to V4 and caudoventral to the middle temporal (MT) cluster. *The Journal of Neuroscience : The Official Journal of the Society for Neuroscience*, 34(31), 10168–10191. <https://doi.org/10.1523/JNEUROSCI.3288-13.2014>
- Koren, V. (2021). Uncovering structured responses of neural populations recorded from macaque monkeys with linear support vector machines. *STAR Protocols*, 2(3), 100746.

<https://doi.org/https://doi.org/10.1016/j.xpro.2021.100746>

- Laland, K. N., & Rendell, L. (2010). *Social Learning: Theory* (J. C. B. T.-E. of A. B. (Second E. Choe (ed.); pp. 380–386). Academic Press. <https://doi.org/https://doi.org/10.1016/B978-0-12-813251-7.00057-2>
- Law, C.-T., & Gold, J. I. (2009). Reinforcement learning can account for associative and perceptual learning on a visual-decision task. *Nature Neuroscience*, *12*(5), 655–663. <https://doi.org/10.1038/nn.2304>
- Li, S. W., Zeliger, O., Strahs, L., Báez-Mendoza, R., Johnson, L. M., McDonald Wojciechowski, A., & Williams, Z. M. (2022). Frontal neurons driving competitive behaviour and ecology of social groups. *Nature*, *603*(7902), 661–666. <https://doi.org/10.1038/s41586-021-04000-5>
- Lidow, M. S., Goldman-Rakic, P. S., Gallager, D. W., & Rakic, P. (1991). Distribution of dopaminergic receptors in the primate cerebral cortex: quantitative autoradiographic analysis using [3H]raclopride, [3H]spiperone and [3H]SCH23390. *Neuroscience*, *40*(3), 657–671. [https://doi.org/10.1016/0306-4522\(91\)90003-7](https://doi.org/10.1016/0306-4522(91)90003-7)
- Luo, T. Z., & Maunsell, J. H. R. (2018). Attentional Changes in Either Criterion or Sensitivity Are Associated with Robust Modulations in Lateral Prefrontal Cortex. *Neuron*, *97*(6), 1382–1393.e7. <https://doi.org/10.1016/j.neuron.2018.02.007>
- Maestriperi, D., & Georgiev, A. V. (2016). What cortisol can tell us about the costs of sociality and reproduction among free-ranging rhesus macaque females on Cayo Santiago. *American Journal of Primatology*, *78*(1), 92–105. <https://doi.org/10.1002/ajp.22368>
- Mahalanobis, P. (n.d.). C.(1936). On the generalised distance in statistics. *Proc. of the Nation. Acad. Sci.,(India)*, *2*, 45–49.
- Makino, H., Hwang, E. J., Hedrick, N. G., & Komiyama, T. (2016). Circuit Mechanisms of Sensorimotor Learning. *Neuron*, *92*(4), 705–721. <https://doi.org/10.1016/j.neuron.2016.10.029>
- Martin, A. B., Cardenas, M. A., Andersen, R. K., Bowman, A. I., Hillier, E. A., Bensmaia, S.,

- Fuglevand, A. J., & Gothard, K. M. (2023). A context-dependent switch from sensing to feeling in the primate amygdala. *Cell Reports*, 42(2). <https://doi.org/10.1016/j.celrep.2023.112056>
- Mathis, A., Mamidanna, P., Cury, K. M., Abe, T., Murthy, V. N., Mathis, M. W., & Bethge, M. (2018). DeepLabCut: markerless pose estimation of user-defined body parts with deep learning. *Nature Neuroscience*, 21(9), 1281–1289. <https://doi.org/10.1038/s41593-018-0209-y>
- McMahon, D. B. T., Russ, B. E., Elnaiem, H. D., Kurnikova, A. I., & Leopold, D. A. (2015). Single-unit activity during natural vision: diversity, consistency, and spatial sensitivity among AF face patch neurons. *The Journal of Neuroscience: The Official Journal of the Society for Neuroscience*, 35(14), 5537–5548. <https://doi.org/10.1523/JNEUROSCI.3825-14.2015>
- Mendres, & FB, de W. (2000). Capuchins do cooperate: the advantage of an intuitive task. *Animal Behaviour*, 60(4), 523–529. <https://doi.org/10.1006/anbe.2000.1512>
- Mesterton-gibbons, & Dugatkin. (1997). Cooperation and the Prisoner's Dilemma: towards testable models of mutualism versus reciprocity. *Animal Behaviour*, 54(3), 551–557.
- Miller, C. T., Gire, D., Hoke, K., Huk, A. C., Kelley, D., Leopold, D. A., Smear, M. C., Theunissen, F., Yartsev, M., & Niell, C. M. (2022). Natural behavior is the language of the brain. *Current Biology: CB*, 32(10), R482–R493. <https://doi.org/10.1016/j.cub.2022.03.031>
- Miller, E. K., & Cohen, J. D. (2001). An integrative theory of prefrontal cortex function. *Annual Review of Neuroscience*, 24, 167–202. <https://doi.org/10.1146/annurev.neuro.24.1.167>
- Miller, E. K., Erickson, C. A., & Desimone, R. (1996). Neural mechanisms of visual working memory in prefrontal cortex of the macaque. *The Journal of Neuroscience: The Official Journal of the Society for Neuroscience*, 16(16), 5154–5167. <https://doi.org/10.1523/JNEUROSCI.16-16-05154.1996>
- Milton, R., Shahidi, N., & Dragoi, V. (2020). Dynamic states of population activity in prefrontal cortical networks of freely-moving macaque. *Nature Communications*, 11(1), 1948.

<https://doi.org/10.1038/s41467-020-15803-x>

- Moessnang, C., Otto, K., Bilek, E., Schäfer, A., Baumeister, S., Hohmann, S., Poustka, L., Brandeis, D., Banaschewski, T., Tost, H., & Meyer-Lindenberg, A. (2017). Differential responses of the dorsomedial prefrontal cortex and right posterior superior temporal sulcus to spontaneous mentalizing. *Human Brain Mapping, 38*(8), 3791–3803. <https://doi.org/10.1002/hbm.23626>
- Molesti, S., & Majolo, B. (2016). Cooperation in wild Barbary macaques: factors affecting free partner choice. *Animal Cognition, 19*(1), 133–146. <https://doi.org/10.1007/s10071-015-0919-4>
- Mosher, C. P., Zimmerman, P. E., & Gothard, K. M. (2014). Neurons in the Monkey Amygdala Detect Eye Contact during Naturalistic Social Interactions. *Current Biology, 24*(20), 2459–2464. <https://doi.org/https://doi.org/10.1016/j.cub.2014.08.063>
- Musall, S., Kaufman, M. T., Juavinett, A. L., Gluf, S., & Churchland, A. K. (2019). Single-trial neural dynamics are dominated by richly varied movements. *Nature Neuroscience, 22*(10), 1677–1686. <https://doi.org/10.1038/s41593-019-0502-4>
- Nahm, F. K., Perret, A., Amaral, D. G., & Albright, T. D. (1997). How do monkeys look at faces? *Journal of Cognitive Neuroscience, 9*(5), 611–623. <https://doi.org/10.1162/jocn.1997.9.5.611>
- Niell, C. M., & Stryker, Mi. P. (2010). Modulation of visual responses by behavioral state in mouse visual cortex. *Neuron, 65*(4), 472–479.
- Noonan, M. P., Sallet, J., Mars, R. B., Neubert, F. X., O'Reilly, J. X., Andersson, J. L., Mitchell, A. S., Bell, A. H., Miller, K. L., & Rushworth, M. F. S. (2014). A neural circuit covarying with social hierarchy in macaques. *PLoS Biology, 12*(9), e1001940. <https://doi.org/10.1371/journal.pbio.1001940>
- Noritake, A., Ninomiya, T., & Isoda, M. (2018). Social reward monitoring and valuation in the macaque brain. *Nature Neuroscience, 21*(10), 1452–1462. <https://doi.org/10.1038/s41593->



- Noudoost, B., & Moore, T. (2011). Control of visual cortical signals by prefrontal dopamine. *Nature*, 474(7351), 372–375. <https://doi.org/10.1038/nature09995>
- O’Connell, L. A., & Hofmann, H. A. (2012). Evolution of a vertebrate social decision-making network. *Science (New York, N.Y.)*, 336(6085), 1154–1157. <https://doi.org/10.1126/science.1218889>
- Okazawa, G., Tajima, S., & Komatsu, H. (2015). Image statistics underlying natural texture selectivity of neurons in macaque V4. *Proceedings of the National Academy of Sciences of the United States of America*, 112(4), E351-60. <https://doi.org/10.1073/pnas.1415146112>
- Ong, W. S., Madlon-Kay, S., & Platt, M. L. (2020). Neuronal correlates of strategic cooperation in monkeys. *Nature Neuroscience*. <https://doi.org/10.1038/s41593-020-00746-9>
- Padilla-Coreano, N., Batra, K., Patarino, M., Chen, Z., Rock, R. R., Zhang, R., Hausmann, S. B., Weddington, J. C., Patel, R., Zhang, Y. E., Fang, H.-S., Mishra, S., LeDuke, D. O., Revanna, J., Li, H., Borio, M., Pamintuan, R., Bal, A., Keyes, L. R., Libster, A., Wichmann, R., Mills, F., Taschbach, F. H., Matthews, G. A., Curley, J. P., Fiete, I. R., Lu, C., & Tye, K. M. (2022). Cortical ensembles orchestrate social competition through hypothalamic outputs. *Nature*, 603(7902), 667–671. <https://doi.org/10.1038/s41586-022-04507-5>
- Parthasarathy, A., Herikstad, R., Bong, J. H., Medina, F. S., Libedinsky, C., & Yen, S.-C. (2017). Mixed selectivity morphs population codes in prefrontal cortex. *Nature Neuroscience*, 20(12), 1770–1779. <https://doi.org/10.1038/s41593-017-0003-2>
- Pasupathy, A., & Connor, C. E. (1999). Responses to contour features in macaque area V4. *Journal of Neurophysiology*, 82(5), 2490–2502. <https://doi.org/10.1152/jn.1999.82.5.2490>
- Pasupathy, A., & Connor, C. E. (2002). Population coding of shape in area V4. *Nature Neuroscience*, 5(12), 1332–1338. <https://doi.org/10.1038/nn972>
- Pasupathy, A., & Miller, E. K. (2005). Different time courses of learning-related activity in the prefrontal cortex and striatum. *Nature*, 433(7028), 873–876.

<https://doi.org/10.1038/nature03287>

- Platt, M. L., Seyfarth, R. M., & Cheney, D. L. (2016). Adaptations for social cognition in the primate brain. *Philosophical Transactions of the Royal Society of London. Series B, Biological Sciences*, *371*(1687), 20150096. <https://doi.org/10.1098/rstb.2015.0096>
- Pojoga, S. A., Kharas, N., & Dragoi, V. (2020). Perceptually unidentifiable stimuli influence cortical processing and behavioral performance. *Nature Communications*, *11*(1), 6109. <https://doi.org/10.1038/s41467-020-19848-w>
- Qiu, J., Kong, X., Li, J., Yang, J., Huang, Y., Huang, M., Sun, B., Su, J., Chen, H., Wan, G., & Kong, J. (2021). Transcranial Direct Current Stimulation (tDCS) over the Left Dorsal Lateral Prefrontal Cortex in Children with Autism Spectrum Disorder (ASD). *Neural Plasticity*, *2021*, 6627507. <https://doi.org/10.1155/2021/6627507>
- Rainer, G., Asaad, W. F., & Miller, E. K. (1998). Selective representation of relevant information by neurons in the primate prefrontal cortex. *Nature*, *393*(6685), 577–579. <https://doi.org/10.1038/31235>
- Rainer, G., & Miller, E. K. (2000). Effects of visual experience on the representation of objects in the prefrontal cortex. *Neuron*, *27*(1), 179–189. [https://doi.org/10.1016/s0896-6273\(00\)00019-2](https://doi.org/10.1016/s0896-6273(00)00019-2)
- Ramsey, R., Kaplan, D. M., & Cross, E. S. (2021). Watch and Learn: The Cognitive Neuroscience of Learning from Others's Actions. *Trends in Neurosciences*, *44*(6), 478–491. <https://doi.org/10.1016/j.tins.2021.01.007>
- Rao, S. C., Rainer, G., & Miller, E. K. (1997). Integration of what and where in the primate prefrontal cortex. *Science (New York, N.Y.)*, *276*(5313), 821–824. <https://doi.org/10.1126/science.276.5313.821>
- Rigotti, M., Barak, O., Warden, M. R., Wang, X.-J., Daw, N. D., Miller, E. K., & Fusi, S. (2013). The importance of mixed selectivity in complex cognitive tasks. *Nature*, *497*(7451), 585–590. <https://doi.org/10.1038/nature12160>

- Rogoff, B., Turkanis, C. G., & Bartlett, L. (Eds.). (2001). Learning together: Children and adults in a school community. In *Learning together: Children and adults in a school community*. (pp. ix, 250–ix, 250). Oxford University Press.
- Rose, M. C., Styr, B., Schmid, T. A., Elie, J. E., & Yartsev, M. M. (2021). Cortical representation of group social communication in bats. *Science (New York, N.Y.)*, *374*(6566), eaba9584. <https://doi.org/10.1126/science.aba9584>
- Rozzi, S., Ferrari, P. F., Bonini, L., Rizzolatti, G., & Fogassi, L. (2008). Functional organization of inferior parietal lobule convexity in the macaque monkey: electrophysiological characterization of motor, sensory and mirror responses and their correlation with cytoarchitectonic areas. *The European Journal of Neuroscience*, *28*(8), 1569–1588. <https://doi.org/10.1111/j.1460-9568.2008.06395.x>
- Russ, B. E., & Leopold, D. A. (2015). Functional MRI mapping of dynamic visual features during natural viewing in the macaque. *NeuroImage*, *109*, 84–94. <https://doi.org/10.1016/j.neuroimage.2015.01.012>
- Saleem, K. S., Miller, B., & Price, J. L. (2014). Subdivisions and connective networks of the lateral prefrontal cortex in the macaque monkey. *The Journal of Comparative Neurology*, *522*(7), 1641–1690. <https://doi.org/10.1002/cne.23498>
- Salvucci, D. D., & Goldberg, J. H. (2000). Identifying Fixations and Saccades in Eye-Tracking Protocols. *Proceedings of the 2000 Symposium on Eye Tracking Research & Applications*, 71–78. <https://doi.org/10.1145/355017.355028>
- Schein, S. J., & Desimone, R. (1990). Spectral properties of V4 neurons in the macaque. *The Journal of Neuroscience: The Official Journal of the Society for Neuroscience*, *10*(10), 3369–3389.
- Schulke, O., Bhagavatula, J., Vigilant, L., & Ostner, J. (2010). Social bonds enhance reproductive success in male macaques. *Current Biology: CB*, *20*(24), 2207–2210. <https://doi.org/10.1016/j.cub.2010.10.058>

- Schultz, W. (1998). Predictive reward signal of dopamine neurons. *Journal of Neurophysiology*, *80*(1), 1–27. <https://doi.org/10.1152/jn.1998.80.1.1>
- Shahidi, N., Parajuli, A., Franch, M., Schrater, P., Wright, A., Pitkow, X., & Dragoi, V. (2022). Population coding of strategic variables during foraging in freely-moving macaques. *BioRxiv*, 811992. <https://doi.org/10.1101/811992>
- Shatz, C. J. (1992). The developing brain. *Scientific American*, *267*(3), 60–67.
- Siegel, M., Buschman, T. J., & Miller, E. K. (2015). Cortical information flow during flexible sensorimotor decisions. *Science (New York, N.Y.)*, *348*(6241), 1352–1355. <https://doi.org/10.1126/science.aab0551>
- Silk, J. B. (2009). Nepotistic cooperation in non-human primate groups. *Philosophical Transactions of the Royal Society of London. Series B, Biological Sciences*, *364*(1533), 3243–3254. <https://doi.org/10.1098/rstb.2009.0118>
- Silk, J. B., Beehner, J. C., Bergman, T. J., Crockford, C., Engh, A. L., Moscovice, L. R., Wittig, R. M., Seyfarth, R. M., & Cheney, D. L. (2009). The benefits of social capital: close social bonds among female baboons enhance offspring survival. *Proceedings. Biological Sciences*, *276*(1670), 3099–3104. <https://doi.org/10.1098/rspb.2009.0681>
- Silk, J. B., Beehner, J. C., Bergman, T. J., Crockford, C., Engh, A. L., Moscovice, L. R., Wittig, R. M., Seyfarth, R. M., & Cheney, D. L. (2010). Strong and consistent social bonds enhance the longevity of female baboons. *Current Biology: CB*, *20*(15), 1359–1361. <https://doi.org/10.1016/j.cub.2010.05.067>
- Sliwa, J., & Freiwald, W. A. (2017). A dedicated network for social interaction processing in the primate brain. *Science (New York, N.Y.)*, *356*(6339), 745–749. <https://doi.org/10.1126/science.aam6383>
- Stalter, M., Westendorff, S., & Nieder, A. (2020). Dopamine Gates Visual Signals in Monkey Prefrontal Cortex Neurons. *Cell Reports*, *30*(1), 164-172.e4. <https://doi.org/10.1016/j.celrep.2019.11.082>

- Stone, V. E., Baron-Cohen, S., & Knight, R. T. (1998). Frontal lobe contributions to theory of mind. *Journal of Cognitive Neuroscience*, *10*(5), 640–656. <https://doi.org/10.1162/089892998562942>
- Strang, S., & Park, S. Q. (2017). Human Cooperation and Its Underlying Mechanisms. *Current Topics in Behavioral Neurosciences*, *30*, 223–239. [https://doi.org/10.1007/7854\\_2016\\_445](https://doi.org/10.1007/7854_2016_445)
- Stringer, C., Pachitariu, M., Steinmetz, N., Reddy, C. B., Carandini, M., & Harris, K. D. (2019). Spontaneous behaviors drive multidimensional, brainwide activity. *Science*, *364*(6437), eaav7893. <https://doi.org/10.1126/science.aav7893>
- Suzuki, S., Harasawa, N., Ueno, K., Gardner, J. L., Ichinohe, N., Haruno, M., Cheng, K., & Nakahara, H. (2012). Learning to simulate others' decisions. *Neuron*, *74*(6), 1125–1137. <https://doi.org/10.1016/j.neuron.2012.04.030>
- Talluri, B. C., Kang, I., Lazere, A., Quinn, K. R., Kaliss, N., Yates, J. L., Butts, D. A., & Nienborg, H. (2022). Activity in primate visual cortex is minimally driven by spontaneous movements. *BioRxiv*, 2022.09.08.507006. <https://doi.org/10.1101/2022.09.08.507006>
- Tang, S., Lee, T. S., Li, M., Zhang, Y., Xu, Y., Liu, F., Teo, B., & Jiang, H. (2018). Complex Pattern Selectivity in Macaque Primary Visual Cortex Revealed by Large-Scale Two-Photon Imaging. *Current Biology : CB*, *28*(1), 38-48.e3. <https://doi.org/10.1016/j.cub.2017.11.039>
- Tanji, J., & Hoshi, E. (2008). Role of the lateral prefrontal cortex in executive behavioral control. *Physiological Reviews*, *88*(1), 37–57. <https://doi.org/10.1152/physrev.00014.2007>
- Tremblay, S., Pieper, F., Sachs, A., & Martinez-Trujillo, J. (2015). Attentional filtering of visual information by neuronal ensembles in the primate lateral prefrontal cortex. *Neuron*, *85*(1), 202–215. <https://doi.org/10.1016/j.neuron.2014.11.021>
- Tremblay, S., Sharika, K. M., & Platt, M. L. (2017). Social Decision-Making and the Brain: A Comparative Perspective. *Trends in Cognitive Sciences*, *21*(4), 265–276. <https://doi.org/10.1016/j.tics.2017.01.007>
- Tremblay, S., Testard, C., DiTullio, R. W., Inchauspé, J., & Petrides, M. (2022). Neural cognitive

- signals during spontaneous movements in the macaque. *Nature Neuroscience*.  
<https://doi.org/10.1038/s41593-022-01220-4>
- Ungerleider, L. G., Galkin, T. W., Desimone, R., & Gattass, R. (2008). Cortical connections of area V4 in the macaque. *Cerebral Cortex (New York, N.Y.: 1991)*, *18*(3), 477–499.  
<https://doi.org/10.1093/cercor/bhm061>
- van Wolken, M., Brosnan, S. F., & de Waal, F. B. M. (2007). Inequity responses of monkeys modified by effort. *Proceedings of the National Academy of Sciences*, *104*(47), 18854 LP – 18859. <https://doi.org/10.1073/pnas.0707182104>
- Venton, B. J., & Cao, Q. (2020). Fundamentals of fast-scan cyclic voltammetry for dopamine detection. *Analyst*, *145*(4), 1158–1168. <https://doi.org/10.1039/C9AN01586H>
- Vinck, M., Batista-Brito, R., Knoblich, U., & Cardin, J. A. (2015). Arousal and locomotion make distinct contributions to cortical activity patterns and visual encoding. *Neuron*, *86*(3), 740–754. <https://doi.org/10.1016/j.neuron.2015.03.028>
- Vinje, W. E., & Gallant, J. L. (2000). Sparse coding and decorrelation in primary visual cortex during natural vision. *Science (New York, N.Y.)*, *287*(5456), 1273–1276.  
<https://doi.org/10.1126/science.287.5456.1273>
- Visco-Comandini, F., Ferrari-Toniolo, S., Satta, E., Papazachariadis, O., Gupta, R., Nalbant, L. E., & Battaglia-Mayer, A. (2015). Do non-human primates cooperate? Evidences of motor coordination during a joint action task in macaque monkeys. *Cortex; a Journal Devoted to the Study of the Nervous System and Behavior*, *70*, 115–127.  
<https://doi.org/10.1016/j.cortex.2015.02.006>
- Viswanathan, P., & Nieder, A. (2013). Neuronal correlates of a visual “sense of number” in primate parietal and prefrontal cortices. *Proceedings of the National Academy of Sciences of the United States of America*, *110*(27), 11187–11192.  
<https://doi.org/10.1073/pnas.1308141110>
- Walker, E. Y., James Cotton, R., Ma, W. J., & Tolias, A. S. (2019). A neural basis of probabilistic

computation in visual cortex. *BioRxiv*, 365973. <https://doi.org/10.1101/365973>

Wallace, K. J., & Hofmann, H. A. (2021). Decision-making in a social world: Integrating cognitive ecology and social neuroscience. *Current Opinion in Neurobiology*, 68, 152–158. <https://doi.org/10.1016/j.conb.2021.03.009>

Wallis, J. D., & Miller, E. K. (2003). Neuronal activity in primate dorsolateral and orbital prefrontal cortex during performance of a reward preference task. *The European Journal of Neuroscience*, 18(7), 2069–2081. <https://doi.org/10.1046/j.1460-9568.2003.02922.x>

Wang, L., Li, X., Hsiao, S. S., Lenz, F. A., Bodner, M., Zhou, Y.-D., & Fuster, J. M. (2015). Differential roles of delay-period neural activity in the monkey dorsolateral prefrontal cortex in visual-haptic crossmodal working memory. *Proceedings of the National Academy of Sciences of the United States of America*, 112(2), E214-9. <https://doi.org/10.1073/pnas.1410130112>

Wickelgren, B. Y. I. (2018). Rebooting Becky 's brain. *Spectrum | Autism Research News*, 1–17.

Williams, S. M., & Goldman-Rakic, P. S. (1998). Widespread origin of the primate mesofrontal dopamine system. *Cerebral Cortex (New York, N.Y.: 1991)*, 8(4), 321–345. <https://doi.org/10.1093/cercor/8.4.321>

Winsky, L., Driscoll, J., & Brady, L. (2008). *CHAPTER 2 - Drug Discovery and Development Initiatives at the National Institute of Mental Health: From Cell-Based Systems to Proof of Concept* (R. A. McArthur & F. B. T.-A. and T. M. for C. N. S. D. D. Borsini (Eds.); pp. 59–74). Academic Press. <https://doi.org/https://doi.org/10.1016/B978-0-12-373861-5.00002-3>

Wutz, A., Loonis, R., Roy, J. E., Donoghue, J. A., & Miller, E. K. (2018). Different Levels of Category Abstraction by Different Dynamics in Different Prefrontal Areas. *Neuron*, 97(3), 716-726.e8. <https://doi.org/10.1016/j.neuron.2018.01.009>

Xiong, Q., Znamenskiy, P., & Zador, A. M. (2015). Selective corticostriatal plasticity during acquisition of an auditory discrimination task. *Nature*, 521(7552), 348–351. <https://doi.org/10.1038/nature14225>

- Xu, N., Harnett, M. T., Williams, S. R., Huber, D., O'Connor, D. H., Svoboda, K., & Magee, J. C. (2012). Nonlinear dendritic integration of sensory and motor input during an active sensing task. *Nature*, *492*(7428), 247–251. <https://doi.org/10.1038/nature11601>
- Yamagata, T., Nakayama, Y., Tanji, J., & Hoshi, E. (2012). Distinct information representation and processing for goal-directed behavior in the dorsolateral and ventrolateral prefrontal cortex and the dorsal premotor cortex. *The Journal of Neuroscience: The Official Journal of the Society for Neuroscience*, *32*(37), 12934–12949. <https://doi.org/10.1523/JNEUROSCI.2398-12.2012>
- Yoshida, W., Seymour, B., Friston, K. J., & Dolan, R. J. (2010). Neural Mechanisms of Belief Inference during Cooperative Games. *The Journal of Neuroscience*, *30*(32), 10744 LP – 10751. <https://doi.org/10.1523/JNEUROSCI.5895-09.2010>



## VITA

Melissa C. Franch was born in North Carolina to Regina and Serafino Franch. She attended West Johnston High School from 2004-2008. That fall, she began her undergraduate degree at North Carolina State University, where she developed her passion for neuroscience research and science education. Melissa graduated in 2012 with a B.S. in Biological Sciences and Science Education. Immediately after undergrad, Melissa's professional career included teaching high school biology and conducting research in cell biology, and systems and cognitive neuroscience for five years. In 2017, she began her PhD in the lab of Valentin Dragoi at MD Anderson Cancer Center UTHHealth Houston Graduate School of Biomedical Sciences.

Permanent address

15818 Cavendish Dr.

Houston, Texas 77059